ELECTRODE KINETICS OF A WATER VAPOR ELECTROLYSIS CELL

Final Report for the Period

August 15, 1971 - June 30, 1974

for

National Aeronautics and Space Administration

Grant # NGR-39-009-123

prepared by

Geoffrey Jacobs

Project Director

Alfred J. Engel

July 1974

TABLE OF CONTENTS

	Page
LIST OF FIGURES	v
LIST OF TABLES	vii
I. SUMMARY	1
II. INTRODUCTION	3
III. STATEMENT OF PROBLEM	5
IV. ELECTROCHEMICAL THEORY OF GENERALIZED REACTION Ox + ne = Red	7
A. A Thermodynamic and Equilibrium Relationship	7
1. Kinetic and Non-Equilibrium Potentials	9
B. Mass Transfer Processes	11
1. Semi-infinite Linear Diffusion to a Plane Electrode Surface at Constant Voltage	12
2. Semi-infinite Linear Diffusion to a Plane Electrode: Continuously Changing Voltage	16
3. Other Mass Transfer Controlled Systems	18
C. Electron Transfer Controlled Processes	20
D. Other Factors Influencing Current-Voltage Relationship	24
1. Reaction Overvoltage	24
2. Crystallization Overvoltage	25
E. Other Sources of Potential Differences	26
1. Electrical Double Layer	26
2. Ohmic Drop	27
3. Liquid-Liquid Potentials	28
4. Adsorption	29
V. LITERATURE SEARCH OF WATER VAPOR ELECTROLYSIS REACTION	32
A. General	32

TABLE OF CONTENTS (Continued)

	Page
B. Oxygen Electrode at Rest	33
1. Oxides	33
2. Adsorbed Oxygen Films	35
3. Mixed Potential Theory	38
4. Conclusions	40
C. Anodic Evolution of Oxygen	40
1. Effects of pH and Adsorbed Ions	42
D. Cathodic Reduction of Oxygen	46
E. Anodic Evolution of O_2 in Sulfuric Acid	48
1. "Dependence of Oxygen-Evolution Overvoltage on Smooth Platinum on the Sulfuric Acid Concentration."	48
2. "Electrolysis of Concentrated Sulfuric Acid Solutions Using Tagged Oxygen."	50
3. "Investigation of the Kinetics of the Electro-oxidation of Sulfuric Acid."	53
F. Water Vapor Electrolysis on Platinum Electrode with an Acid Gel Electrolyte	58
1. "Design and Development of a Water Vapor Electrolysis Unit."	58
2. "A Water-Vapor Electrolysis Cell with Phosphoric Acid Electrolyte."	61
3. "Cycled Operation of a Water Vapor Electrolysis Cell."	66
VI. EXPERIMENTAL APPARATUS AND PROCEDURE	73
A. Apparatus	73
1. Controlled Humid-Air Supply System	74
2. Electrochemical Cell	76
3. Electrochemical Measurement and Control	81

TABLE OF CONTENTS (Concluded)

	Page
B. General Procedure	83
C. Automatic Potential and Current Control	84
VII. RESULTS AND DISCUSSION OF RESULTS	86
A. Experimental Results and Discussion	86
1. "Free Electrolyte" Results	94
2. Standard Cell Results	98
3. Comparison of "Free Electrolyte" Results and Standard Cell Results	99
B. Physical and Electrochemical Implications of Experimental Results	101
1. Concentration Polarization	101
2. IR Losses	104
3. Water Absorption and Overvoltage Decrease	106
4. Adsorption	107
5. Oxygen Coverage	111
VIII. CONCLUSIONS AND RECOMMENDATIONS	119
IX. NOMENCLATURE	121
X. BIBLIOGRAPHY	124
XI. APPENDICES	128
A. Appendix A - Experimental Data	129
B. Appendix B - Sample Calculations	147

LIST OF FIGURES

Figure		Page
1.	Variation of current ration i/i_d with electrode potential	15
2.	Current-potential curve with continuously changing potential	19
3.	Electrical double layer	25
4.	Adsorption current-voltage behavior (a) Adsorption causing constant current. (b) Adsorption causing peak current.	30
5.	Potential sweep obtained on Pt in 2.3 M H_2SO_4 at 25°C and a sweep rate of 0.5 V/sec	37
6.	Oxygen overvoltage on a Pt anode in 0.01 N H_2SO_4 after cathodic and anodic pre-electrolysis.	41
7.	Oxygen overvoltage curves on a bright Pt anode in O_2 saturated 2 N H_2SO_4	43
8.	Anodic polarization curves on Pt in solutions of $HClO_4$ of various concentrations	45
9.	Oxygen overvoltage curves of V.L. Kheifets and I. Ya. Rivlin	49
10.	Oxygen overvoltage curves of Kagancvich, et al.	52
11.	Oxygen overvoltage curves of E. A. Efimov and N. A. Izgrayshev.	56
12.	Electrode polarization characteristics in 9.5 M H_2SO_4	59
13.	Current-voltage behavior in phosphoric acid	65
14.	Constant flow/humidity air supply	75
15.	Disassembled water vapor electrolysis cell.	77
16.	Standard cell, reference electrode, and cathode assembly.	78
17.	Electrochemical measurement and control circuit	82
18.	"Free Electrolyte" Tafel plot, #1	87

LIST OF FIGURES (Concluded)

Figure		Page
19.	"Free Electrolyte" Tafel plot, #2 and #3	88
20.	Standard Cell Tafel plot, #1 and #2	89
21.	Standard Cell Tafel plot, #3 and #4	90
22.	Standard Cell Tafel plot, #5 and #6	91
23.	Comparison of different Standard Cells	92
24.	Comparison of Standard Cell and "Free Electrolyte"	93
25.	Water absorption rate on H_2SO_4 at different gas flow rates	149

LIST OF TABLES

Table		Page
1.	Potentials of platinum oxide couples	34
2.	Oxygen evolution efficiency	51
3.	Characteristic constants of water vapor electrolysis	54
4.	Voltage analysis for free liquid and liquid/matrix cells	62
5.	Cyclic operation power consumption data	68
6.	Free Electroylte - Downward Scan-Figure 1B, #1	130
7.	Free Electrolyte - Upward Scan-Figure 19, #2	132
8.	Free Electrolyte - Downward Scan-Figure 19, #3	134
9.	Standard Cell - Upward Scan-Figure 20, #1	136
10.	Standard Cell - Downward Scan-Figure 20, #2	138
11.	Standard Cell - Downward Scan-Figure 21, #3	140
12.	Standard Cell - Upward Scan-Figure 21, #4	142
13	Standard Cell - Upward Scan-Figure 22, #5	144
14.	Standard Cell - Downward Scan-Figure 22, #6	146

I. SUMMARY

An investigation of the anodic electrochemical behavior of the water vapor electrolysis cell was undertaken. A theoretical review of various aspects of cell overvoltage is presented with special emphasis on concentration overvoltage and activation overvoltage. Other sources of overvoltage are described in less detail. An understanding of these electrochemical fundamentals is of primary importance in explaining the experimental results of this work.

The actual water vapor electrolysis cell consists of a bright platinum anode screen immersed in a thick, viscous sulfuric acid silica gel electrolyte. The cathode was a gray platinum screen and the reference electrode was a mercury-mercurous sulfate sleeve junction electrode. A humid air stream flowed over the anode assembly, and water was absorbed from the airstream by the high concentration sulfuric acid. Although the major investigation was performed on this cell, results are compared to the current-voltage results of a "free electrolyte" cell, using only sulfuric acid as the electrolyte.

The experimental apparatus controlled and measured anode potential and cell current. Potentials between 1.10 and 2.60 V (vs NHE) and currents between 0.1 and 3000 mA were investigated. Different behavior was observed between the standard cell and the "free electrolyte" cell. The "free electrolyte" cell followed typical Tafel behavior (i.e. activation overvoltage) with Tafel slopes of about 0.15, and the exchange current densities of 10^{-9} A/cm^2, both in good agreement with literature values. The standard cell exhibited this same Tafel behavior at lower current densities but deviated toward lower than expected current densities at higher potentials. This behavior and other results were

examined to determine their origin. After a one by one elimination of possible explanations (e.g. concentration polarization, IR losses, and adsorption), a theory of "oxygen entrapment" was shown to be compatible with experimental results. This included the results of this work and the results of others, especially Bloom's work (69) on cycled operation (i.e. turning the cell "on," "off," and "on" again). Considerable indirect evidence is presented for proof of the "oxygen entrapment" proposition which states that evolved oxygen is trapped on the electrode surface by the thick gel electrolyte and this reduces the area available for electrolysis. Much of the discusstion of this theory revolves around the ease of removal of the trapped bubbles and the subsequent changes in surface coverage.

Some limited direct evidence for the existence of trapped oxygen is presented although it is not entirely conclusive. Recommendations for future experiments suggest work on investigating the nature of the trapped oxygen.

II. INTRODUCTION

Of the several oxygen producing life support systems investigated by NASA, the water vapor electrolysis cell still remains a strong possibility for actual use in outer space. The water vapor electrolysis cell operates by absorbing water from a passing humid air stream and electrolyzing the water into gaseous oxygen and hydrogen. The oxygen is inhaled by astronauts and is excreted as water vapor by breathing and perspiration. This water is subsequently electrolyzed again and the cycle is complete. Recycle of oxygen avoids the necessity of storing large quantities of oxygen for extended space flights.

The water vapor electrolysis cell is attractive from several standpoints. Possibly the foremost advantage is its zero gravity characteristic. By maintaining the electrolyte in the form of a thick, viscous gel the cell can be used easily under zero gravity conditions. By using concentrated sulfuric acid in the gel, a gradient exists for the absorbtion of water from a passing air stream.

The major disadvantage of the water vapor electrolysis cell is its power requirement. At the present state of research, a small decrease in the power requirement would make the water vapor electrolysis cell even more attractive for actual use in outer space. Therefore, research directed at determining the major component of the cell overvoltage is of primary importance. By identifying the major source of power consumption, research can be directed toward improving that particular aspect of the cell. Previous studies (8, 13,14) have produced conflicting results as to the major cause of the large required cell voltage. Moreover, these studies have produced other anomalous results regarding cell operation which must be explained in order to exactly describe the

behavior of the water vapor electrolysis cell.

Whereas previous work has primarily investigated the physical behavior of the water vapor electrolysis cell (e.g. heat and mass transfer), this work attempts to explain the electrochemical behavior.

III. STATEMENT OF PROBLEM

Previous studies (8, 13,14) of the water vapor electrolysis cell have produced some contradictory and unexplained results. It was the purpose of this thesis to investigate this cell from an electrochemistry perspective so that more understanding could be given to previous claims about the behavior of the cell. In particular, there have been contradictory statements regarding the nature of the large observed cell overvoltage. Some claim that this overvoltage is due to electrochemical kinetics. Others claim that the large observed overvoltage is due to mass transfer phenomena. It was the direct task of the experimental work of this thesis to settle this dispute. The experimental analysis consists of measurement of cell current and anode potential. The nature of the cell's overvoltage is described by the relationship between current and potential, as will be shown in the "Electrochemical Theory" section of this thesis. Comparison of experimental results with literature findings further aids proper interpretation of the experimental data.

Another task of this work was to apply the understanding of the electrochemical behavior of the water vapor electrolysis cell to other unexplained phenomena reported in previous studies. Of foremost concern was the unusual behavior of the cell observed by Bloom (69) during cycled operation. Here, cycled operation of the cell is turning the cell "on", then "off", then "on" again. Bloom observed that this type of operation had a beneficial effect on the power requirements of the cell. Moreover, Bloom found that there were optimum values of the "on" and "off" parameters. Many other experimental observations from previous studies were also kept in mind during the work on this thesis.

These are too many to be described here, but will be described in detail in the "Discussion" section of this work.

Finally, recommendations were to be made as to what can be done in future work to fully determine the behavior of the water-vapor electrolysis cell.

IV. ELECTROCHEMICAL THEORY OF THE GENERALIZED REACTION: Ox + ne = Red

Concepts and equations are developed here for the generalized redox electrochemical reaction, oxidized form + stoichiometric number of electrons = reduced form (Ox + ne = Red). These concepts and equations can be used experimentally to investigate such reactions; in particular, the water vapor electrolysis reaction will later be investigated using an understanding of the fundamentals presented here.

First, the thermodynamic and equilibrium relationships are investigated and electrochemical kinetics are discussed. Finally, an assortment of other factors are presented.

A. Thermodynamic and Equilibrium Relationships.

Consider the electrochemical reaction

$$aA + bB + ne = cC + dD \qquad [1]$$

where i is the stoichiometric number of moles of component I and n is the total number of electrons involved in the reaction. The Gibbs free energy change for the reaction is

$$\Delta G = \Delta G^{\circ} + RT \ln \left[a_C^{c} \, a_D^{d} \, / \, a_A^{a} \, a_B^{b} \right] \qquad [2]$$

In the above equation

ΔG = change in Gibbs free energy due to reaction, cal/mol

ΔG° = change in Gibbs free energy due to reaction with all constituents in their standard states, cal/mol

R = gas law constant, 1.98 cal/mol - °K

T = absolute temperature, °K

a_I^i = activity of component I raised to the ith power.

Since the reaction takes place at an electrode surface, the activities of the reaction constituents are those at the electrode surface.

The Gibbs free energy change is related to the equilibrium potential[1] of the cell by:

$$\Delta G = -n F \varepsilon_e \qquad [3]$$

where

ε_e = equilibrium cell voltage, volt

n = number of equivalents of reactants converted in the reaction as written

F = Faraday constant, 23060 cal/volt-equivalent

nF = charge flow accompanying reaction as written, coulomb (converted to cal/volt)

The equilibrium potential of the cell is, then

$$\varepsilon_e = E^\circ - \frac{RT}{nF} \ln \left\{ a_C^c \, a_D^d \; / \; a_A^a \, a_B^b \right\} \qquad [4]$$

where E° is the standard potential of the cell. The standard potential

[1]The differentiation made by Vetter (79) between three types of equilibrium potentials will be adopted here.

1. Metal/ion potentials, created when ions of the same metal are bound to different ligands in two phases which are in equilibrium with each other. For example, copper ion bound in copper metal and hydrated (or complexed in an electrolyte.)

2. Redox potentials (oxidation-reduction potentials), created when the two phases exchange electrons with one another and whereby the electrons of both phases are in equilibrium.

3. Donnan and membrane potentials, created when several types of ions, which may be in the same or different valence states, are present in both phases; of these at least one type must be able to pass through the boundary (by mechanical means, such as bonding by ion-exchangers). The ions capable of passing from one phase to the other must be bound in the same manner in both phases (for example, they must be hydrated in both phases).

Study of the water vapor electrolysis reaction involves only the use of redox potentials.

is simply the equilibrium potential when all activities are made unity. For each electrode E° is a characteristic standard potential which is referenced to the normal hydrogen electrode (NHE), arbitrarily set at 0.0 volts. The above equation, commonly called the Nernst equation, was thermodynamically derived, and is an expression of electrochemical equilibrium.

The equilibrium cell potential is defined as the potential of the cell when no net current flows, i.e. the anodic and cathodic currents identically compensate for each other. This state must be attainable from both directions, a requirement analogous to that of thermodynamic reversibility. This latter restriction takes care of the case of extremely slow kinetics where essentially no current flows in either direction.

For a redox system the metal electrode acts only as a source or sink of electrons. The metal electrode is therefore completely inert in the reaction sequence.

1. Kinetic and Non-Equilibrium Potentials.

When a net current flows in an electrochemical cell, the potential is different from the equilibrium potential (i.e. when no net current flows). This difference, $E-E_e$, is defined as the overvoltage. There are several possible causes of the existence of a particular overvoltage. These can best be explained by examining the net process by which an electrochemical reaction occurs.

Consider the general redox reaction:

$$Ox + ne = Red \qquad [5]$$

where Ox is the oxidized form of the electroactive species and Red is the reduced form. Following the simplified approach of Adams (2), this reaction is actually composed of three consecutive individual processes:

$$(Ox)_{bulk} \rightarrow (Ox)_{electrode} \quad [6]$$

$$(Ox)_{electrode} + ne \rightarrow (Red)_{electrode} \quad [7]$$

$$(Red)_{electrode} \rightarrow (Red)_{bulk} \quad [8]$$

These equations actually represent a series of reaction steps. The first equation is a mass transfer process and the second equation is an electron or charge transfer process. These processes have finite rates and determine the actual reaction rate (i.e. current).

The mass transfer process can occur via three common mechanisms: migration, convection, and diffusion. The migration current results from the force exerted on a charged particle by an electric field (e.g. negative ions being attracted to a positively charged electrode). In a large excess of supporting electrolyte, the migration current is negligible.

Convection occurs as a result of thermal, mechanical or other disturbances. Common examples are stirring, vibration, and density variations. Diffusion current occurs when there is a concentration gradient of the species which is being reduced or oxidized.

The electron or charge transfer step is the electrochemical reaction itself. The rate of electron transfer is an exponential function of the applied potential.

Overvoltage resulting from the mass transfer rate determining process is often called diffusion or concentration overvoltage. Over-

voltage resulting from electron transfer as the rate determining process is called activation overvoltage or charge transfer overvoltage.

Mass transfer and electron transfer processes will now be discussed in detail The appropriate equations will be derived whereby the important variables (i.e. current, voltage, concentration, and temperature) are related.

B. Mass Transfer Processes

If the rate of an electrochemical reaction is determined by the rate of mass transfer to the electrode surface, this reaction is often called reversible or Nernstian. This terminology results because the Nernst equation applies to the cell conditions at the electrode surface, i.e. the electron transfer is fast, hence electrochemical equilibrium is established at the electrode surface. The actual current is limited by how fast the oxidized or reduced species can reach the electrode surface. Mass transfer controlled processes are sometimes referred to as reversible processes. Conversely, a process which is controlled by electron transfer and where the Nernst equation does not apply at the electrode surface is often called an irreversible process. Charge transfer controlled processes therefore are sometimes referred to as irreversible processes.

In general, the particular equations which relate current, voltage, concentration, etc. in mass transfer controlled processes result from the particular mode of transport and the particular geometry of the cell. In other words, the equations describing linear diffusion to a spherical electrode are different from those describing hydrodynamic transport past a wire electrode. Each particular case of mass transport must be solved separately. The case of semi-infinite linear diffusion

to a plane electrode surface will be discussed here in detail. Other cases which have been solved will be listed with references.

1. Semi-infinite Linear Diffusion to a Plane Electrode Surface at Constant Voltage.

Consider the cathodic reduction

$$Ox + ne = Red \qquad [5]$$

where the concentration of the oxidized form in the bulk phase is C_{Ox}^{b}. Similarly C_{Red}^{b} is the concentration of the reduced form in the bulk phase.

According to Fick's second law, one can write

$$\frac{\partial C_{Ox}(x,t)}{\partial t} = \frac{\partial}{\partial x} D_{Ox}\left\{\frac{\partial C_{Ox}(x,t)}{\partial x}\right\} \qquad [9]$$

for the oxidized form of the electroactive species and

$$\frac{C_{Red}(x,t)}{\partial t} = \frac{\partial}{\partial x} D_{Red}\left\{\frac{\partial C_{Red}(x,t)}{\partial x}\right\} \qquad [10]$$

for the reduced form. In these equations x is the distance from the electrode surface, t is time, and D_{Ox} and D_{Red} are the diffusion coefficients of the oxidized and reduced forms respectively. The diffusion coefficient is a function of concentration and consequently x, but in the presence of a large excess of supporting electrolyte the diffusion coefficient can be considered to be independent of x. Hence the above equations can be written

$$\frac{\partial C_{Ox}(x,t)}{\partial t} = D_{ox} \frac{\partial^2 C_{Ox}(x,t)}{\partial x^2} \qquad [11]$$

for the oxidized form. An analogous expression exists for the reduced form. Two initial and two boundary conditions are required for solution of these equations. The initial conditions are: $C_{Ox}(x,0)=C_{Ox}^{b}$ and

$C_{Red}(x,0) = 0$ if the reduced form is not present before electrolysis.

The first boundary condition is derived from the Nernst equation. Since electrochemical equilibrium is assumed at the electrode surface,

$$E = (\varepsilon_o) = E^{\circ} + \frac{RT}{nF} \ln \left[\frac{F_{Ox} C_{Ox}(0,t)}{F_{Red} C_{Red}(0,t)} \right] \qquad [12]$$

where F's are the activity coefficients.

The second boundary condition is derived from the conservation of mass, i.e. one mole of the reduced form is produced by transformation of a mole of the oxidized form. The sum of the fluxes of the oxidized and reduced forms at the surface is equal to zero,

$$D_{Ox} \left[\frac{\partial C_{Ox}(x,t)}{\partial x} \right]_{x=0} + D_{Red} \left[\frac{\partial C_{Red}(x,t)}{\partial x} \right]_{x=0} = 0 \qquad [13]$$

Finally, for semi-infinite conditions,

$$C_{Ox}(x,t) \to C^{b} \text{ as } x \to \infty \qquad [14]$$

and

$$C_{Red}(c,t) \to 0 \text{ as } x \to \infty. \qquad [15]$$

Solution for the concentrations of the oxidized and reduced forms yields:

$$C_{Ox}(x,t) = C^{b}_{Ox} \frac{\psi\theta + \operatorname{erf}\left[\frac{x}{2 D_{Ox}^{1/2} t^{1/2}} \right]}{1 + \psi\theta} \qquad [16]$$

and

$$C_{Red}(x,t) = C^{b}_{Ox} \frac{\psi \operatorname{erfc}\left[\frac{x}{2 D_{Red}^{1/2} t^{1/2}} \right]}{1 + \psi\theta} \qquad [17]$$

where

$$\psi = [D_{Ox}/D_{Red}]^{1/2} \qquad [18]$$

and

$$\theta = \frac{C_{Ox}(0,t)}{C_{Red}(0,t)} = \frac{F_{Red}}{F_{Ox}} \exp\left\{\frac{nF}{RT}(E-E^{\circ})\right\} \quad [19]$$

The most useful expressions of the above equations are those which give current (i.e. reaction rate) as some function of potential, or vice-versa. The above relationship for the concentration profile of the oxidized form can thus be transformed:

$$i = \frac{i_d}{1 + \psi\theta} \quad [20]$$

which, upon proper substitution is equivalent to the following equation:

$$E = E^{\circ} - \frac{RT}{nF} \ln\left(\frac{F_{Red}}{F_{Ox}}\right)\left(\frac{D_{Ox}}{D_{Red}}\right)^{1/2} + \frac{RT}{nF} \ln \frac{i_d - i}{i} \quad [21]$$

In the above expressions i_d is the maximum diffusion current possible, i. e. when the concentration of the oxidized species at the electrode surface is essentially equal to zero and the maximum concentration gradient exists. The current-voltage relationship for the reduction reaction is given graphically in Figure 1.

Qualitatively in Figure 1 one notices the existence of a limiting current, i_d The limiting current is reached at potentials where the term

$$\psi\theta = \left(\frac{D_{Ox}}{D_{Red}}\right)^{1/2} \frac{F_{Ox}}{F_{Red}} \exp \frac{nF}{RT}(E-E^{\circ})$$

becomes small. In other words, as the potential becomes more negative with respect to the standard potential, E°, the (cathodic) reduction of the oxidized species reaches a limiting (cathodic) current The opposite holds true for the reverse (i e. oxidization) reaction. The cathodic limiting current is directly proportional to the concentration

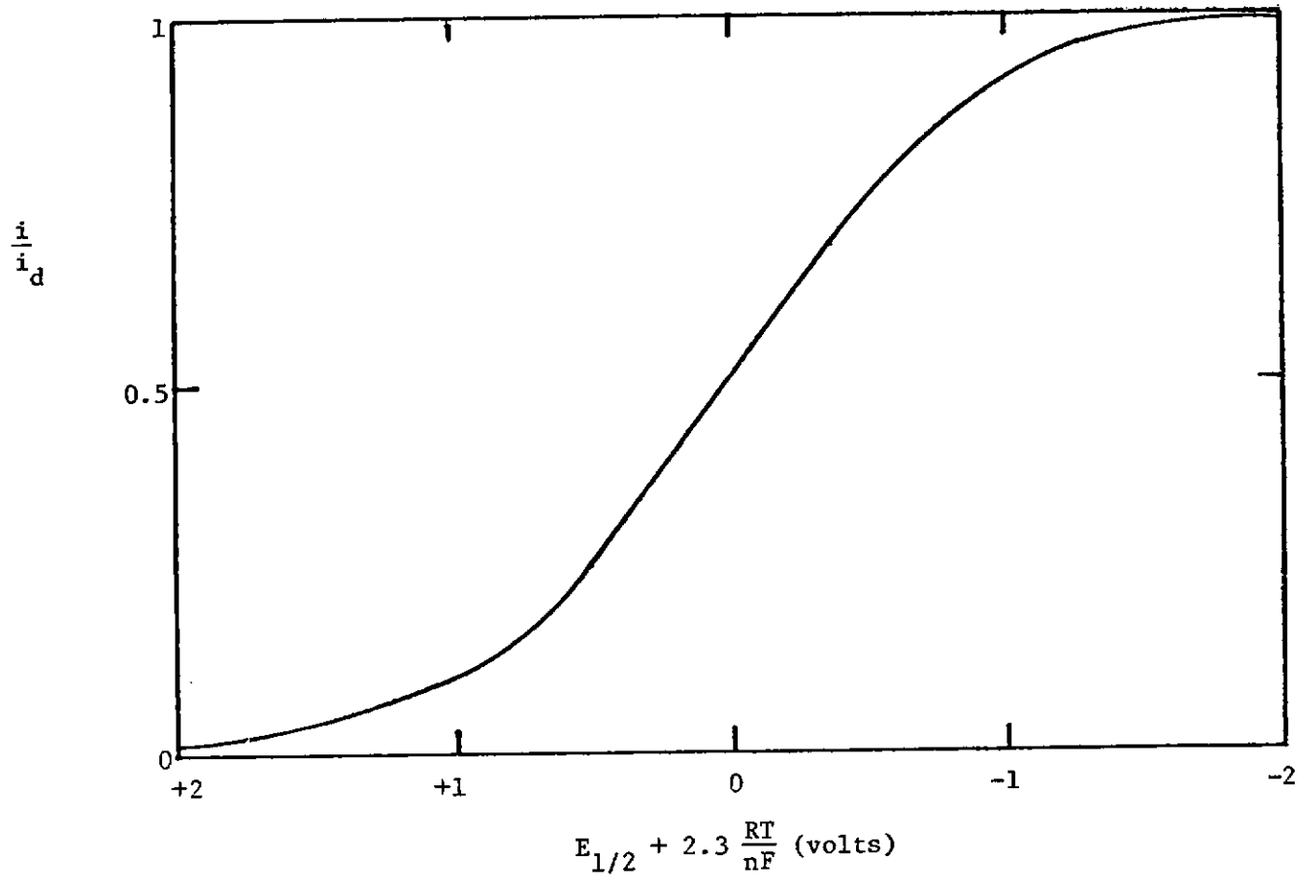

Figure 1. VARIATION OF CURRENT RATIO i/i_d WITH ELECTRODE POTENTIAL

of the oxidized form; similarly, the anodic limiting current is directly proportional to the concentration of the reduced form. In general, for all diffusion controlled processes, the limiting current is directly proportional to the bulk concentration of the electroactive species.

Note: In Figure 1, the current ratio i/i_d is plotted versus $E_{1/2} + 2.3 \frac{RT}{nF}$.

$E_{1/2}$ is called the half-wave potential, as Equation 21 can be rewritten

$$E = E_{1/2} + \frac{RT}{nF} \ln \frac{i_d - i}{i} \qquad [22]$$

The half-wave potential is defined as the potential at which $i = i_{d/2}$. For many situations $E_{1/2}$ is a characteristic constant of a particular system. By taking the second derivative of the current-voltage equation $E_{1/2}$ can be shown to correspond to the inflection point of the current-voltage equation.

Finally, many redox reactions are represented by the form:

$$Ox + mH^+ + ne = Red + Z\ H_2O. \qquad [23]$$

In this case

$$E_{1/2} = E^\circ + m \frac{RT}{nF} \ln a_H + - \frac{RT}{nF} \ln \left|\frac{F_{Red}}{F_{Ox}}\right| \left|\frac{D_{Ox}}{D_{Red}}\right|^{1/2} \qquad [24]$$

2. Semi-infinite Linear Diffusion to a Plane Electrode: Continuously Changing Voltage.

A constant voltage electrochemical process refers to a steady state process. In partice, depending on the particular physical properties of the electroactive species, steady state measurements can be made while changing the potential very slowly. Julian and Ruby (49) found current-potential curves in agreement with the constant voltage

equations derived above for sweep rates up to 40 mv/min. This maximum sweep rate was recommended for a platinum-wire electrode in an unstirred solution.

One can obtain unsteady state behavior by varying the voltage at a constant rate such that

$$E = E_i - vt \qquad [25]$$

where E_i is the initial potential and v is the sweep rate in volts/min. In practice if v is 200 mv/min or greater, unsteady state behavior will be observed.

For the case of semi-infinite linear diffusion to a plane electrode, equations can be derived similar to that obtained above for the constant voltage case. Only important results together with a qualitative description are presented here.

One finds that the current-potential curve reaches a maximum current and then decreases. In the constant voltage case, recall that the current reached a maximum value and maintained that value. In the case of constantly changing potential a peak value of the current is reached which is given by

$$i_p = k\, n^{3/2}\, A\, D_{Ox}^{1/2} C_{Ox}^{b}\, v^{1/2} \qquad [26]$$

where

i_p = peak current, amps

A = area of electrode, cm^2

v = rate of potential change, V/min.

k = Randles-Sevcik constant.

The important characteristics of equation 26 are:

1. The peak current is proportional to the bulk concentration.

2. The peak current is proportional to the sweep rate to the one-half power.

A typical example of the peak current characteristic is given in Figure 2.

Delahay (20) gives an excellent qualitative explanation of the existence of the peak current phenomenon.

"Initially the rate of the electrochemical reaction is so low that virtually no current flows through the cell. As the voltage varies in the proper direction, the rate of electron transfer at the electrode increases, and the current increases accordingly. The substance reacting at the electrode is progressively removed from the solution in the immediate vicinity of the electrode, and this tends to decrease the current. This effect of depletion becomes progressively dominant, and the current-potential curve exhibits a maximum "

3. Other Mass Transfer Controlled Systems

Many electrochemical systems which have mass transfer controlled reaction rates have been investigated These systems can be divided into "quiet" solutions and stirred solutions. Quiet solutions are those in which diffusion is the principle mass transfer process. Several quiet systems for which the current-voltage characteristics have been solved are listed below.

1. Semi-infinite spherical diffusion (57)
2. Semi-infinite cylindrical diffusion (21)
3. Diffusion toward an expanding sphere (52)
4. Cylindrical diffusion with a constantly changing potential (68)

The current-voltage characteristics of several stirred solution

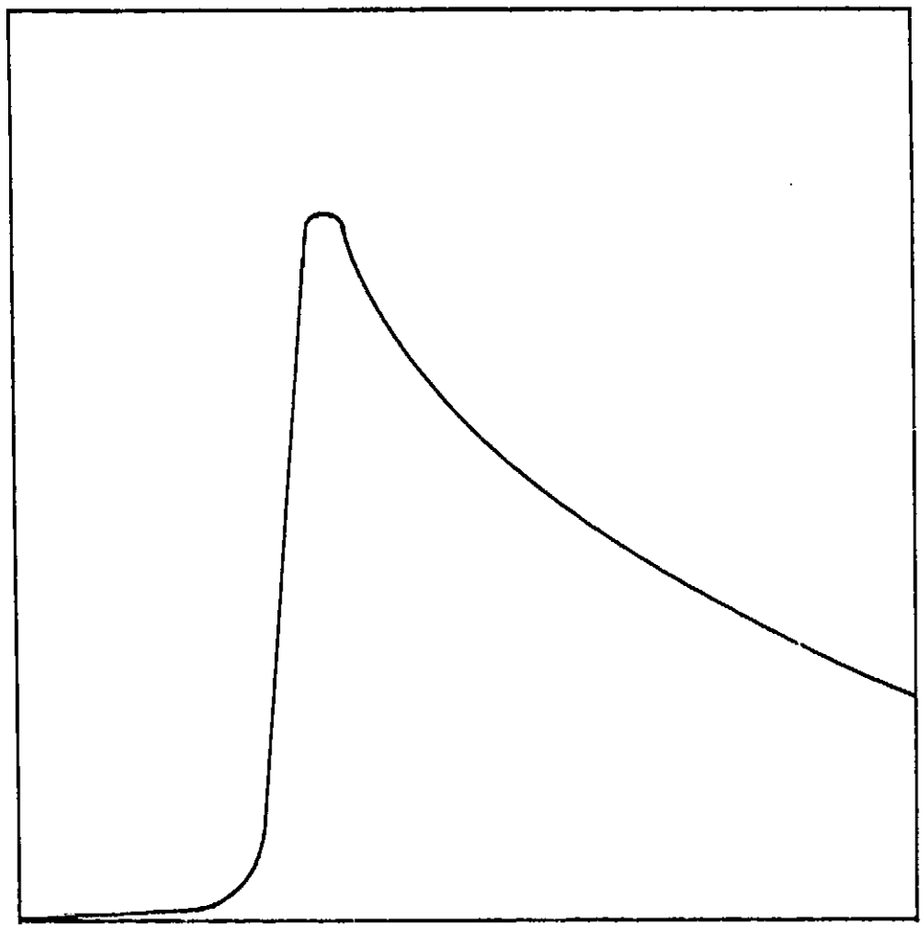

Figure 2. CURRENT-POTENTIAL CURVE WITH CONTINUOUSLY CHANGING POTENTIAL

systems and systems with moving electrodes have been investigated. Some of these are listed below.

1. Rotating disc electrode in the case of laminar flow (59)
2. Plane electrode in the case of laminar flow (60)
3. Limiting currents for turbulent flow (61)
4. Rotating wire electrode (78)
5. Rotating mercury electrode (58)

Electrochemical literature concerning stirred solutions is replete with the concept of the Nernst diffusion layer. Essentially, this is a theory which proposes the existence of a small stagnant diffusion layer (order of 5×10^{-3} cm) at the electrode surface. A linear concentration gradient of the electroactive species is assumed across the completely still diffusion layer. Both of these assumptions have been shown to be grossly incorrect (7); nevertheless, the concept of a diffusion layer proves to be a useful one. This concept (the diffusion layer) can be used to predict the effect of speed of rotation of the electrode and bulk concentration on the limiting current. The relationship between the limiting current and the speed of rotation is often given in the form:

$$i_L = a\, r^b \qquad [27]$$

where r is the speed of rotation (rpm) and a and b are constants.

C. Electron Transfer Controlled Processes

If the kinetics of an electrochemical reaction are rate determining then this is called an electron or charge transfer process. The equations governing this process are developed below.

The electrochemical redox reaction

$$Ox + ne = Red \qquad [5]$$

is assumed to have first order kinetics.

Hence

$$-\frac{dN_{Ox}}{dt} = k_{f,h}\, C_{Ox} = \frac{dN_{Red}}{dt} = k_{b,h}\, C_{Red} \qquad [28]$$

where

N_{Ox} = flux of oxidized species, moles/cm^2

N_{Red} = flux of reduced species, moles/cm^2

$k_{f,h}$ = forward heterogenous rate const., cm/sec.

$k_{b,h}$ = backward heterogeneous rate const., cm/sec.

and C_{Ox}, C_{Red}, and t have their usual significance.

The cathodic current is obtained by multiplying the rate of reduction of the oxidized form by the area and the charge required (to reduce one mole of the oxidized form). Hence

$$i_c = -\frac{dN_{Ox}}{dt}\,(nFA) = k_{f,h} C_{Ox}\,(nFA). \qquad [29]$$

Similarly, one can write for the anodic current:

$$i_a = \frac{dN_{Red}}{dt}\,(nFA) = -k_{b,h}\, C_{Red}\,(nFA). \qquad [30]$$

The net current is simply the sum of the anodic and cathodic currents:

$$i = i_c + i_a \qquad [31]$$

or

$$i = k_{f,h}\, C_{Ox}\, nFA - k_{b,h}\, C_{Red}\, nFA. \qquad [32]$$

The rate constants are exponential functions of the applied potential. These are given in Equations 33 and 34 below:

$$k_{f,h} = k^{\circ}_{f,h} \exp\left[-\frac{\alpha nF}{RT} E\right] \qquad [33]$$

and

$$k_{b,h} = k^{\circ}_{b,h} \exp\left\{\frac{(1-\alpha)\ nF}{RT} E\right\} , \qquad [34]$$

where k_f°'s are the rate constants at E = 0 versus the normal hydrogen electrode.

The postulate that the reaction is an exponential function of the applied potential was first formulated by Eyring (32) from the absolute reaction rate theory. This postulate was further verified in a quantum theoretical treatment by Gerisher (30).

Alpha, α, is a constant called the transfer coefficient. There is considerable controversy over the physical significance of the transfer coefficient. The most common interpretation is that the fraction of the potential αE favors the cathodic reduction reaction and the fraction $(1-\alpha)E$ favors the anodic oxidation reaction. Typical values for α are between 0.15 and 0.65, most values of the transfer coefficient being close to 0.5.

At the equilibrium potential there is no net current and hence,

$$k_{f,h}\ C_{Cx}\ nFA = k_{b,h}\ C_{Red}\ nFA \qquad [35]$$

and

$$k^{\circ}_{f,h}\ C_{Ox} \exp\left\{-\frac{\alpha nF}{RT}\varepsilon_{\circ}\right\} = k_{b,h}\ C_{Red} \exp\left\{\frac{(1-\alpha)\ nF}{RT}\varepsilon_{\circ}\right\}. \qquad [36]$$

It is a simple matter to reduce this expression to a statement of the Nernst equation. Note here that there are cathodic and anodic currents at the equilibrium potential; however, the cathodic and anodic currents identically cancel each other. The value of the cathodic (or anodic) current density at the equilibrium potential is called the ex-

change current density, i_o. The relative magnitude of the exchange current density is often used to determine the catalytic activity of a particular electrode material: the higher the activity, the higher the exchange current density.

A combination of equations yields the equation:

$$i = nFA\, k_{s,h} \left\{ C_{Ox} \exp\left[-\frac{\alpha\, nF}{RT} (E - \varepsilon_o) \right] - C_{Red} \exp\left[\frac{(1-\alpha)nF}{RT} (E - \varepsilon_o) \right] \right\} \qquad [37]$$

where $k_{s,n}$ is the standard rate constant at the equilibrium potential. A still more common expression of the current-voltage relationship is

$$i = i_o \left\{ \exp\left[\frac{\alpha nF}{RT} \eta \right] - \exp\left[-\frac{(1-\alpha)nF}{RT} \eta \right] \right\} \qquad [38]$$

where η is defined as the overvoltage, i. e. $\eta = E - \varepsilon_o$.

This equation can be written in the following simplified form:

$$i = i_o \left(e^{-A\eta} - e^{B\eta} \right) \qquad [39]$$

where A and B are constants. It is easily seen that as E varies in the proper direction one component of Eqn.39 (i.e. either $i_o e^{-A\eta}$ or $i_o e^{B\eta}$) becomes large while the other becomes small. In general, if the potential is more than $\frac{0.012}{n}$ volts different from the equilibrium potential the current will be either 99% cathodic or 99% anodic. Therefore, at large positive or negative values of the overvoltage, η is a logarithmic function of i,

$$\eta = a + b \log i \qquad [40]$$

Such a plot of η versus log i is known as a Tafel plot and b is known as the Tafel slope. In general, if a Tafel plot (i.e. a plot of η vs log i which yields a straight line) is obtained from experimental data, then it can be concluded that the overvoltage is charge transfer

overvoltage. Furthermore, extension of the Tafel line to $\eta = 0$ yields a value of the exchange current density. Often the slope of the Tafel line is characteristic of a certain type of mechanism, e.g. if b = .12, then a one-electron transfer step is often assumed to be rate determining. The value of the Tafel slope also yields a value of the transfer coefficient, α.

Equation 40 is very important in electrochemical studies. Tafel plots are powerful analytical tools for determining the nature of electrochemical cell overvoltages. This type of plot is used extensively in the analysis of the experimental results presented in this thesis.

D. Other Factors Influencing Current-Voltage Relationship.

Unfortunately, the world of electrochemistry is not governed solely by the Nernst equation, diffusion overvoltage, and charge-transfer overvoltage. There are many complicating factors which come into play; some of these are more dominant under certain conditions than under other conditions. In many instances, these other factors can be safely overlooked. Nevertheless, it is necessary to understand what they are, where they derive from, and how significant they are. These other factors include other sources of overvoltage and other sources of potential drop. These factors are discussed below in a less-than-rigorous fashion.

1. Reaction Overvoltage.

Reaction overvoltage exists when a separate chemical reaction is the rate determining step in the overall electrochemical reaction. In other words, if an electroactive species must undergo a chemical reaction which has a much smaller rate constant than the other partial rate processes, (e.g. diffusion or electron transfer), then there exists

reaction overvoltage. By definition, a chemical reaction is independent of the applied cell potential.

Vetter (80) gives a quantitative expression for the reaction overvoltage:

$$\eta = \nu \frac{RT}{nf} \ln \frac{a(i)}{\bar{a}} \qquad [41]$$

where ν is the stoichiometric factor of the reactant species being produced or consumed by a particular partial electrode reaction. $\bar{a}$ is the activity of the substance at equilibrium. The activity, a(i), is the activity of the substance at any current density, i. Reaction overvolatge is generally accompanied by diffusion since the activities of the species are changing. However, the concurrent diffusion overvoltage is generally very small. In the literature, reaction overvoltage plus difussion overvoltage is called concentration overvoltage.

A distinction is made between homogeneous and heterogeneous reaction overvoltage For a homogeneous rate-limiting step, the overvoltages will be independent of the properties and state of the electrode surface. Conversely, a heterogeneous chemical reaction process will be highly dependent on the properties and state of the electrode surface.

In practice, the existence of a dominant reaction overvoltage is rare, although there are definite cases where it does exist, e.g. HNO_3/HNO_2 redox electrode and the cathodic generation of hydrogen.

Although reaction overvoltage does not play a role in the study of water vapor electrolysis, it is nevertheless worthwhile to be aware of its existence in this presentation of the generalized electrochemical reaction

2. Crystallization Overvoltage.

Since this paper deals almost exclusively with redox reactions,

no discussion of crystallization overvoltage is presented here, as it occurs only at metal/ion electrodes. Crystallization overvoltage is related to the difficulty in the inclusion or release of "ad-atoms" into and from, respectively, the lattice of the solid metal electrode. Quantitative expressions of crystallization overvoltage have been developed and are presented by Vetter (81). As in the case of reaction overvoltage, crystallization overvoltage plays no part in water vapor electrolysis.

E. Other Sources of Potential Differences.

1. Electrical Double Layer.

At an electrode which is positively charged an adjacent layer of negatively charged ions will form. This layer of ions is characterized as compact or diffuse, depending on the relative concentration of ionic charge near the surface of the electrode. For any other negative ion diffusing or migrating to the positive electrode surface, a repulsive force will arise between the negative ion and the negatively charged layer of ions. The existence of the two layers (i.e. the positively charged electrode surface and the surrounding layer of negatively charged ions) is called the electrical double layer. See Figure 3.

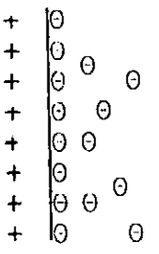

Figure 3. ELECTRICAL DOUBLE LAYER

The electrical double layer is characterized by the double layer capacitance, C_{dl} and the double layer zeta potential, ζ. Vetter (82) gives quantitative expressions to evaluate these parameters. Experimental values of the double-layer capacity of bright platinum lie between 10 to 40 $\mu F/cm^2$. The actual value depends on the electrolyte, its composition, and the potential. It can be shown that for electrochemical cells operating at relatively large current densities (e.g. $> 10^{-4}$ A/cm^2), the effect of the electrical double layer is negligible. also, at high concentrations (e.g. $> 10^{-1}$ M) of the electroactive species, the capacity current, i. e., due to the double layer can be neglected. On the other hand, at low current densities one cannot neglect the double layer. Because studies of water vapor electrolysis are carried out in aqueous solutions (water being a concentrated electroactive species), the effect of the double layer can be neglected. This is true even at low current densities.

2. Ohmic Drop

The actual potential of a particular system includes the ohmic drop due to the resistance of the cell and connections. The ohmic drop is simply equal to the product of the total resistance and the cell current. In general, the resistance of the cell and connections is of the order of 100 ohms and the net contribution to the overall potential drop can most often be neglected. Usually, selection of a supporting electrolyte of high concentration assures a minimal ohmic drop.

The net potential drop, E_r, is given simply by

$$E_r = E_i + IR \qquad [42]$$

where E is the initial potential and R the total resistance. In practice, however, the potential is often varied as a linear function

of time, v·t where v is the sweep rate in volts/min. Since, the current i is a function of the potential, E, the actual potential dependence on time can be complex if the ohmic drop is not small. Delahay gives an approximate mathematical interpretation (22).

At high currents, when the contribution of ohmic drop is significant, current-voltage curves must be corrected to account for this IR drop. A measureable IR drop occured in the experimental work of this thesis and an analysis of the data includes corrections for these ohmic losses.

3. Liquid - Liquid Potentials.

A common complicating factor in electrolytic cells is the potential difference which exists at the contact zone between two different electrolytes. This is often the case at the contact zone between the cell electrolyte and the reference electrode solution. This added potential difference must be taken into account, as it can be relatively large. The potential which exists as described above is called the liquid - liquid junction potential, E_{L-L}.

The general expression for this potential is:

$$E_{L-L} = \frac{RT}{F} \sum_{j=1}^{n} \int_{a_{j,1}}^{a_{j,2}} \frac{t_j}{z_j} \, d \ln a_j \qquad [43]$$

where $a_{j,1}$ is the activity of the j^{th} species in phase 1, t_j is the transference number of the j^{th} species, and z_j is the charge number of the j^{th} species. The transference is the fraction of current carried by the j^{th} species. The exact solution of this equation depends on the particular characteristics of the diffusion zone.

In the special case of a liquid junction potential at

different concentrations of the same dissolved species, the above equation can be simplified to give:

$$E_{L-L} = \frac{RT}{F} \Sigma \frac{t_j}{z_j} \ln \frac{a_{j,2}}{a_{j,1}} \qquad [44]$$

This equation is commonly called the Henderson equation.

By placing a common ionic solution between two different electrolytes, one can greatly reduce the magnitude of the liquid - liquid junction potential. This is frequently done in practice by insertion of a concentrated KCl solution "salt bridge" between the two electrolytes. Vetter (83) gives the corresponding equations.

Awareness of the liquid - liquid potential influenced the selection of a proper reference electrode for the experimental work of this thesis. Details of this particular problem are given later.

4. Adsorption.

Ralph Adams has written a recent text on the electrochemistry of solid electrodes (1). In the preface of the text he writes, "Also, more important to the concept of the book, there is no organized treatment of adsorption phenomena. Critics may well ask, 'How ... can one write a book on solid electrodes and not adequately treat adsorption?' ... Unlike some, I do not feel that adsorption is the single, most important part of every electrode reaction ... When adsorption processes are better understood, and particularly when their role in the overall electrode process can be assessed better, then these discussions can be properly modified ..."

At this point in time, reliable quantitative expressions of the effect of adsorption on current-voltage relationships are still nonexistent. In fact, recent publications (15, 16) have shown that previous

Interpretations of adsorption phenomena at solid electrodes are often ill-founded. Conway (16) has concluded that in "complex anodic reactions it seems, therefore, that the method (i.e. potential) sweep must be applied with caution and that only qualitative or semi-quantitative kinetic and coverage information can be derived."

In general, a current-voltage curve will exhibit a leveling off of the current at the potentials where adsorption is occurring on the electrode. Depending on the magnitude of the potential sweep rate, "adsorption peaks" may even be descerned. Figure 4 gives typical examples of adsorption processes.

Adsorption processes generally occur at potentials preceding the potentials at which the kinetic currents occur. This is so because the adsorbed intermediates often act as the new catalytic surface at which the electrochemical reaction occurs.

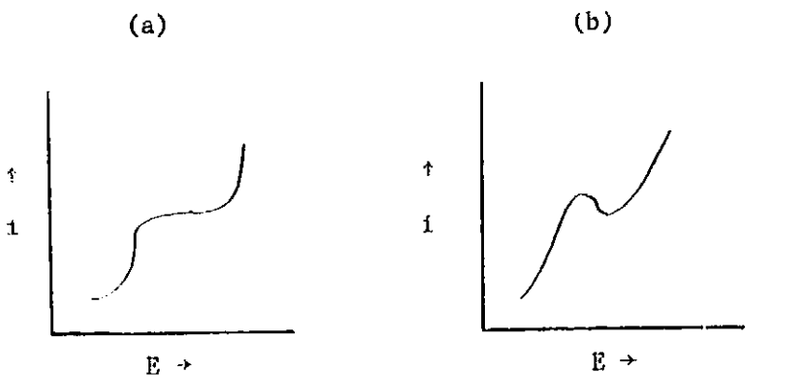

Adsorption causing constant current

Adsorption causing peak current

Figure 4. ADSORPTION CURRENT-VOLTAGE BEHAVIOR

The quantitative expressions which do exist are extremely complex. The adsorption layer is characterized by its capacitance, C_{Ad}, and the electrode surface is characterized by its fractional coverage, θ. Simple expressions do not exist to evaluate these properties. Conway (26) gives quantitative expressions, for what they are worth.

Since an adequate theory of adsorption phenomena at electrodes does not exist, present practice is the individual interpretation of each particular electrode process. This is true in the case of the water vapor electrolysis reaction and is an important part of the related discussion which is presented later in this thesis.

V. LITERATURE SEARCH[1] OF THE WATER VAPOR ELECTROLYSIS REACTION

A. General.

The oxygen electrode has been the subject of much controversy throughout its study. This is still true today, as Vetter (82) writes, "The mechanism of the oxygen electrode is simply not clear at present." Nevertheless, several aspects of the oxygen electrode have been fruitfully studied. Some of these observations include:

1. The equilibrium potential is unattainable except under very special conditions.
2. The evolution of oxygen occurs at high overvoltages.
3. The current-voltage characteristics are dependent on the pre-treatment of the electrode.
4. Oxides and adsorbed layers affect the current-voltage relationship.

Determination of the actual mechanism of the oxygen electrode has been the heart of most research on it.

This work investigates only the anodic evolution of oxygen in concentrated (approx. 8M) sulfuric acid in a silica gel matrix at a brite platinum electrode. However, the observations of other conditions of the oxygen electrode add much insight to the investigation of the afore-mentioned system. Therefore, the oxygen electrode at rest and the

[1]The bulk of the material in this section is taken from the excellent review of the oxygen electrode by J. P. Hoare, entitled The Electrochemistry of Oxygen. Since this book was copyrighted in 1968, it was only necessary to search from 1968 to 1972 for other pertinent literature. Hoare's basic format in explaining the oxygen electrode is followed here.

reduction of oxygen are also discussed below. In order to shorten the discussion somewhat, only observations at platinum electrodes in acid solutions are presented.

B. Oxygen Electrode at Rest

It has been long known that, under open circuit conditions, the usually observed potential of the oxygen-hydrogen cell is only about 1.10v. This is considerably lower than the equilibrium potential of 1.299 V. The standard potential for the overall reaction $O_2 + 2H_2 = 2H_2O$ has been calculated from the standard heat and entropy of formation of water (-68,317 cal/mole and -39.0 cal/deg-mole, respectively) (28).

The large discrepancy between the observed potential and the theoretical equilibrium potential can be found to derive from the fact that platinum and the other noble metals are not inert to oxygen saturated electrolytes. This gives the oxygen electrode its irreversibility and poor reproductibility.

Studies of the oxygen electrode under open circuit conditions have been directed at determining the actual state of the electrode surface, i.e. the type of adsorbed films, the extent of coverage, and the effect of impurities. Some of the significant results of these studies are presented below.

1. Oxides.

The first explanations of the observed potentials of the oxygen electrodes proposed an oxide/oxygen couple instead of the metal/oxygen couple as determining the rest potential. Such an explanation is commonly called the "oxide theory." Researchers have suggested that the surface of the platinum was oxidized, thus causing the low potentials of the oxygen-hydrogen (or Grove) cell (29, 30, 31). Several oxides were

Table 1

POTENTIALS OF PLATINUM OXIDE COUPLES

Electrode couple	Lorenz and Spielmann (65,66,75)	Grube (33)	Nagel and Dietz (67)	Latimer (56) and de Bethune (18)	Hoare (45)
Pt/Pt-O					0.88 V
Pt/PtO		0.9 V			
$Pt/Pt(OH)_2$			0.98 V	0.98 V	
$Pt/PtO.2H_2O$	0.95 V	1.04 V			
$Pt/PtO_2.2H_2O$	0.96 V				
$Pt/PtO_2.3H_2O$	0.98 V				
$Pt/PtO_2.4H_2O$		1.06 V			
Pt/PtO_3		1.5 V			
Pt/PtO_4		1.6 V			
Pt/Pt_3O_4			1.11 V		
$Pt(OH)_2/PtO_2$			1.1 V	1.1 V	

subsequently identified and the potentials of the metal-metal oxide were determined. These are given in Table 1.

Foerster (26) argued that the open-circuit potentials were the result of a combination of oxides, PtO_x.

The oxide theory is generally considered to be incorrect due to the following observations:

1. Plateaus in the potential-time curves can not be found which correspond to any of the measured oxide potentials (26).
2. Oxides of other noble metals (Pd, Au, Rh, Os, Ir, and Ru) had potentials which approached a common value with time, instead of different values as one would expect with the oxide theory (4).

2. Adsorbed Oxygen Films.

The technique of using constant current curves to investigate the formation and reduction of adsorbed films on platinum has been widely used. Hoare (37) cites 33 papers on this technique. In general, it has been found that the adsorbed layer of oxygen is a monolayer of atomic oxygen (6). The thickness of the oxygen layer has been determined by analysis of charging curves (11, 73) and, more recently, by ellipsometric methods (69, 70).

Constant current charging curves yield information on the number of coulombs required to form a monolayer of oxygen, Qa, and the number of coulombs required to reduce it, Qc. It is always found experimentally that Qa = Qc. Slow charging techniques (54) show that Qa > Qc, while fast charging techniques (10) yield Qa = Qc. After about 20 cycles of anodic and cathodic polarization in 8m $HClO_4$ between 5 and 1.4 V, Feldberg, Enke, and Bricker (10) reported that Qa/Qc approached a

value of 1, whereas initially Qa/Qc = 2. It is now generally accepted that the reason Qa > Qc for fast charging techniques and for repeated cycling is the dissolution of oxygen into the platinum metal itself. Only a monolayer exists on the surface; the rest is dissolved into the body of the metal. Schuldiner and Warner (74) showed that with rapid charging, only the adsorbed oxygen was measured to determine Qa and Qc. On the other hand, with slow charging both the oxygen dissolved in the platinum and the adsorbed oxygen were measured. Similarly, repeated cycling tends to saturate the platinum metal with oxygen; the equivalent of several monolayers of oxygen can be dissolved in platinum metal before it is saturated. Once it is saturated, only the adsorbed layer determines Qa and Qc (dissolved oxygen is difficult to remove), hence, Qa = Qc when the platinum metal is saturated. Thacker and Hoare (76) distinguish between oxygen on the surface, dermasorbed oxygen (in the "skin" of the metal), and oxygen absorbed into the bulk metal.

Rapid potential sweep methods have also yielded information about the nature of the adsorbed films of oxygen. A typical curve (38) for the oxygen-hydrogen cell in acid solution is given in Figure 5.

The interpretation of this curve is as follows: oxygen adsorption begins at about 0.85 V and oxygen evolution at about 1.4 V; hydrogen peaks exist below 0.4 V. Note that the anodic and cathodic peaks for hydrogen occur at the same potentials, implying a reversible process. On the other hand, the cathodic sweep must proceed further than the anodic oxygen adsorption potential to reduce the oxygen. This indicates an activation barrier in the adsorption of oxygen. The same principle of oxygen dissolution into the platinum metal applies to fast potential sweeps as well as constant charging curves.

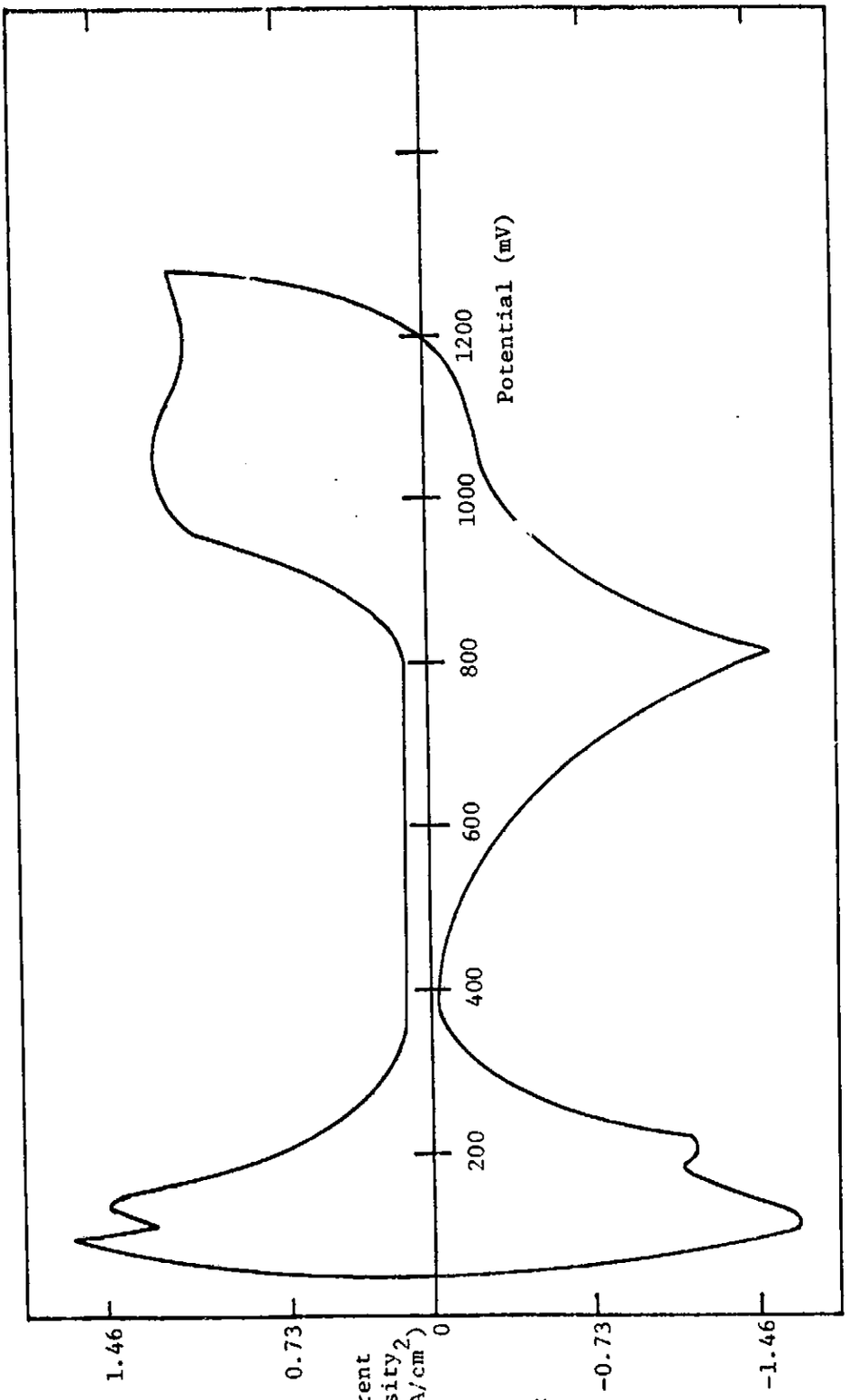

Figure 5. POTENTIAL SWEEP OBTAINED ON Pt IN 2.3 M H_2SO_4 AT 25°C AND A SWEEP RATE OF 0.5V/Sec.

Unfortunately fast triangular sweep curves are difficult to interpret quantitatively. Conway (15, 16) points out that many of the present interpretations of rapid potential sweep curves are somewhat incorrect because the capacitance of the adsorbed intermediates has a complex effect on the current-voltage relationship. Furthermore, the capacitance is a function of the magnitude of the potential sweep rate. Hence, quantitative interpretations of rapid potential sweep curves are suspect. Conway cautions that qualitative or semi-quantitative interpretations are all that can be made, based on the present state of the knowledge of adsorbed intermediates.

Bockris and Huq (9) were able to maintain a complete electronically conducting monolayer of oxygen on a platinum electrode. The reversible potential was obtained for an hour in oxygen saturated H_2SO_4 solutions (.001N to 0.1N). Impurities were rigorously controlled. This is especially important for the oxygen electrode because the exchange current density, i_o, is very low (approx. 10^{-9} A/cm^2). Impurity reactions could, therefore, be potential-determining at potentials below the reversible potential (1.23V). Bockris and Huq calculated an impurity level of less than 10^{-11}M for their experiments. The platinum electrodes were pre-treated to insure a complete monolayer of electronically conducting oxygen. The electrodes were prepared for two hours at 500°C before plunging them into the pre-purified, oxygen-saturated sulfuric acid solutions. After about an hour, the potential dropped to lower values.

3. Mixed Potential Theory.

The most widely held explanation of the low value of the rest potential of the oxygen electrode is the mixed potential theory. Two

prominent versions of what the combining reactions might be are presented below. Others are given by Hoare (40).

Hoar (36) was the first to suggest a mixed potential mechanism. He proposed that cracks exist in an oxide surface film whereby oxygen is reduced and a platinum oxide is formed on the platinum surface, i. e. a local cell is set up. By applying a countercurrent of 2×10^{-7} A/cm^2 the reversible potential has been maintained. This countercurrent is equal to the local cell current.

A mixed potential theory of two reactions occurring at different points on the surface of the electrode has been proposed by Lewartowicz (62). Hoare (39) suggests the O_2/H_2O reaction and a Pt/Pt-O reaction:

$$Pt\text{-}O + 2H^+ + 2e = Pt + H_2O \qquad E_o = 0.88V. \qquad [45]$$

Pt-O is a layer of adsorbed oxygen atoms (as opposed to PtO, an oxide layer). (Further discussion of the oxidation of Pt is given by Appleby (3)) Oxygen is reduced on the PtO sites, and Pt-O sites are formed by reacting with water (Eqn.45). This should ultimately produce a complete Pt-O layer and the reversible potential, 1.23V, would be obtained. However, Hoare concludes that a complete Pt-O layer is unstable in acid solutions, hence some bare Pt sites always exist. Therefore, the mixed potential of the O_2/H_2O and Pt/Pt-O reactions is determining. (Note that the mixed potential, E_m, must lie between the values of the two combining potentials).

The mixed potential can thus be used to explain the dependence of the rest potential on the extent of surface coverage. This dependence has been reported by several workers (10, 31, 71) and is a function of electrode pretreatment. Therefore, the mixed potential theory can also

be used to explain the dependence of the rest potential on electrode pretreatment. Unfortunately, there is little positive evidence for the existence of a mixed potential at the oxygen electrode. It has not been proven to exist nor has it been disproven. It can explain, however, the many anomalies of the oxygen electrode. The only positive evidence thus far is that cathodic stripping measurements have shown that the maximum quantity of oxygen stripped is less than a complete monolayer. This means that there must be some bare Pt sites available.

4. Conclusions.

In summary of the phenomena of the oxygen electrode at rest, the following important facts have been determined:

1. The reversible potential is attainable only under strict control of impurities.
2. The reversible potential is attainable only when a complete adsorbed layer of Pt-O exists.
3. Oxygen is dissolved into massive platinum.
4. The existence of bare Pt sites gives rise to lower rest potentials.

C. Anodic Evolution of Oxygen.

Overvoltage curves (i.e. log i vs. E) of oxygen evolution at Pt electrodes are characterized by high overvoltages. Under ordinary conditions Tafel behavior begins at an overvoltage of about 0.4V. Between current densities of 10^{-6} A/cm^2 and 10^{-2} A/cm^2, a typical Tafel slope is 0.10 to 0.13, and the extrapolated exchange current density is about 10^{-9} A/cm^2 for systems with controlled impurities. A typical plot is given below (9) in Figure 6

Note that the initial potential sweep does not follow Tafel

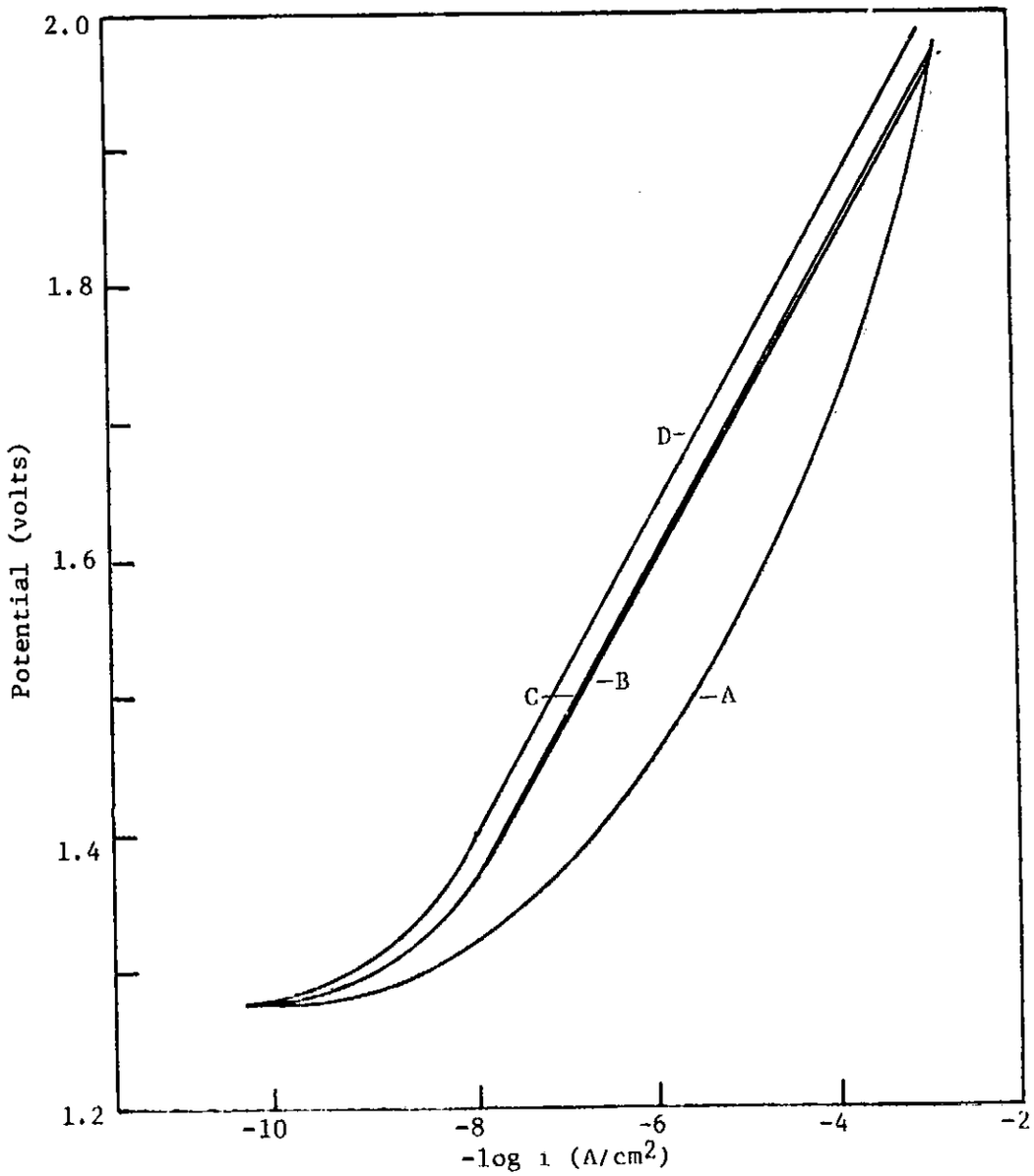

Figure 6. OXYGEN OVERVOLTAGE ON A Pt ANODE IN 0.01 N H_2SO_4 AFTER CATHODIC AND ANODIC PRE-ELECTROLYSIS (A) increasing current followed by (B) decreasing current followed by (C) increasing current followed by (D) decreasing current.

behavior. This is due to the fact that the adsorbed monolayer of oxygen is still being formed. Once it has been formed, the curves become reproducible.

Hoare (41) points our that the anodic evolution of oxygen on platinum is activation (or charge transfer) controlled because a Tafel region is observed and because the overvoltage, η, decreases as the temperature increases, while the value of the Tafel slope remains the same.

An oxygen overvoltage curve shows the changes in the surface of the Pt electrode. Figure 7 below, is interpreted as follows (42).

In the region BC a limiting current is observed and is considered to be the potential range where the Pt-O film is being built up. Oxygen evolution begins at point C and the region DE has been interpreted to represent a conversion of Pt-O to PtO_2 (despite the previous arguments against an oxide theory). At point E, a stable Pt-O film has been formed and the subsequent EF region is the Tafel region. A slope of 0.14 is obtained and the exchange current density, i_o, is 8.5×10^{-9} A/cm^2 in good agreement with other results.

Although most workers believe that the rate determining step is an electron transfer, the mechanism of the oxidation of oxygen (i.e. evolution of oxygen) is still unknown Various factors which affect the evolution of oxygen have been studied to help determine the mechanism. Although these studies have not succeeded in pinning down a particular mechanism, they have been illuminating Some of the important aspects of these studies are presented below.

1. Effects of pH and Adsorbed Ions

It has been found (9) that on bright platinum, the overvoltage

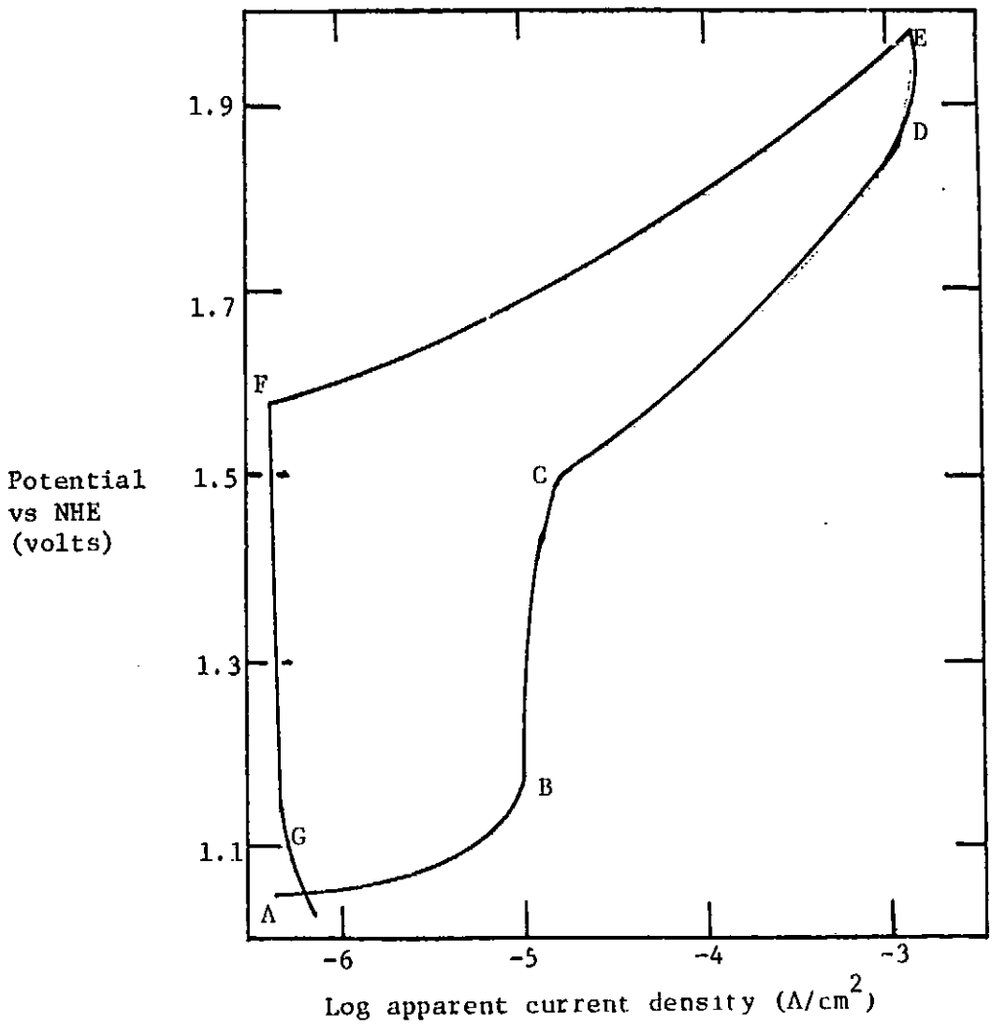

Figure 7. OXYGEN OVERVOLTAGE CURVES ON A BRIGHT Pt ANODE IN O_2- SATURATED 2N H_2SO_4.

decreases for the lower pH's but increases in very strong acid solutions. As acid strength increases, the effect is often clouded by the adsorption on ions and the presence of other reactions. In particular, high concentrations of H_2SO_4 (51) produce $H_2S_2O_8$ and H_2SO_5 and also cause an oxygen exchange with the water (29), whereas high concentrations of $HClO_4$ do not exhibit these problems. In both cases, the anions ($SO_4^=$ and ClO_4^-) are rapidly adsorbed and an abrupt shift in the overvoltage curve is noticed. An example of this is given in Figure 8 (54)

Frumkin (28) found using $HClO_4$ with tagged oxygen, O^{18}, that O^{18} did not exist in the lower Tafel region, but did exist in the upper region. This behavior led him to conclude that ClO_4^- ions are specifically adsorbed.

Two distinct Tafel regions separated by a limiting current region were also found by Beck and Moulton (5). By showing that the limiting current was identical on rotating and stationary electrodes, they concluded that the process was not diffusion controlled. They, too, concluded that the break was due to the specific adsorption of ClO_4^-. At high current densities other reactions were found to occur, namely

$$ClO_4^- \rightarrow ClO_2 + O_2 \qquad [46]$$

and

$$3\ ClO_4^- + H_3O^+ + e \rightarrow 3\ HClO_3 + 2O_2. \qquad [47]$$

Note that the effect of these reactions is to produce more oxygen than can be accounted for from the electrolysis of water.

The formation of ozone, O_3, is also common to the electrolysis of very high acid concentrations. Briner (12) has detected ozone in the

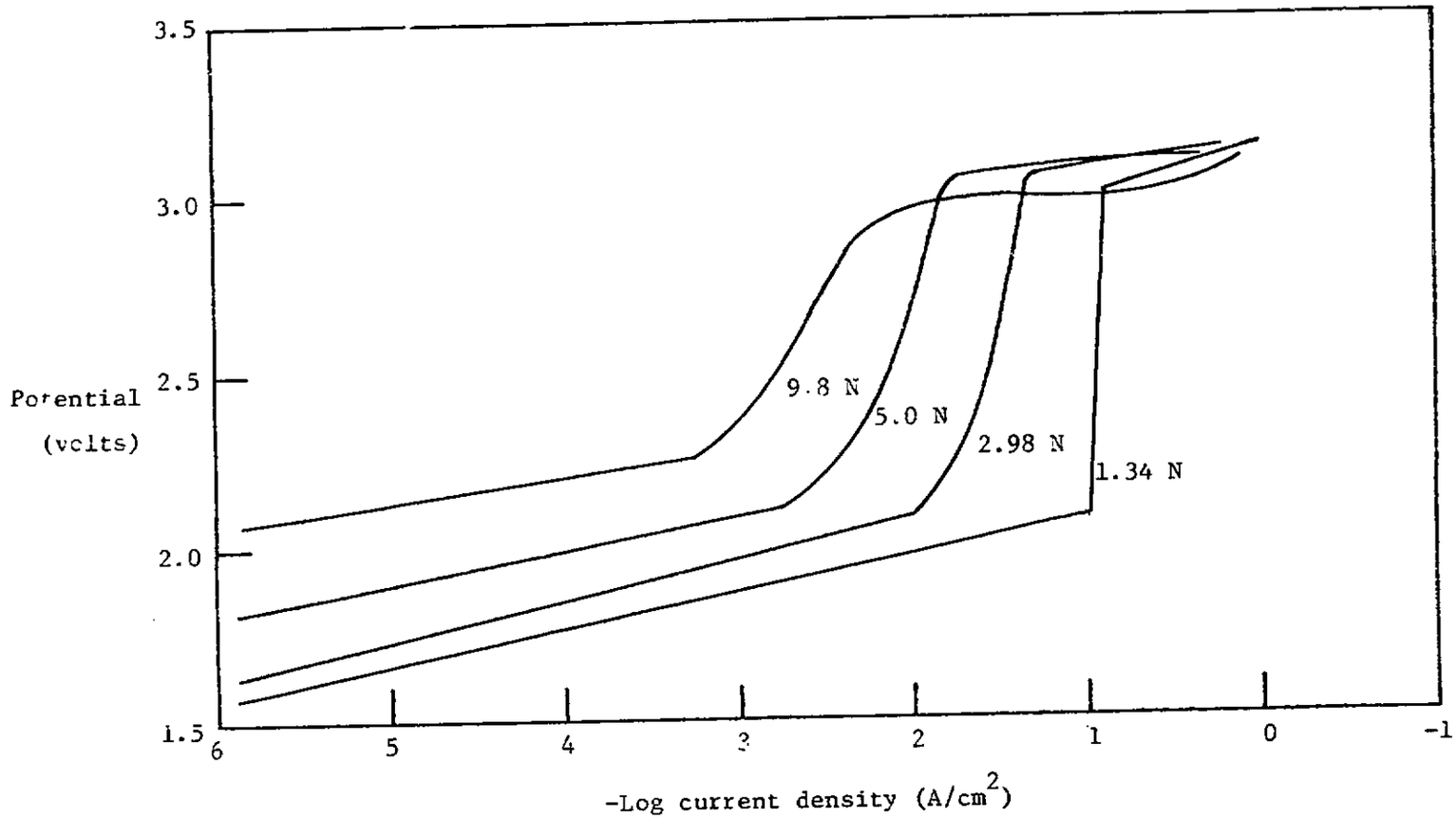

Figure 8. ANODIC POLARIZATION CURVES ON Pt IN SOLUTIONS OF $HClO_4$ OF VARIOUS CONCENTRATIONS.

electrolysis of concentrated solutions of H_3PO_4, KOH, H_2SO_4, and $HClO_4$.

Addition of reducing agents, e.g. $NaNO_2$ and Na_2S, have been found to increase the overvoltage (35); however, Bockris and Huq (9) found that the addition of Na_2SO_4 lowers η. All workers agree that the actual effect of adsorbed ions is difficult to interpret.

D. Cathodic Reduction of Oxygen.

Although the reaction under investigation by the research is the anodic oxidation of oxygen, the cathodic reduction is discussed here because it sheds light on the nagging problem of the presence of H_2O_2.

The generally accepted reaction mechanism consists of the following slow step:

$$(O_2)_{ads} + e \overset{slow}{\rightarrow} (O_2^-)_{ads} \qquad [48]$$

and the subsequent fast steps:

$$(O_2^-)_{ads} + H^+ = (HO_2)_{ads} \qquad [49]$$

$$(HO_2)_{ads} + e = (HO_2^-)_{ads} \qquad [50]$$

$$(HO_2^-)_{ads} + H^+ = (H_2O_2)_{ads} \qquad [51]$$

The formation of H_2O_2 is an important step of this mechanism. The main evidence for this theory is that the cathodic reduction is accompanied by the presence of the stable intermediate, H_2O_2. (This intermediate is never found, under proper control of impurities in the oxidation reaction.) The H_2O_2 is then decomposed at the electrode by

$$2(H_2O_2)_{ads} \overset{cat}{\rightarrow} 2H_2O + O_2 \qquad [52]$$

Typical η vs. log i curves yield a Tafel region in the current density range from 10^{-6} to 10^{-3} A/cm^2 with a slope approximately 0.1. The corresponding exchange current density, i_o, is about 10^{-9} A/cm^2 (86).

A plot of overvoltage versus log P_{O_2} shows change of η of 60 mv for a unit step in log P_{O_2}. This has been interpreted (46) to mean that the rate determining step is an electron transfer with O_2.

The presence of H_2O_2 has been found experimentally to depend on the magnitude of the current density (43). In particular, for i less than 10^{-4} A/cm^2, H_2O_2 does accumulate and reaches a steady state value around 10^{-6} to 10^{-5} M. The observations have been interpreted as being due to the relative ability of the platinum surface to decompose H_2O_2. The platinum surface changes with current densities having more bare sites at higher current densities, and having fewer bare sites at lower current densities. The presence of adsorbed oxygen inhibits the reduction of O_2 to H_2O but promotes the decomposition of H_2O_2 to O_2 (53). It is on the bare Pt surface that steady-state reduction occurs.

One other significant reaction scheme has been proposed, in which H_2O_2 is a side product rather than an intermediate (17). The experimental evidence for this is that H_2O_2 is not found present when impurities are removed from the system. Hoare (44) argues that, in the absence of impurities, the Pt surface can decompose the H_2O_2 as fast as it is formed; consequently H_2O_2 is not detected. Obviously the point of whether H_2O_2 is a side product or an intermediate is a critical one, and as yet, has not been unequivocably resolved.

Study of the nature of the electrode surface in contact with the O_2, has revealed that O_2 dissolved in the Pt surface enhances the reduction of O_2, but an adsorbed layer of oxygen inhibits the reduction of O_2 (47). On the other hand, an adsorbed layer enhances the decomposition of H_2O_2. This phenomenon of the adsorbed layer of O_2 innibiting the reduction of O_2 is exactly contrary to the oxidation

reaction. For the oxidation reaction potentials approaching the theoretical reversible potential have only been obtained in the presence of an adsorbed oxygen layer.

E. Anodic Evolution of O_2 in Sulfuric Acid.

There are many studies of oxygen evolution which have been carried out in sulfuric acid solutions. In fact, sulfuric acid is the most common solution to be used on oxygen electrode studies. However, almost all studies in sulfuric acid are limited to one or two concentrations of H_2SO_4 and these are concentrations less than 2N H_2SO_4.

There are three excellent reviews which do cover the spectrum of sulfuric acid concentrations. These reviews are discussed here separately.

1. "Dependence of Oxygen-Evolution Overvoltage on Smooth Platinum On the Sulfuric Acid Concentration" by V. L. Kheifets and I. Ya. Rivlin (51)

Several important observations are made in this paper. First, reproducible overvoltage curves are attainable only after prolonged preanodization. Initial experiments showed a continuous shift toward more positive potentials with successive experiments. Long interruptions also affected the reproducibility of the current voltage curves. Fig. 9 presents the results of their steady state overvoltage determinations.

Increasing the sulfuric acid concentration has the effect of shifting the overvoltage curve toward more positive potentials. This is expected because the activity of water decreases as the concentration of sulfuric acid increases. According to Equation 53 below,

$$\epsilon_o = E_o + \frac{2.3RT}{4F} \log \frac{a_{H^+}^4}{a_{H_2O}^2} \qquad [53]$$

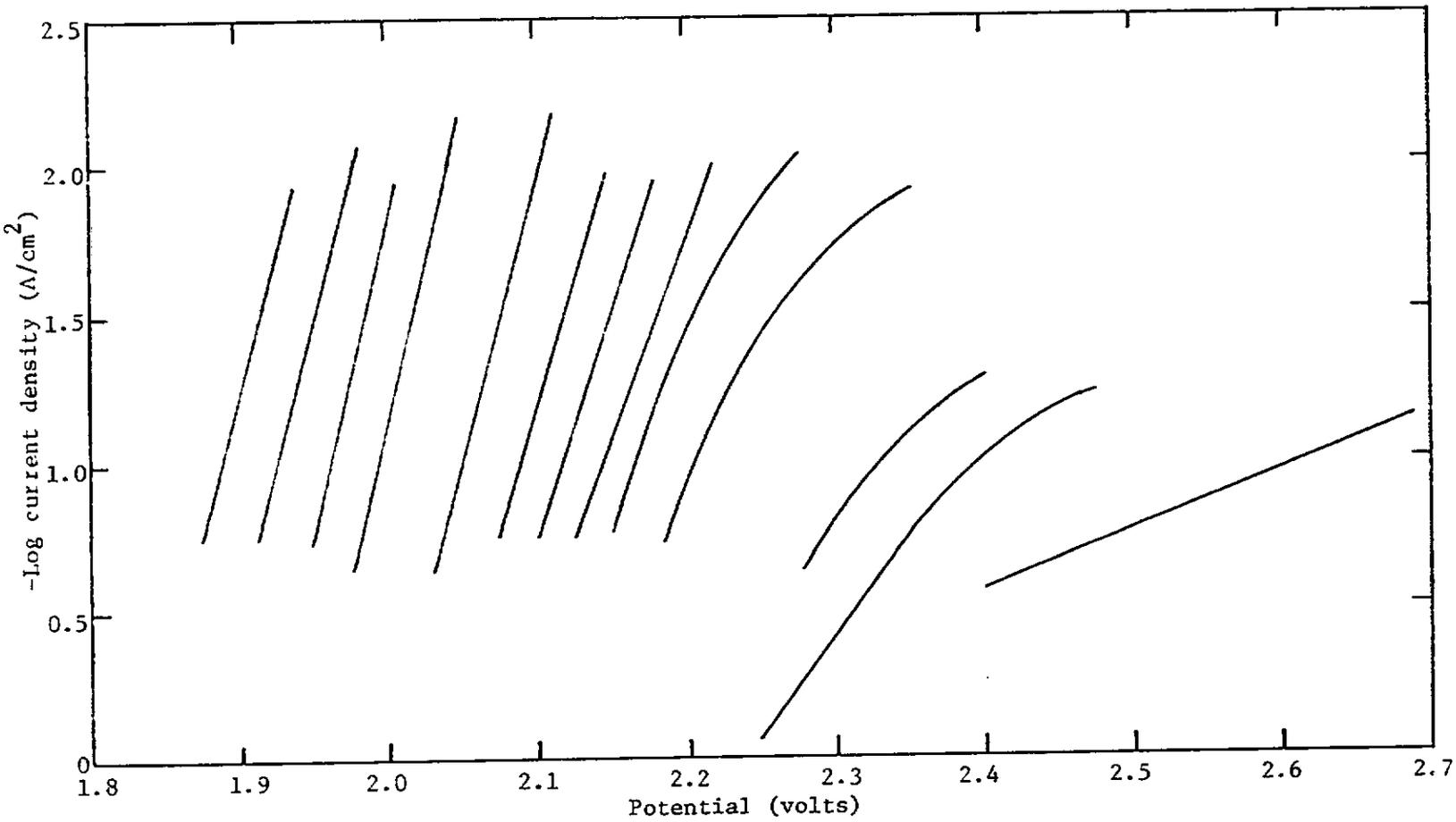

Figure 9. OXYGEN OVERVOLTAGE CURVES OF V.L. KHEIFETS AND I. YA. RIVLIN. SULFURIC ACID CONCENTRATIONS OF (l. to r.) 0.038M, 0.078M, 0.260M, 0.525M, 1.034M, 2.374M, 3.760M, 5.000M, 6.615M, 7.805M, 10,397M, 15.2M, 21.761M.

where ϵ_o is the particular equilibrium potential, E_o is the standard potential (1.23 V), a_{H+} is the activity of the hydrogen ion, and a_{H_2O} is the activity of water. The equilibrium potential increases as a_{H_2O} decreases. The observed shift in the overvoltage curves is much greater than that due simply to the shift in the equilibrium potential. Therefore, strong polarization must be occurring, i.e. there is a strong increase in the activation energy required to make the reaction occur.

Finally, Kheifets and Rivlin point out that at high concentrations of sulfuric acid (>6.6M), there is an inflection in the overvoltage curves. Two distinct slopes can be distinguished from these curves. While other authors attribute the inflection in these curves to a change in the reaction mechanism (50), Kheifets and Rivlin attribute this to a strengthening of the bond between the oxygen and the platinum. They also note that, at high concentrations, persulfuric acid is formed by

$$2\ HSO_4^- - 2e \rightarrow H_2S_2O_8. \qquad [54]$$

Table 2 gives the information describing their observations of the efficiency of O_2 production. The increased production of $H_2S_2O_8$ causes a decrease in the production of O_2, as one would expect from stoichiometric considerations.

2. "Electrolysis of Concentrated Sulfuric Acid Solutions Using Tagged Oxygen" by Kaganovich et.al. (50).

A break exists in the Tafel plots which yields two distinct Tafel lines of essentially the same slope (see Fig. 10). In contrast to the paper discussed above, Kaganovich et.al. suggest that the break corresponds to a change in mechanism, namely, that oxygen evolution at

Table 2

OXYGEN EVOLUTION EFFICIENCY

Current Density Measured by O_2 Evolution (mA/cm^2)	Current Density in $H_2S_2O_8$ Formation (mA/cm^2)	Anode Potential (V vs NHE)	O_2 Yield (%)
4.46	0.34	2.431	92.9
6.25	0.84	2.510	88.7
10.36	3.75	2.605	73.4
12.59	8.57	2.655	59.5
14.37	13.85	2.781	50.9
16.33	18.94	2.706	45.2
17.65	24.68	2.722	41.7

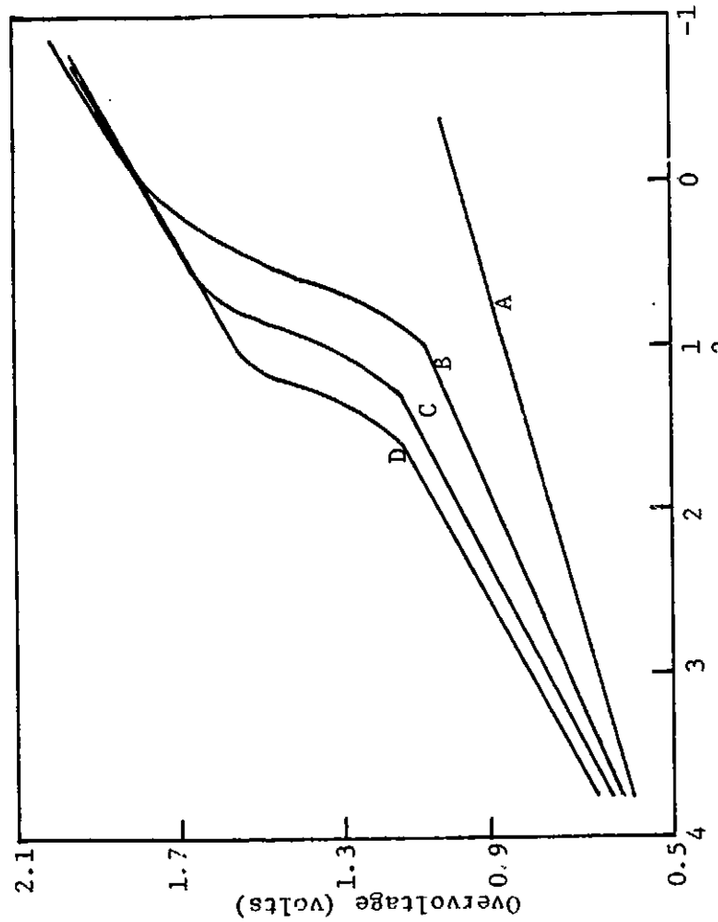

Figure 10. OXYGEN OVERVOLTAGE CURVES OF KAGANOVICH et.al.
(A) 1N, (B) 7N, (C) 10N, (D) 15N.

the higher current densities involves anions in some fashion. Analysis for tagged oxygen, O^{18}, supports this view. They conclude that tagged oxygen is found at increasing concentrations in the evolved gas in the break range and beyond. This is attributed to surface isotopic exchange which is possible because of strong anion adsorption at high overvoltages and high anion concentration.

Table 3 gives the constants characteristic of the electrochemical system which was used.

Kaganovich et.al. pretreated a smooth platinum electrode by repeated anodic and cathodic polarization. The anodic current density was kept less than 7×10^{-6} A/cm^2 before measurements. The current was changed continuously and the potential was measured two minutes after a current change.

3. "Investigation of the Kinetics of the Electro-oxidation of Sulfuric Acid" by E. A. Efimov and N. A. Izgaryshev (23).

This study of the electro-oxidation of sulfuric acid to persulfuric and monopersulfuric acid is the most thorough and highly regarded study of the polarization of high concentrations of sulfuric acid.

The basic reaction in question was:

$$2HSO_4^- - 2\,e = H_2S_2O_8 \text{ (persulfuric acis)} \qquad [55]$$

with the following side reactions:

$$2H_2O - 4e = 4H^+ + O_2 \qquad [56]$$

$$H_2S_2O_8 + H_2O = H_2SO_5 \text{ (monopersulfuric acid)} \qquad [57]$$

$$SO_5^= + H_2O - 2e = H_2SO_4 + O_2 \qquad [58]$$

$$H_2SO_5 + H_2O = H_2SO_4 + H_2O_2 \qquad [59]$$

$$H_2SO_5 + H_2O_2 = H_2SO_4 + H_2O + O_2 \qquad [60]$$

Table 3

CHARACTERISTIC CONSTANTS OF WATER VAPOR ELECTROLYSIS

Concentration	i_o (A/cm^2)	α
1N H_2SO_4	3×10^{-9}	0.39
7N H_2SO_4	1×10^{-7}	0.32
10N H_2SO_4	2×10^{-7}	0.29
15N N_2SO_4	2×10^{-7}	0.28

$$HO_2^- - 2\epsilon = H^+ + O_2 \qquad [61]$$

$$H_2S_2O_8 + H_2O = 2H_2SO_4 + 1/2\ O_2 \ . \qquad [62]$$

Efimov and Izgaryshev found that reactions 57 - 62 were unimportant. However, the existence of $H_2S_2O_8$ and $H_2S_2O_5$ was found to be characteristic of the variables of the electrochemical system.

Their polarization data are presented in Figure 11. These data were obtained on smooth platinum in sulfuric acid concentrations from 5.0 to 36.0 N. The anode was a platinum wire, 0.3mm diameter. Analysis for $H_2S_2O_5$ was made in the current density range of 4.2×10^{-3} to 2.0 A/cm^2, as $H_2S_2O_8$ and H_2SO_5 were not detected below $i = 4.2 \times 10^{-3}$ A/cm^2. The electrode was preanodized for 30 minutes at $i = 2.1 \times 10^{-3}$ A/cm^2. Three minutes after a particular current density was established, the anode potential was measured. At each sulfuric acid concentration, 3 to 6 plots were made, and average values were taken. The repoducibility of the potentials was 5 to 20 mV. This is reasonably good repoducibility and it might have been improved by extending the preanodization time.

Efimov and Izgaryshev made several significant observations and conclusions:

1. The current efficiency for the production of $H_2S_2O_8$ passes through an optimum. These optima lie in the H_2SO_4 concentration range of approximately 15 - 27 N H_2SO_4. Lower concentrations require higher potentials to produce $H_2S_2O_8$.
2. The optimum production of $H_2S_2O_5$ is independent of current density (hence potential) and depends only on H_2SO_4 concentration and occurs at approximately 25 N H_2SO_4.

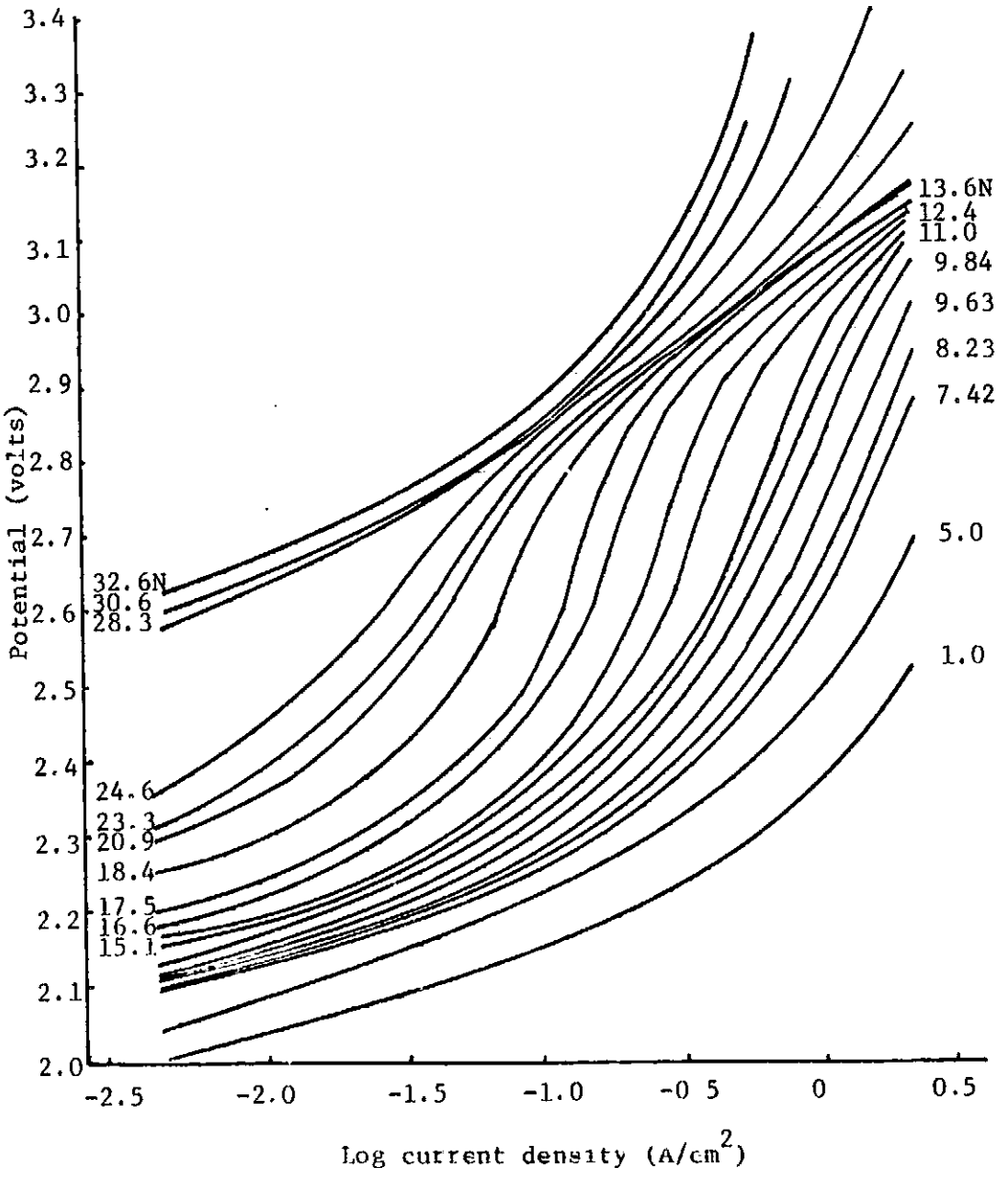

Figure 11. OVERVOLTAGE CURVES OF E. A. EFIMOV AND N A IZGARYSHEV. VARIOUS CONCENTRATIONS OF H_2SO_4 AT BRIGHT Pt ANODE.

This can be expected because Equation 57 is a chemical (not an electrochemical) process.

3. Tafel behavior for the production of oxygen is observed until i = 10^{-3} to 10^{-2} A/cm^2. At this point the curves bend toward higher potentials, after which time another inflection is reached and the curves bend back.
4. Efimov and Izgaryshev agree with the explanation of Kaganovich e.al. (50) that the upward bend results from a change in the mechanism of oxygen evolution. They disagree with Kheifets and Rivlin (51) that the break is caused by the production of $H_2S_2O_8$ (which Efimov and Izgaryshev had also believed earlier (48)).
5. The second bend is attributed to the depolarizing effect of the decompostion of SO_5^{-2}. Although mixing the solution before the second inflection produced no change in potential, mixing above this point increased the potential 20-30 mV. This effect results from the excess accumulation of $S_2O_5^-$ near the electrode. As the S_2O_5 is dispersed, the potential increases.
6. In extremely concentrated H_2SO_4 solutions, there was a physical hindrance to any increase in current (e.g. 35.9 N at 0.3A/cm^2). This occurred because of obstruction by oxygen bubbles. The surface of the anode was covered by these bubbles which could only be removed by the application of a tremendous overvoltage (approx. 18.5 V). This obstruction phenomenon occurred at 3.4 to 3.5 V.
7. The most rapid change in current with potential occurs in the middle concentration range, 5N to 20N

F. Water Vapor Electrolysis on Platinum Electrodes with an Acid Gel Electrolyte.

Previous studies of water vapor electrolysis on platinum electrodes with acid gel electrolyte have produced contradictory conclusions regarding the characteristics of the electrode processes. Three studies address themselves to the problem above. These are by Connor et.al. (14), Clifford et.al. (13), and Bloom (8). These studies are discussed separately below.

1. "Design and Development of a Water Vapor Electrolysis Unit" by W. J. Conner et.al. (14).

Conner's report give experimental information on cell operation with liquid electrolyte and with an acid impregnated gel electrolyte matrix.

Polarization data taken in the liquid electrolyte are presented in Figure 12. A normal hydrogen electrode with 6.1 M H_2SO_4 was the reference cell. There are several questionable aspects of the reliability of these data. First of all, Connor notes a hysteresis in the anodic and cathodic sweeps and a difference in polarization values when the system is left idle. These are typical "symptoms" of the aforementioned irreproducibility of oxygen electrode overvoltage data. It is apparent that Connor did not sufficiently preanodize the system so as to insure a complete electronically conducting layer of oxygen on the electrode surface. Moreover, oxygen may have been continually absorbed into the massive Pt during his measurements and never have reached saturation.

Secondly, Connor notes that the solutions of the various electrode systems were of approximately the same concentration. Previous

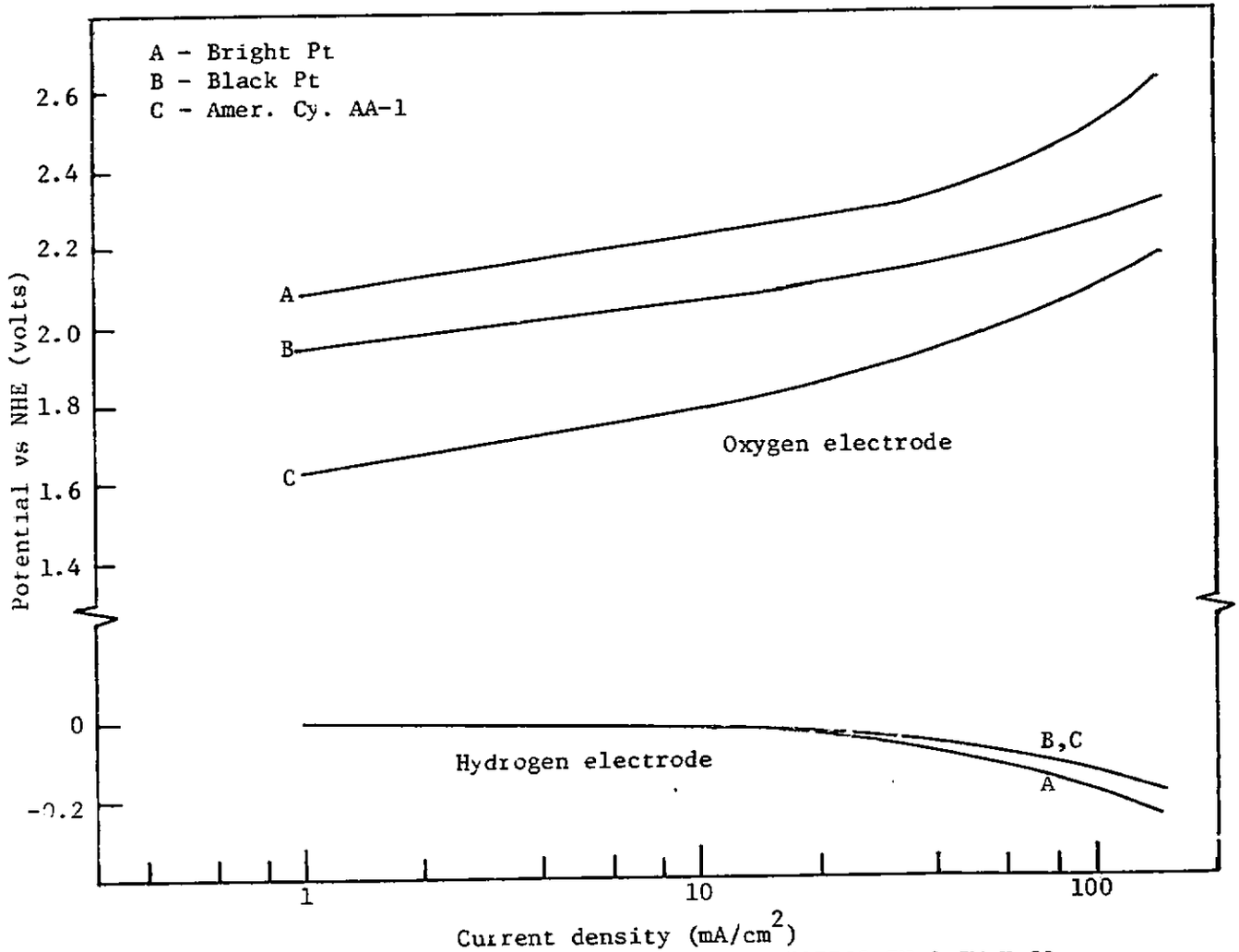

Figure 12. ELECTRODE POLARIZATION CHARACTERISTICS IN 9.5M H_2SO_4.

figures have shown that overvoltage data depend strongly on the electrolyte concentration, especially at high concentrations and high current densities.

Finally, although, correction was made for the ohmic, or IR loss, no calculations are given or data presented to assure that this was done properly. The net polarization is thus attributed to activation overvoltage and IR losses. In light of the above factors, the reliability of Connor's overvoltage data is suspect.

Connor investigated the performance of the water vapor electrolysis cell using an immobilized silica gel electrolyte matrix. The gel consisted of 10 wt % fine silica[1] and 90 wt % 8.1 M H_2SO_4. Initial cell operating conditions were 1.96 V and 35 mA/cm^2. After six hours, operation was at 2.06 V and 35 mA/cm^2; the voltage requirement had increased to maintain a current density of 35 mA/cm^2. The electrode material used in these experiments was not specified by Connor; hence, comparison with data for operation with liquid electrolyte is not possible.

Conner states that failure of the gel matrix cell occurred because of severe cross-leakage. This cross-leakage resulted from localized drying and cracking of the matrix. Apparently, the matrix was so immobilizing that water could not creep from wetter areas to drier areas.

Finally, separate tests on the silica gel gave a mixture-to-liquid conductivity ratio of 67% (specific resistance = 4.4 ohm-cm). The gel resistance was measured by a 1000 cps impedance bridge Connor

[1]Cab-o-sil, Cabot Corporation, Boston, Massachusetts.

reported an initial specific resistance of 11.5 ohm-cm for the gel during the cell operations.

2. "A Water-Vapor Electrolysis Cell with Phosphoric Acid Electrolyte" by Clifford et.al., (13).

Clifford et.al. also performed experimental work on both the liquid electrolyte system and the acid gel system. The bulk of their experiments were performed on phosphoric acid systems. Clifford's group analyzed the electrode overvoltage in terms of its components in order to determine the dominant sources of overvoltage.

A current-interruption technique (77) was used whereby voltage-time curves were obtained. The variations in the slopes of the curves determined the magnitude of the various components of the cell over-voltage.

The working electrode was a platinized platinum sheet and overvoltage data were recorded versus an autogeneous hydrogen electrode. No mention was made of correction for the liquid-liquid potential between the reference electrode and the test solution. This could introduce serious error. The current-interruption technique yielded values of ohmic losses which agreed well with calculated values using a specific conductivity of 0.105 ohm^{-1}-cm^{-1} for 83% H_3PO_4

A component overvoltage analysis is given in Table 4 for both the free-liquid and liquid-matrix cells. Clearly, the most interesting aspect of Table 4 is the magnitude of anodic concentration polarization: 1.09 to 1.18 V. All previous indications would point to no concentration overvoltage at all or very little at most; nevertheless, Clifford et al have interpreted their data to say that the major component of the over-voltage is concentration overvoltage. A simple experiment of changing

Table 4

VOLTAGE ANALYSES FOR FREE LIQUID AND LIQUID/MATRIX CELLS

Item	Liquid/Matrix Cell		Free-Liquid Cell	
	Individual-Electrode Cell Analysis	Total-Cell Analysis	Individual-Electrode Cell Analysis	Total-Cell Analysis
Average Current Density, amp/sq. ft.	33	33	33	33
Total Cell Voltage, volts	3.41	3.42	3.14	3.18
Potential Anode Versus Autogenous Hydrogen Electrode, volts	2.90	-	2.83	-
Potential Cathode Versus Autogeneous Hydrogen Electrode, volt	0.51	-	0.30	-
E_r, Theoretical Cell-Decomposition Voltage, volts	1.23	1.23	1.23	1.23
E_{aa}, Anode-Activation Polarization, volt	0.04	-	0.05	-
E_{ac}, Anode-Concentration Polarization, volt	1.09	-	1.18	-
E_{ca}, Cathode-Activation Polarization, volt	0.00	-	0.00	-
E_{cc}, Cathode-Concentration Polarization, volt	0.07	-	0.06	-
E_{IR}, Total-Cell Ohmic Polarization, volt[c]	0.95	0.95	0.67	0.67
E_{ta}, Total-Cell Activation Polarization, volt	$E_{aa} + E_{ca}$ 0.04	0.05	$E_{aa} + E_{ca}$ 0.05	0.04

Table 4 (Concluded)

Item	Liquid/Matrix Cell		Free-Liquid Cell	
	Individual-Electrode Cell Analysis	Total-Cell Analysis	Individual-Electrode Cell Analysis	Total-Cell Analysis
E_{rc}, Total-Cell Concentration Polarization, volt	$E_{ac} + E_{cc}$ 1.16	1.18	$E_{ac} + E_{cc}$ 1.25	1.25

(a) See text of report for cell details and operating conditions.

(b) Slight changes of about ± 0.03 v in cell voltage occurred during the course of making the voltage-analysis runs; these changes were not large enough to affect the overall cell analysis significanly.

(c) The E_{IR} polarization values are characteristic of the geometry of the experimental cells used.

the rate of stirring would have told them straightaway if their analysis was correct. Moreover, the value of concentration overvoltage was higher in the free-liquid cell than in the immobilized liquid-matrix cell! This means that it is easier for the water to diffuse to the electrode surface in the gel than in the free liquid. This seems extremely unlikely.

The above discussion pertained to a phosphoric acid electrolyte; Clifford et.al. arrived at identical conclusions for overvoltage data on a free-liquid sulfuric acid electrolyte (50 and 77 wt. % concentrations).

During extended operational testing of the water vapor electrolysis cell, current-voltage data were recorded. Since the cell had been operating for more than 1000 hours, it can be safely assumed that the cell was more than sufficiently pre-anodized. Therefore, the data can safely be considered to be repoducible. These data are presented in Fig. 13, with Clifford's component overvoltage breakdown. The IR loss was not calculated. Instead, a value for specific resistance was selected by which the straight dotted line could be obtained.

Note that despite the existence of a straight dotted line, Clifford still analyzed the overvoltage components as being almost entirely concentration overvoltage (1.05 V) and practically no activation overvoltage (.04V). In other words, a Tafel plot is obtained clearly indicating a charge transfer controlled system, yet Clifford interprets this as mass transfer control. Furthermore, no limiting current has been reached. Clearly, the analysis of Clifford et.al must be incorrect.

Finally, this author (not Clifford) calculated an exchange current density, i_o, of 1.1×10^{-7} A/cm^2 from an extrapolation of the straight dotted line of Fig. 13. This value of i_o is in good agreement

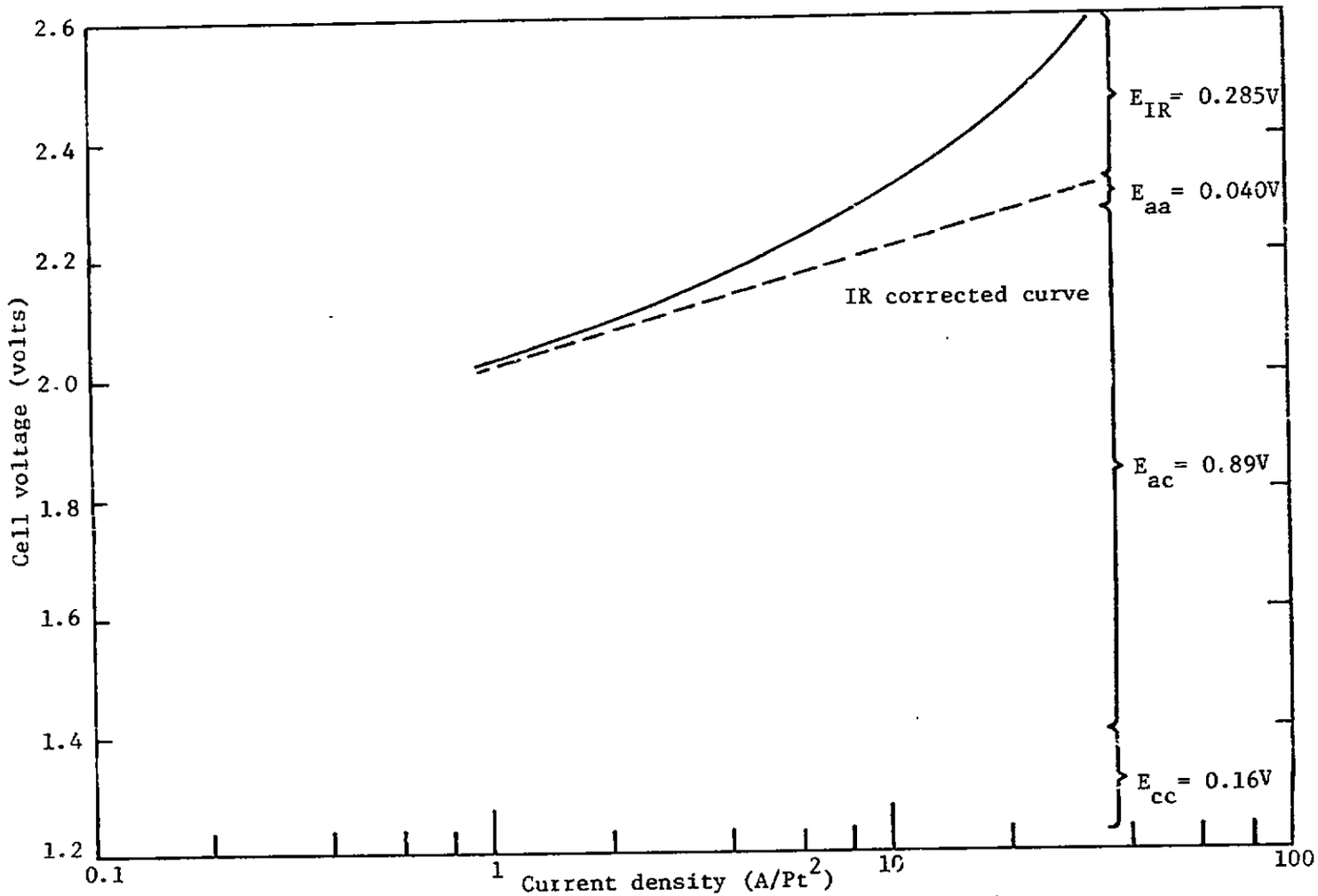

Figure 13. CURRENT-VOLTAGE BEHAVIOR IN PHOSPHORIC ACID.

with the data of Kaganovich. Similarly, the semi-log slope of b = 0.196 (α = 0.40) is in reasonably good agreement with other oxygen electrode Tafel slopes. Both of these findings support an activation controlled electrode process.

3. "Cycled Operation of a Water Vapor Electrolysis Cell" by A. M. Bloom (8).

Bloom's investigation dealt mainly with cycled operation of the water vapor electrolysis cell, i.e. turning the cell on and off. He also treated theoretically the topic of concentration polarization. The experimental work of Bloom is presented below.

All experimental results were performed on bright platinum screen electrodes and platinum-tantulum screen electrodes in a sulfuric acid sicila gel electrolyte. Water was constantly added to the system via a humid air stream passing over the silica gel. The gel consisted of 10% by weight fine silica and 90% by weight 8.1 m H_2SO_4. Gas cross-leakage between the anode and cathode was prevented by a microporous PVC membrane[1] inserted in the electrolyte. Steady state operation was carried out at 2.60 V and .92 amps for the bright platinum and 2.20 V and 1.00 amps for the platinum-tantulum. Voltage measurements were only good to within ± 50 mV. Current efficiency was determined from the rate of hydrogen collection. Bloom made the following observations and conclusions:

1. The Pt-Ta electrodes were unsuitable for long operation because of deterioration of the electrode.
2. Bright platinum electrodes have a considerably higher

[1]Synpor, Electic Storage Battery, Yarldley, Pa.

overvoltage (approx. 0.3 to 0.4 V) than the platinum-tantulum.

3. Proper cyclic operation was found to decrease specific power consumption.
4. Both "on" and "off" times were found to have optimal values, i. e. 5 minutes "on" and 5 seconds "off" for the bright platinum electrode. This caused a 12.9% decrease in specific power consumption (see Table 5).
5. "Off" times were followed by a current surge (sometimes greater than 5 amps) at the beginning of the "on" times.
6. Spurts of excess water into the system caused a sudden rise in cell current which required considerable time (e.g. two hours) to dissipate.
7. Doubling the humid air supply flow rate (from 25 to 50 cc/sec) caused a decrease in specific power consumption (from 12.7 to 17.6%).
8. Specific power consumption increased as "on" time goes toward zero. This results from the reduction (or "fuel cell") reaction which occurs while an adsorbed layer of oxygen (and hydrogen) is still present on the electrode. This layer is gradually stripped as the cell is "off" or grounded.
9. Pt-Ta and bright platinum electrodes exhibited opposite tendencies in specific power consumption characteristics near zero "off" time. This was attributed to differences in specific surface area of the two electrodes.
10. Current efficiency measurements assured that the elec-

Table 5

CYCLIC OPERATION POWER CONSUMPTION DATA

Cells No. 3 through 8, BRITE Anodes, E = 2.60 V

Cell No.	ON[1] (min)	OFF[2] (sec)	N[3]	$Work_M$[4] (watt-sec)	Error[5]	Coll[6] Eff	$Work_T$[7] (watt-sec)	%[8] IMP
3	3	1.5	10	1242	14	0.95	1175	-4.9
	4		19	1104	11		1044	6.8
	5		8	1075	8		1017	9.2
	6		12	1107	19		1047	6.5
	7		8	1162	12		1099	1.8
4	2	5	6	1034	4	0.99	1025	8.5
	3		6	1023	2		1013	9.6
	4		7	1005	3		996	11.1
	5		14	988	4		979	12.7
	6		10	1004	1		995	11.2
	7		4	1013	3		1004	10.4
5	5	0.5	11	1054	8	0.98	1036	7.5
		3	9	1013	4		996	11.1
6		10	4	1140	2	0.97	1106	1.3
6	3	7	4	1076	10	0.97	1049	6.3
7	3		12	1064	5	1.00	1064	5.0
6	5		3	1026	6	1.00	1026	8.4
6	7		6	1050	4	0.97	1023	8 7
7	7		12	1021	5	1.00	1021	8.8
7	9		6	1032	13		1032	7.9
8	5	5	5	976	2	1.00	976	12 9

Table 5 (Concluded)

[1]"ON" cycle time.

[2]"OFF" cycle time.

[3]Number of measurements.

[4]Ave. measured electrical work to produce 50 standard cc H_2.

[5]Estimate of maximum error in measurement to 95 percent confidence, assuming data follow t-distribution.

[6]Hydrogen collection system efficiency

[7]Average electrical work corrected for H_2 collection efficiency.

[8]Percent improvement in power consumption efficiency, related to steady state power consumption of 1120 watt-sec for production of 50 standard $cm^3 H_2$ at 2.60 V.

trolysis of water was the only reaction occurring.

The previous studies of Kaganovich et.al. (50) and Efimov and Izgaryshev (23) give sufficient evidence to doubt the reliability of point 10. If $H_2S_2O_8$ and $H_2S_2O_5$ are produced in Bloom's electrochemical cell the proper amount (i.e.~ 100%) of hydrogen will still be produced, but less oxygen will be evolved as O_2.

Bloom, himself, admits that his conclusion of point 9 is very tenuous. He cites "incomplete data" and a decomposing electrode surface as the prime sources for his skepticism. In the final conclusions of his report he is only willing to state that "incomplete data showed measured efficiency increases of up to ten percent" and that "it is believed that cyclic operation efficiency improvement will be observed with any electrode displaying oxygen overvoltage." Bloom is unwilling to make specific statements about the nature of this improvement in his final presentation of results, although he has made such tenuous claims in the body of his discussions. Similarly, point 7, the effect of air flow rate, is questionable. Only six measurements were taken to make this startling conclusion. No further investigation of this matter was undertaken by Bloom. Furthermore, evaluation of the significance of the air flow effect is the comparison of increases in efficiency Bloom cites a 17.6% increase in efficiency due to a doubling of air flow rate as compared to a 12.7% increase due to normal air flow rate (and optimum cycling parameters). The tendency here is to compare 17.6% to 12.7% and cite a 40% improvement due to doubling air flow rate, by the ratio of 17.6 to 12.7. This is a tempting, but incorrect, approach. The actual improvement is the ratio of 117.6% to 112.7% or a 4.3%. A 4.3% improvement due a doubling of air flow rate is not as startling as a

40% improvement. As for the reason for this improvement, Bloom states that what "caused the efficiency increase is not understood." He then states that the "increased supply of feed water, causing electrolyte dilution, was apparently the reason for the performance increase with increased feed air flow rate." In light of investigations presented above and given the finite amount of electrolyte in Bloom's cell, it is probably true that any increase in cell current improvement from increased air flow resulted from electrolyte dilution and larger currents in general. This ties in well with point 6, i.e. that increased currents were observed with attendant spurts of water into the system. This is still more credible when one is considering a 4% improvement and not a 40% improvement. Further discussion of this point is given later in this thesis.

Bloom offers no explanation for 3, 5 and 6. He does point out that IR loss is decreased as water is adsorbed because the resistance of the gel decreases with increasing water content. However, it hardly seems likely that the small change which occurs in the IR loss in 5 seconds could cause a 12.9% decrease in specific power consumption over 5 minutes (300 seconds). Engel (24) has hypothesized some sort of "electrode regeneration" and Bloom has simply stated he does not know what causes improved behavior of the electrolysis cell with cyclic operation.

Finally, Bloom's theoretical investigation of concentration overvoltage leads to the conclusion that concentration overvoltage is negligible. This is in direct conflict with the experimental analysis of Clifford et.al. (13).

The critical equations in Bloom's analysis are given below:

$$E_c = - \frac{RT}{nF} \ln (1.0 - i/i_L) \qquad [63]$$

and

$$i_L = nFDC_b/\delta. \qquad]64]$$

Where E_c is the concentration overvoltage, i_L is the limiting current density, D is the diffusivity of the electroactive species in the electrolyte, C_b is the concentration of the electroactive species in the bulk solution, and δ is the thickness of the Nernst diffusion layer (see "Theory" section). In particular Bloom investigated the diffusion of H^+ ions to the cathode surface to form H_2. The calculated value for E_c is 0.0002 V, i.e. negligible concentration overvoltage. The following values were used for the variables:

$$T = 25°C$$

$$\delta = .005 \text{ cm}$$

$$D = 2.7 \times 10^{-5} \text{ cm}^2/\text{sec}$$

$$i = 0.1 \text{ A/cm}^2$$

These values yield $i_L = 24 \text{ A/cm}^2$ and consequently i/i_L is very small and E_c is very small. The value of the diffusivity which Bloom used was that of H^+ in 60 wt % H_2SO_4. It is not unreasonable to expect that the value of the diffusivity of H^+ in an immobilizing silica gel matrix could be <u>considerably less</u> than $2.7 \times 10^{-5} \text{ cm}^2/\text{sec}$. Moreover, for the evolution of O_2, the electroactive species is H_2O (a much larger species than H^+). It is difficult to guess at the real value of D_{H_2O} or D_{H^+} in a silica gel matrix, but it could be orders of magnitude smaller than in the free-electrolyte solution. In that case, i_L would be much smaller, hence i/i_L would be larger and E_c would be larger. Whether or not E_c would be larger enough to be signifiicant (e.g. 50 mv), is difficult to say.

VI. EXPERIMENTAL APPARATUS AND PROCEDURE

The basic scheme of the experimental work of this thesis was to produce current-voltage data for the water vapor electrolysis system which Bloom (8) studied. The experiments themselves were designed to provide accurate measurements of cell current and anode potential on a continuous basis. The analysis of such data provided the information necessary to solve the problems set forth at the beginning of this work. For example, an exponential dependence of cell current on anode potential indicates that the anode overvoltage is electron transfer controlled.

It was impossible to use Bloom's total experimental system for this purpose because of the new requirement of a reference electrode. A reference electrode must have an electrolytic connection with the working electrode, in this case the oxygen electrode (anode). In Bloom's system the electrochemical cell was enclosed in a tight, compact unit. There was no way to place a reference electrode inside this unit or to make an electrolytic connection, e.g. a salt bridge, with it.

The new system which was developed not only had a reference electrode but also had more sophisticated electronic monitoring equipment than Bloom used. The new system also had an essentially infinite supply of electrolyte as compared to the finite supply of Bloom's system.

The experimental apparatus and experimental procedure are detailed below.

A. Apparatus.

The experimental apparatus was designed to duplicate that of Bloom (8) wherever possible. The reason for this was that it made comparison of the present results with those of Bloom more meaningful.

There are three basic systems of apparatus which make up the total experimental assembly. These are the controlled humid-air supply system, the electrochemical cell, and the controlling and monitoring electronic equipment. Each of these systems is described separately below.

1. Controlled Humid-Air Supply System.

This is the same system as that used by Bloom (8). The feed air stream was monitored as to its temperature, humidity, and flow rate.

Since it was known beforehand that temperature has a negligible effect on the cell reaction, no great care was taken to control the feed air temperature. It was allowed to be at room temperature. Experiments were performed during the late summer and the room temperature ranged from 75° F to 85° F. The temperature was measured on a precision potentiometric-output hygrometer[1] to ±1° F accuracy.

The humidity of the feed air stream was measured by the same hygrometer. Control of the humidity was maintained by the apparatus shown schematically in Figure 14. Dried compressed air passed through two-stage pressure reduction and regulation and entered the humidification section. The air stream was then split, part to be passed through a second container filled with calcium chloride particles. The humidified and dry air streams were then recombined, forming a mixture whose relative humidity depended upon the proportion of the total stream which passed through each container. Control of humidity and flow rate was effected by the two-stage pressure regulator and needle valves in each stream of the humidification system. The humidity was maintained at 50%

[1]Model 15-3001, Hygrodynamics Inc., Silver Spring, Maryland

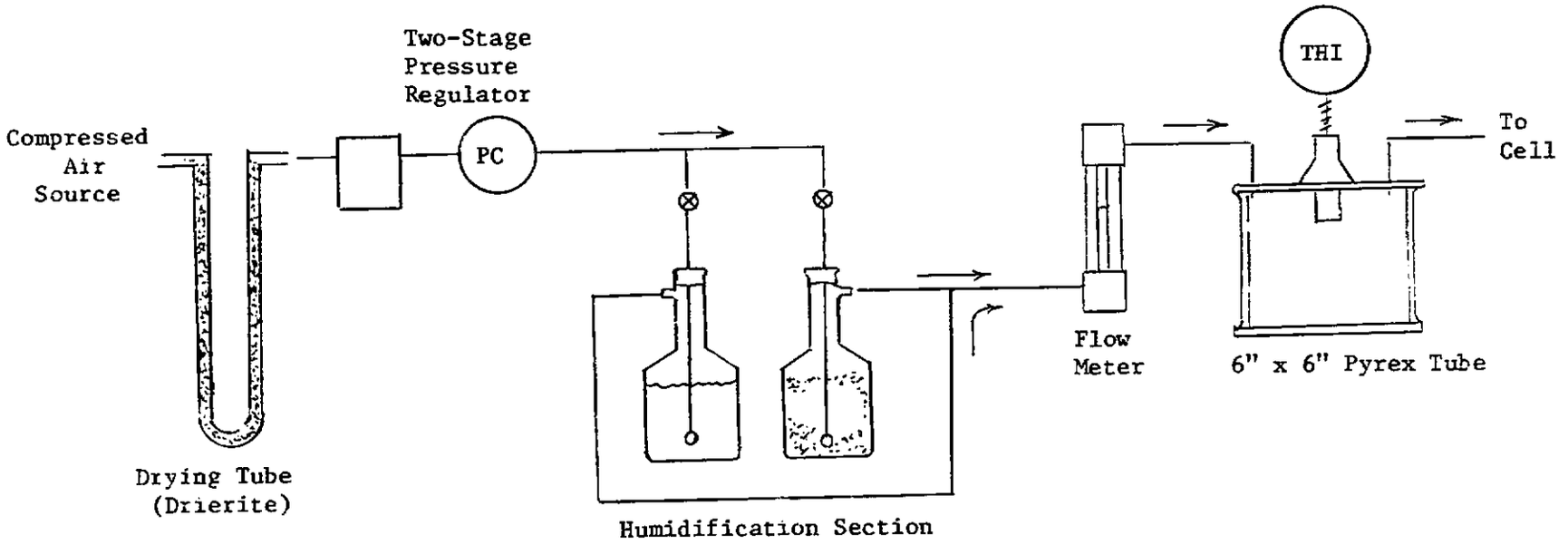

Figure 14. CONSTANT FLOW/HUMIDITY AIR SUPPLY

relative humidity $\pm$ 1%. Within the operating temperature range of the experiments, the relative humidity was very insensitive to temperature changes. Bloom (8) noted the occurrence of slugs of water in the air supply system. This caused a simultaneous increase in cell current. Although Bloom noted the increase in current, he failed to state that it was due to the decrease in sulfuric acid concentration. This had the attendant effect of decreasing the anode overvoltage, as Efimov and Izgaryshev (48) have shown conclusively. No slugs of water in the air feed stream occurred during the experimental stages of this work.

Air flow rate was measured with a rotameter and was held constant at 24 cc/sec. at room temperature and atmospheric pressure. Variation in air flow rate was $\pm$ 1 cc/sec. This small variation had a negligible effect on the experimental data.

Finally, no measurements were taken on the pressure of the entering or ambient air streams. As with temperature, it was known beforehand that minor variations in pressure (in this case pressure of O_2) had no measurable effect on the experimental data.

2. Electrochemical Cell.

The electrochemical cell consisted of a PVC compartment to which a platinum screen was secured. Silica gel, impregnated with sulfuric acid, was spread on the platinum screen. A microporous PVC membrane covered the silica gel and screen. The entire sandwich of platinum screen, silica gel, and membrane was secured in the PVC anode compartment by a PVC block clamped tightly to the PVC anode compartment. Figure 15 and 16 show the unassembled and assembled units respectively. The entire unit was submerged in sulfuric acid. A mercury-mercurous sulfate reference electrode (+0.61 V vs NHE) was attached to the anode

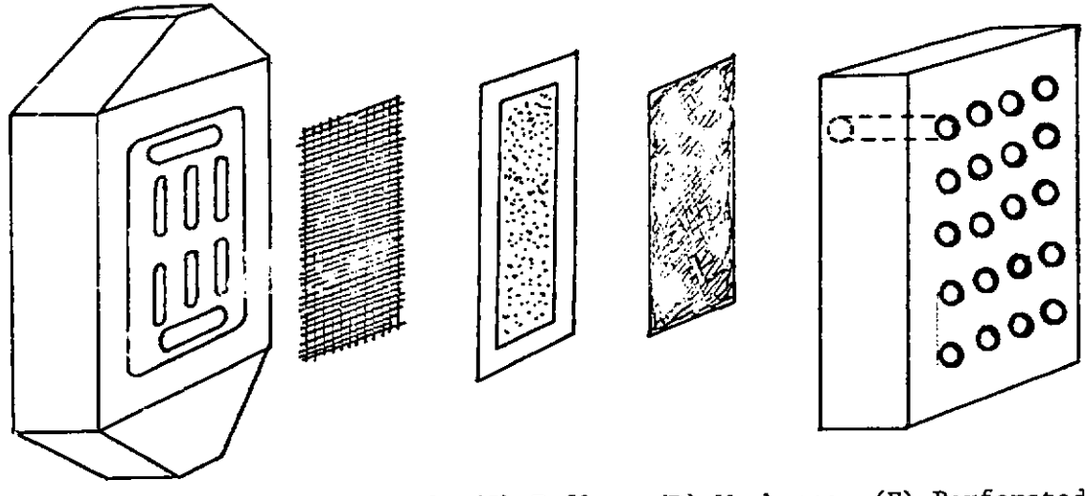

Figure 15. DISASSEMBLED WATER-VAPOR ELECTROLYSIS CELL.

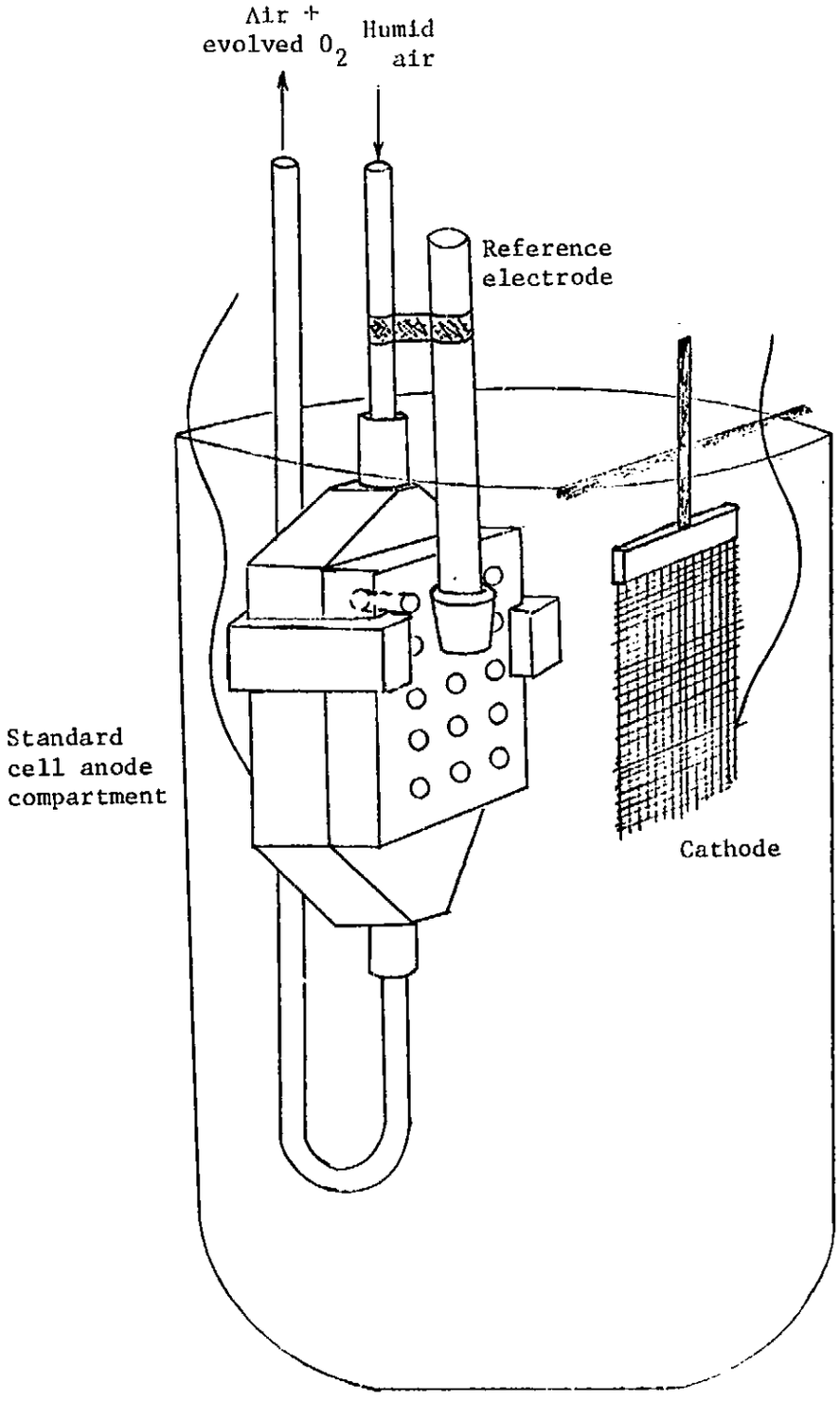

Figure 16. STANDARD CELL, REFERENCE ELECTRODE, AND CATHODE ASSEMBLY.

assembly. Another platinum screen, suspended at a variable distance from the anode, acted as the cathode.

The anode compartment was a machined block of PVC which not only served to hold the cell anode, but also provided passage for the humid air supply. Air entered through the top of the air manifold (anode compartment) and flowed over the anode screen and silica gel before passing out through the bottom of the air manifold and out a long stainless steel tube. The air manifold section was 4.75 cm square by 0.159 cm deep. Small supports protruded from the wall of the air manifold. These supports kept the anode screen at a fixed distance from the compartment wall. Two small holes were provided in the compartment wall so that wire leads could be drawn from the screen to the outside of the cell assembly.[1] These small holes were sealed by clear silicone rubber.

The anode was a 4-inch by 4-inch 45-mesh bright platinum screen.[2] The leads from this screen were also platinum wire. The cathode screen was gray platinum as supplied by NASA. Its dimensions and type were not investigated, as they were irrelevant to the experimental data.

The silica gel consisted of 90% by weight of 8 1 M H_2SO_4 and the remaining 10% dry fine silica.[3]

The silica was preheated to 100° F for a minimum of two days prior to mixing with H_2SO_4. This ensured a true dry weight of silica.

[1]The original supply of the cell compartments was obtained from NASA. However, these were made of methyl methacrylate. The PVC replicas were made by Microtol Corporation, State College, Pennsylavnia.

[2]Englehard Industries, 700 Blair Road, Carteret, New Jersey.

[3]Cabot Corporation, Boston, Massachusetts.

(Bloom (8) pointed out the significant effects of adsorbed water on the silica.) The silica gel was applied to the surface of the platinum anode screen with a stainless steel spatula. The gel was "pushed" through the pores in the screen and the screen was entirely covered by the gel. The thickness of the gel was of the order of one millimeter. A teflon gasket was placed over the edges of the screen and made water-tight with an O-ring situated in the PVC compartment.

The microporous membrane was stored in 8.1 M H_2SO_4 for a minimum of two weeks to use in the cell. This ensured saturation of the membrane by the electrolyte. The purpose of the membrane was to prevent O_2 and H_2 gas from cross-leaking within the cell. It is assumed that the membrane added no additional resistance to the electrochemical cell, as it was saturated with electrolyte.

Since the entire system operated immersed in 8.1 M H_2SO_4, great care was exercised in choosing the materials which made up the entire electrochemical cell assembly. Consequently, the cell anode compartment and the perforated cover were made of PVC. This was found to be entirely resistant to attack by 8.1 M H_2SO_4. Similarly, the clamps were made of the same PVC. The entrance and exit tubes and fittings were stainless steel which was found to resist attack. Screws made of a different type of stainless steel were found to dissolve in the acid; therefore, they were covered with silicone grease (after they were screwed in the clamps). This prevented further dissolution of the screws. The support for the cathode screen was made of teflon. Screws for this support were also treated with silicone grease to prevent dissolution.

Similar care was exercised in choosing a proper reference

electrode. Not only was the corrosiveness of 8.1 M H_2SO_4 a factor, but the high concentration of sulfuric acid can also result in a liquid-liquid junction potential. A mercury-mercurous sulfate reference electrode with a sleeve junction[1] solved both of these problems. First of all, the sleeve junction is simply a ground glass joint which is not susceptible to corrosive attack. Secondly, the electrolyte of the reference electrode was concentrated potassium sulfate. There was, therefore, only a minor difference in the activities of the electrolyte of the cell and the electrolyte of the reference electrode (i.e. both were concentrated sulfate ion). Hence, there was no measurable liquid-liquid junction potential.

3. Electrochemical Measurement and Control.

The overall experimental system is shown schematically in Figure 17. This system was a simple potentiostat with current measurement. The voltage control was a direct variable voltage source[2] and controlled the voltage drop across the anode and cathode. The cell current was measured on a standard ammeter. The other piece of equipment was a high impedance digital voltmeter[3] which measured the voltage drop between the anode and the reference electrode.

Although the variable voltage source contained its own voltmeter and ammeter, these meters were not used. The ammeter only had an accuracy of $\pm$ 0.2 amps. Moreover, the voltmeter gave only the potential difference between the anode and cathode. Since the cathode did not have a fixed potential, this could not be used to measure the anode potential.

[1] Beckman Instruments, Pittsburg, Pennsylavnia.
[2] Kepco, 0-8V, Model CK8-5M.
[3] Honeywell "Digitest", Model 333.

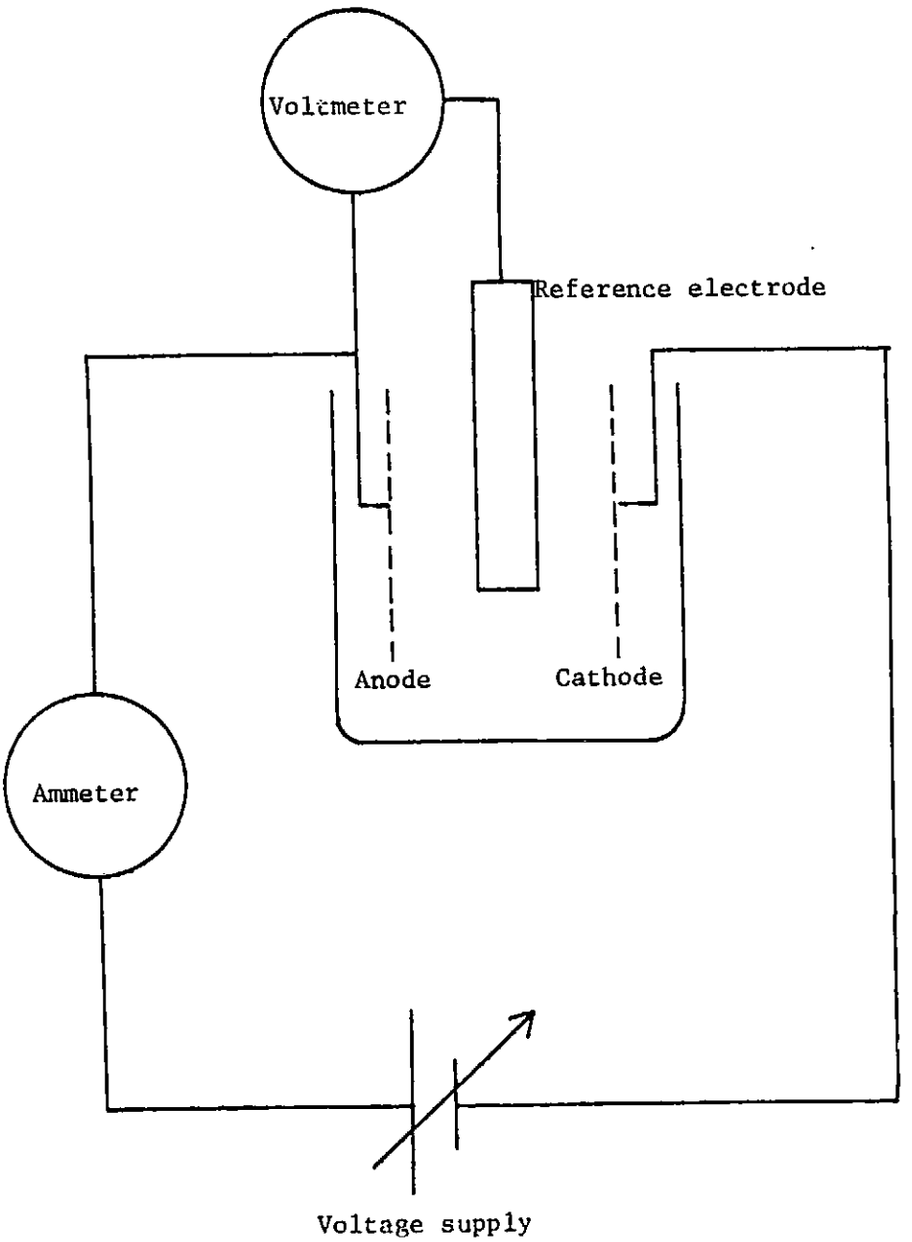

Figure 17. ELECTROCHEMICAL MEASUREMENT AND CONTROL CIRCUIT.

Therefore, the voltage source was only used to adjust the potential difference between the anode and the reference electrode. The digital voltmeter which measured this potential drop was accurate to ± 10 mV.

In practice, the potential difference between the anode and the reference electrode was set at some initial potential. This was either 1.16 V or 2.00 V, depending on the direction the potential was to be changed. The potential difference was changed by 20 mV for each data point. After each potential step the current was recorded. After approximately 15 seconds the potential was changed again, and the current was recorded within ten seconds after the step change. Each step change in potential required about fifteen seconds to attain a new stable potential. A sequence of increasing potentials was followed, without pause, by a sequence of decreasing potentials. Potentials were scanned between 1.16 V and 2.00 V against the mercury-mercurous sulfate electrode (MMSE) (+0.61 V). This range was chosen because oxygen evolution generally does not occur below 1.8 V versus NHE, and 2.6 V versus NHE was the maximum operating voltage used by Bloom.

Current was recorded with an accuracy of ± 3%. The largest part of any inaccuracy was due to minor fluctuations in the current at a particular current level. This was especially noticeable at the higher currents. Currents were recorded in a range of 0.1mA to 1A.

B. General Procedure.

Two reliable sets of current-voltage data were required. One set of experiments was performed on the electrochemical cell as described above. The second set was carried out on the "free-electrolyte", i.e. in 8.1 M sulfuric acid solution only. This was necessary for comparison with a reference system. The same procedure was used in varying the

potential in both cases. In the free electrolyte, the anode and cathode screens were suspended at a known distance from each other. The reference electrode (MMSE) was placed between the two platinum screen electrodes.

The distance between the electrodes was measured with a ruler to $\pm$ 0.25 cm. This information was required to calculate the cell IR drop. Although the distance between electrodes varied between experimental data sets, the usual distance was approximately 2.5 cm.

The information obtained from experiments on the free electrolyte turned out to be very important to the conclusions of this thesis.

C. Automatic Potential and Current Control.

At this point it should be pointed out that a considerable amount of effort went into development of another experimental system which has not been discussed thus far. The reason for the lack of discussion about it is that the system turned out to be unworkable. A Heath polarograph was purchased for current and potential measurement. This device had the capability of very accurate potential sweep control, i.e. varying the applied potential at a known constant rate. A sophisticated dual channel linear recording device was attached to the Heath polarograph for current and potential recording. Preliminary experiments were performed with this apparatus on known electrochemical systems, e.g. the ferrocyanide-ferricyanide redox couple. These experiments were performed in order to familiarize this author with polarographic techniques. It was also desirable to reproduce a known electrochemical system to assure that the apparatus was functioning properly. The particular experiments that were performed were measurements of half-wave potentials. In general, for a given redox system in which both the

reduced and oxidized forms are soluble the potential corresponding to one half the limiting current has a characteristic value. The experiments performed on known systems were very successful. The half wave potentials found experimentally agreed well with literature values. The working electrode in these experiments was a rotating platinum drop electrode and the reference electrode was a mercury-mercurous sulfate electrode. These experiments were successful in acquainting this author with polarographic technique.

The reason why this apparatus was not used for the experimental work in studying the water vapor electrolysis reaction was that the maximum current attainable on the Heath polarograph was one milliamp. Since the currents of the water vapor electrolysis cell are roughly about one amp, the apparatus was unsuitable as it was purchased. Considerable effort was made by the electronics group of the Department of Chemistry of the Pennsylvania State University to adjust the current measurement range to two amps. These attempts proved unsuccessful, hence the automatic current-potential apparatus was not used. A manual set up, as described previously, was assembled. This information is presented here so that others might not make the same mistake.

VII. RESULTS AND DISCUSSION OF RESULTS

This section is organized in a format such that the experimental results are first presented, then analyzed from an experimental viewpoint. This is followed by a discussion of the physical and electrochemical implications of these experimental results, i.e. what were the real electrochemical phenomena which caused the observed results, and how could these phenomena also explain the experimental results of others, especially Bloom's (69) cycling experiments.

Several "theories" are proposed in order to explain the experimental results. The argumentative approach adopted to evaluate these theories is to 1) assume that a particular theory is correct, 2) find evidence which supports that particular theory, 3) find evidence which negates that particular theory, and 4) weigh and evaluate the various evidence to arrive at whatever conclusions are possible for a particular theory.

A. Experimental Results and Discussion.

The experimental results are presented graphically in Figures 18 - 24. Figures 18 and 19 are the results of current-voltage experiments on the "free electrolyte" cell. This cell, as described in the apparatus section, consists of a bright platinum screen anode in 8.1M H_2SO_4 electrolyte solution. The electrochemical reaction is the electrolysis of water into oxygen gas and hydrogen gas. The "free electrolyte" results serve as the "base case", i.e. this is the behavior one would expect without any complicating factors.

Figures 20, 21, and 22 present the results of the same experiments on a standard cell. The standard cell, as described in the apparatus section, consists of the same anode, but in a 8.1M H_2SO_4 silica

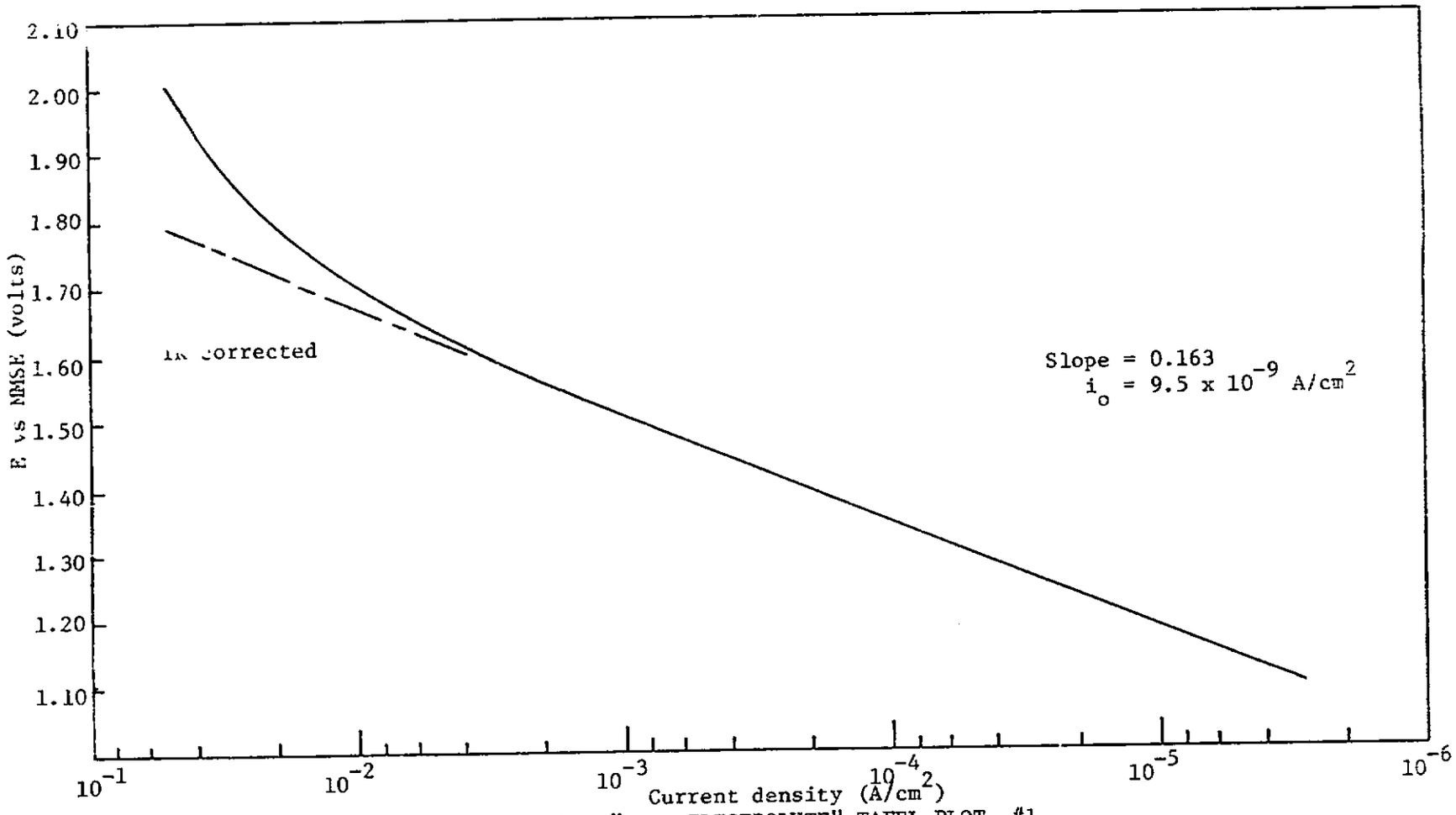

Figure 18. "FREE ELECTROLYTE" TAFEL PLOT, #1.

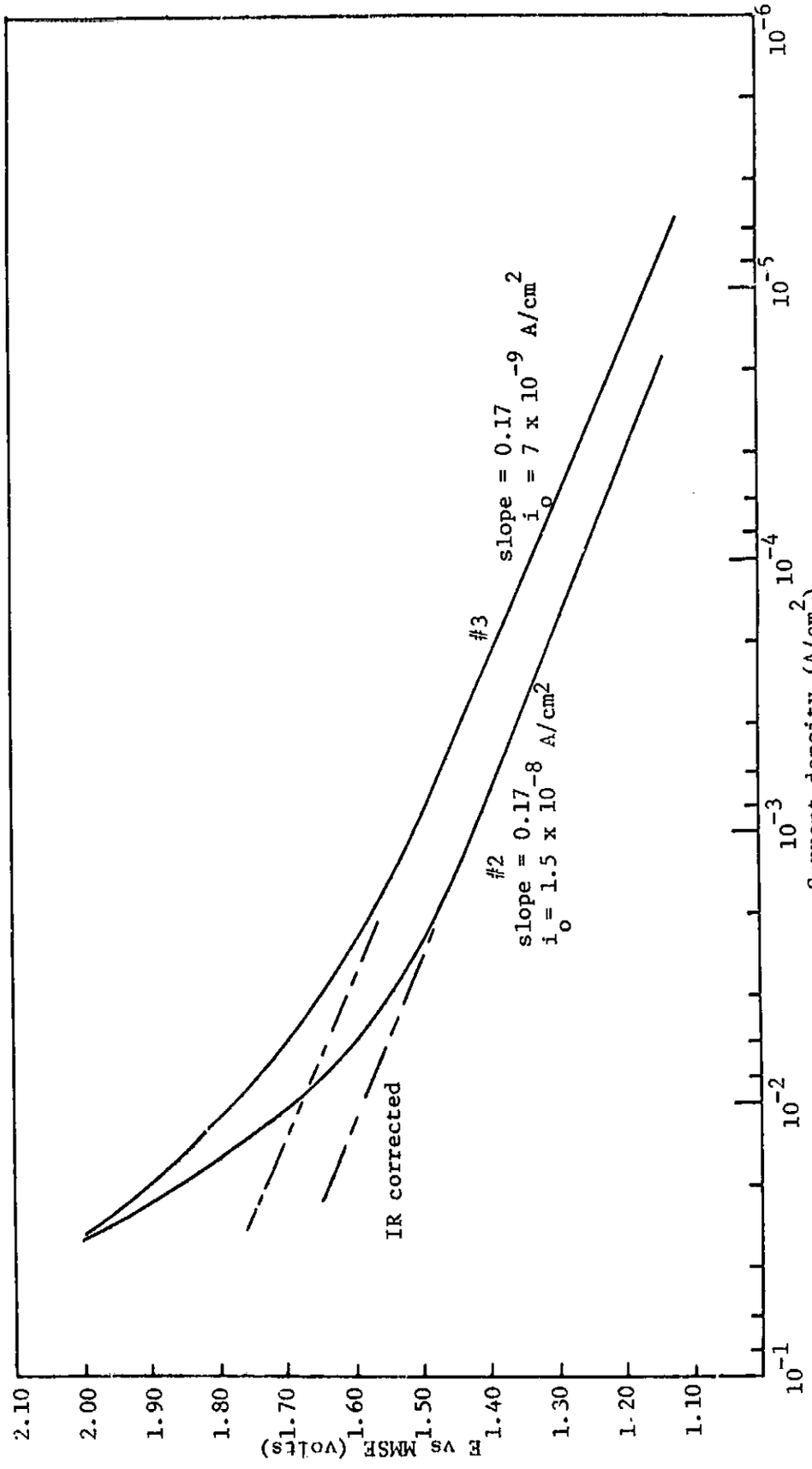

Figure 19. "FREE ELECTROLYTE" TAFEL PLOT, #2 AND #3.

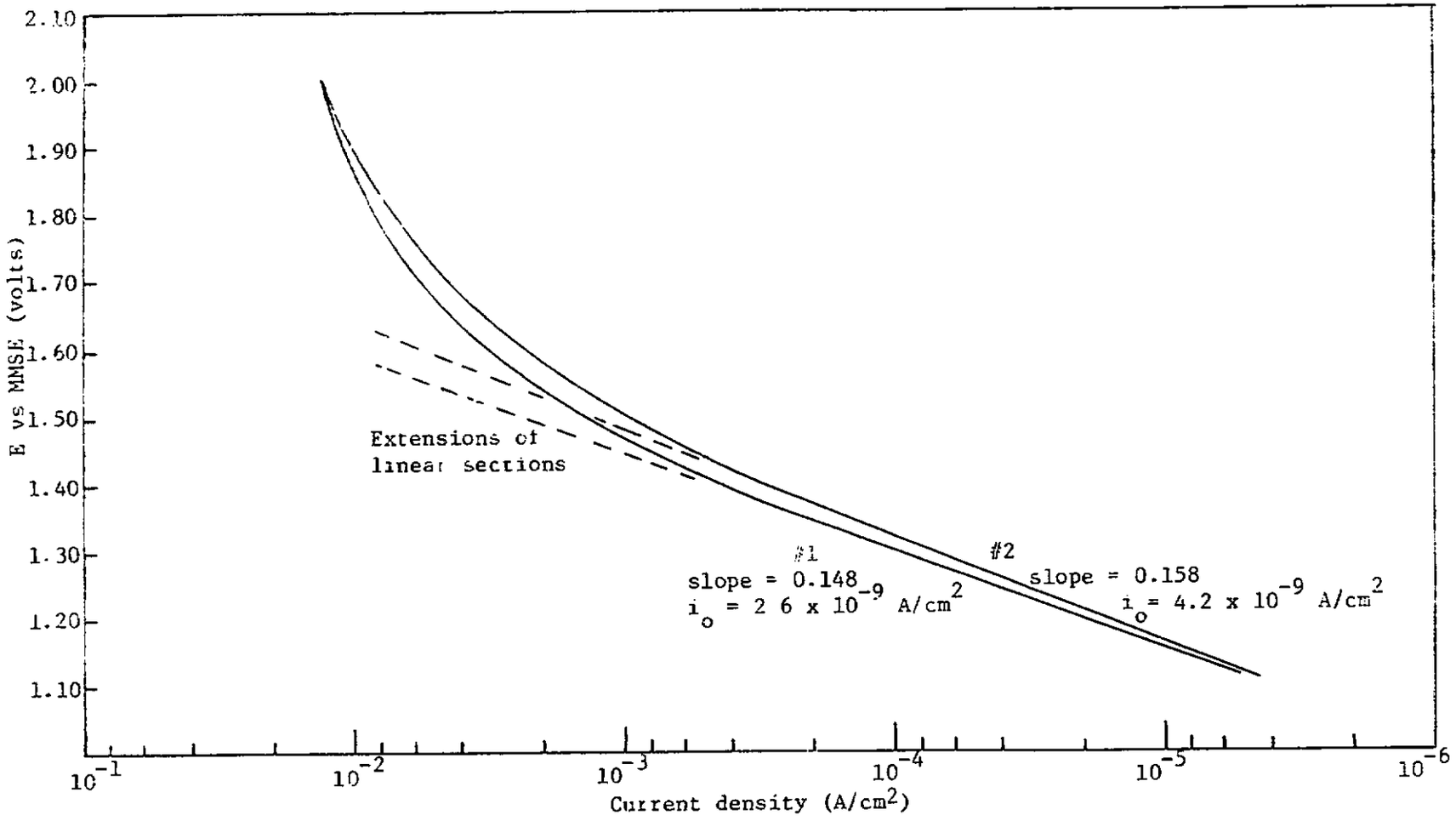

Figure 20. STANDARD CELL TAFEL PLOT, #1 AND #2

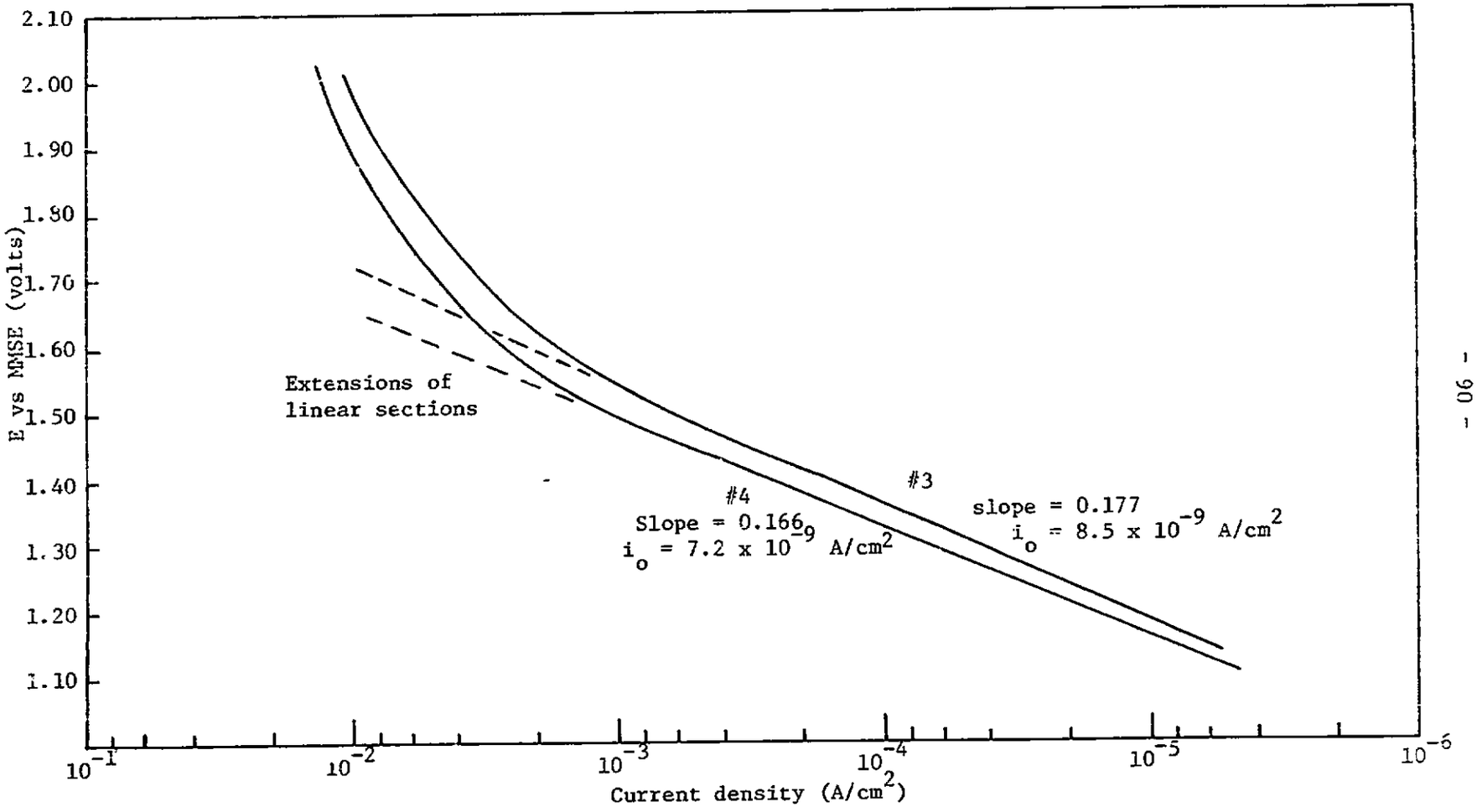

Figure 21. STANDARD CELL TAFEL PLOT, #3 AND #4

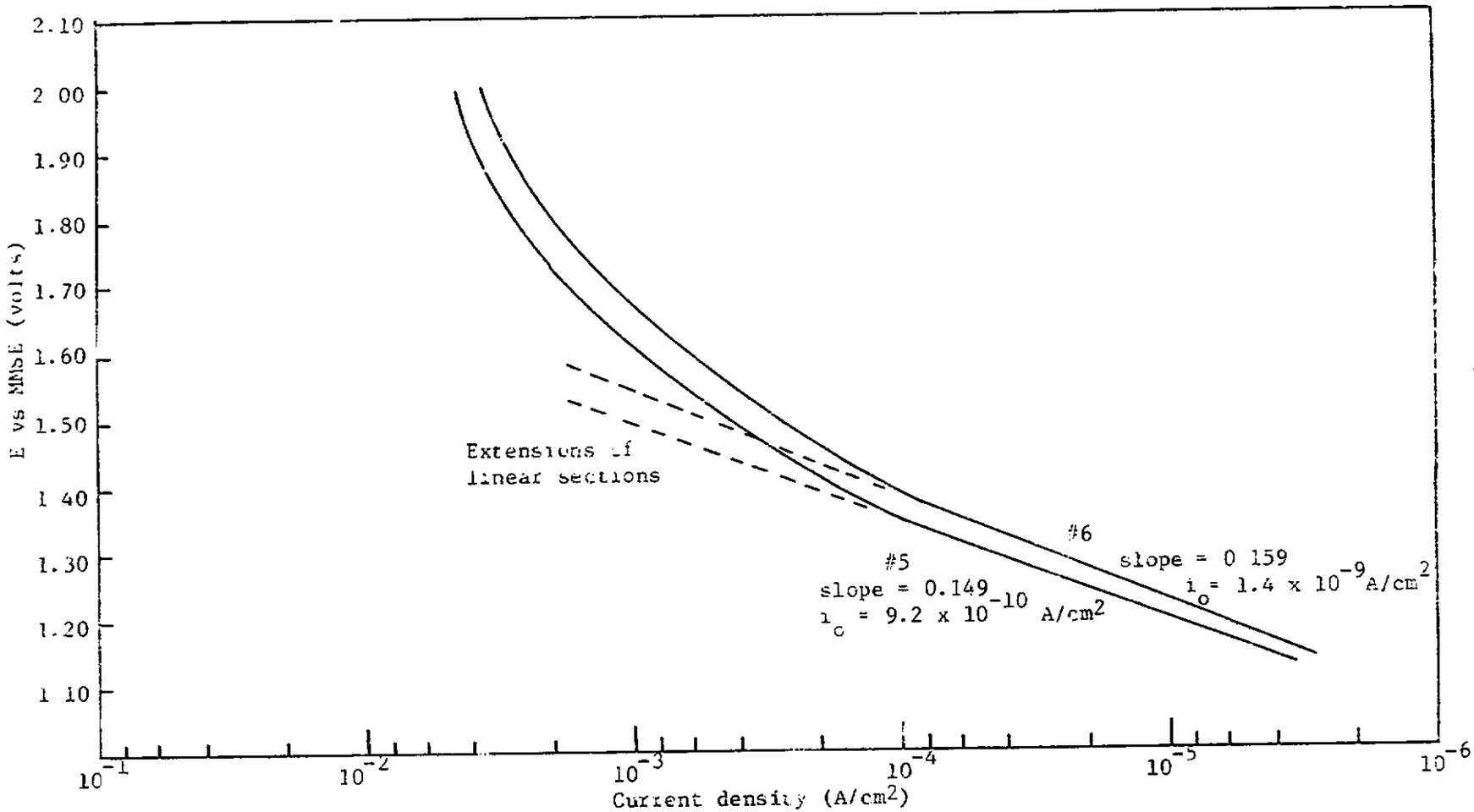

Figure 22. STANDARD CELL TAFEL PLOT, #5 AND #6.

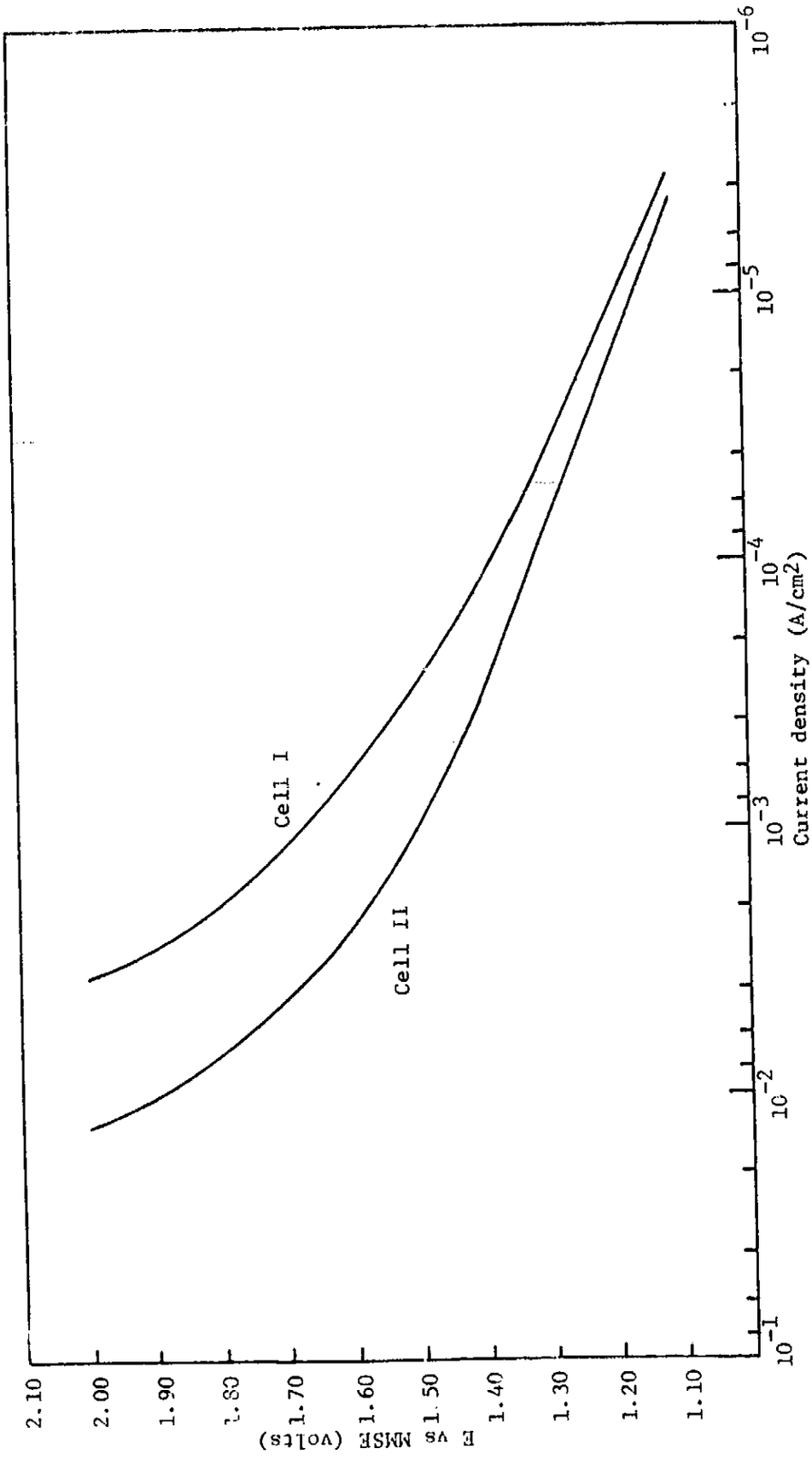

Figure 23. COMPARISON OF DIFFERENT STANDARD CELLS

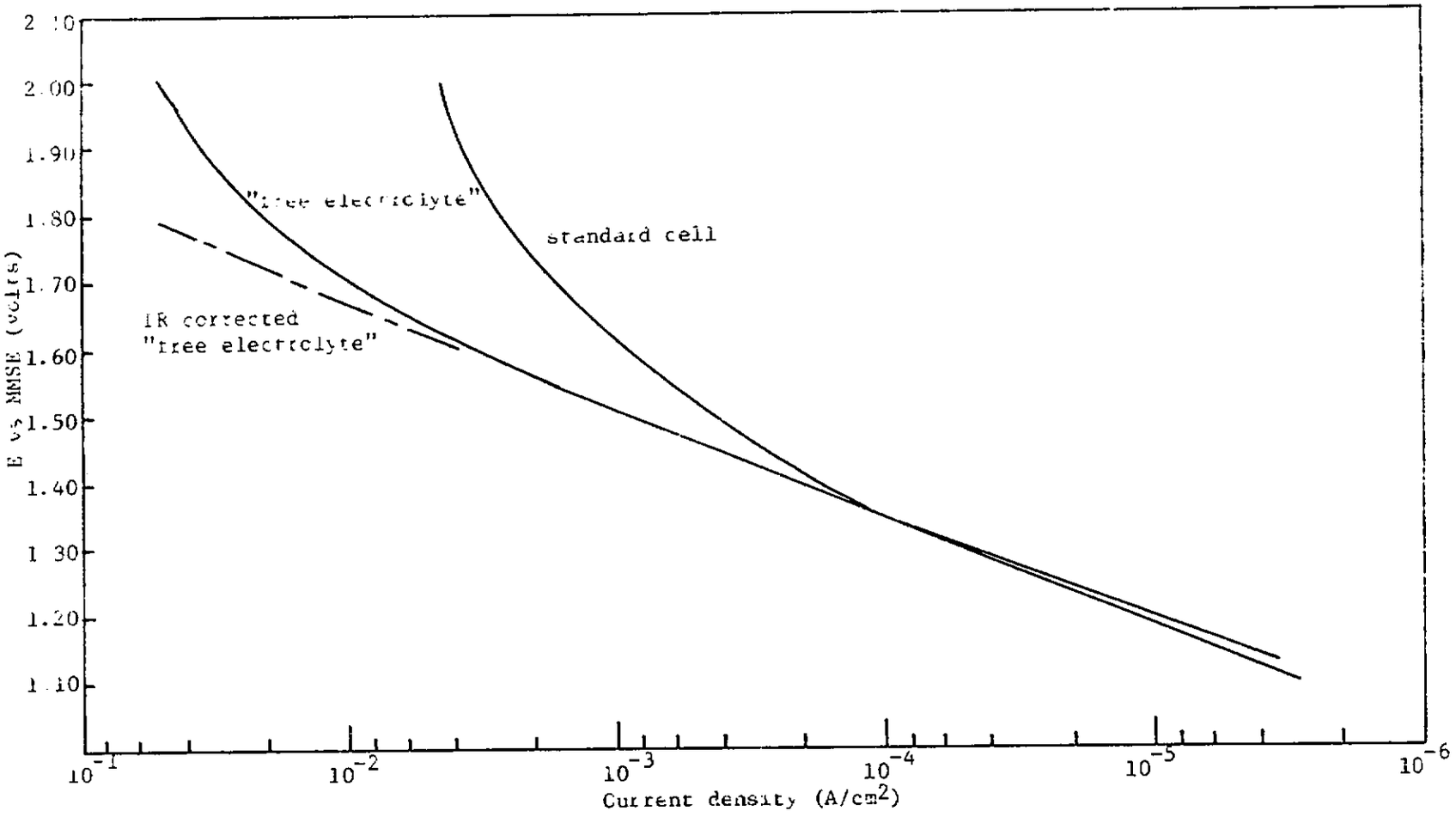

Figure 24. COMPARISON OF STANDARD CELL AND "FREE ELECTROLYTE".

gel electrolyte. This cell operates with humic air at room temperature and pressure flowing over the gel and anode screen. Figure 23 is a comparison of two different standard cell current-voltage curves.

Figure 24 is a comparison of the results of the standard cell and the "free electrolyte" cell. It is this comparison which is the most significant aspect of the experimental work.

All figures are semi-logarithmic plots of current density versus ancde potential. These are the usual Tafel graphs, voltage being the linear coordinate and current density the logarithmic coordinate.

1. "Free Electrolyte" Results.

Figure 18 is a downward scan of potential between 2.00 V and 1.12 versus the reference electrode.[1] The actual results are the solid line; the dashed line represents the IR-corrected results. The correction was made by subtracting the IR loss from the measured potential difference. The value of the IR loss was calculated using a specific resistance of 1.91 ohm cm (72) for 55 weight per cent sulfuric acid at 25°C, an interelectrode distance of 2.0 to 2.5 cm, and an electrode surface area of 61.9 cm^2. A sample calulation is given in the Appendix.

A straight line can be readily drawn with a Tafel slope of 0.163 and an intercept at E_o = 1.23 V versus NHE of 9.5 x 10^{-9} A/cm^2. This intercept is the exchange current density, i_o. These values of the Tafel slope and exchange current density agree well with literature values of 0.14 and 10^{-9} to 10^{-10} A/cm^2, respectively (9, 41, 42) for the anodic evolution of oxygen. Exact literature values of the

[1]The reference electrode was a mercury-mercurous sulfate electrode (MMSE) with a constant potential of + 0.61 V versus the normal hydrogen electrode (NHE). The potential of the normal hydrogen electrode is 0.0 V by convention.

Tafel slope and i_o do not exist due to wide variation in experimental conditions. Coupled with visual observations of the evolution of gases at the anode and cathode, the experimental results mark the electrochemical reaction unmistakably as the electrolysis of water.

The existence of a straight line of the log i-E plot denotes that the electrochemical reaction is activation controlled, i.e. the slowest step in the evolution of O_2 under these experimental conditions is the transfer of an electron at the anode surface. This is an expected result (41, 42).

Figure 19 gives results of an upward voltage scan followed by a downward scan. Two Tafel lines are observed, with equal slopes of 0.17. The upward scan has an exchange current density of 7×10^{-9} A/cm^2; the downward scan's i_o is 1.5×10^{-8} A/cm^2.

The upward scan produces higher current densities than the downward scan. This behavior is exactly opposite to what is expected (9), namely, during the upward scan, an electronically conducting monolayer of oxygen is being built up. During the downward scan, therefore, this layer should already exist, hence the current should be higher. Undoubtedly, the oxygen layer is being built up during the upward voltage scan However, its effect is small compared to the other considerations of the experimental technique. In particular, the time between current measurement and voltage adjustment is an important factor. In practice, it was observed that an increase in the voltage gave an initial rise in current which gradually decreased. In order to maintain a consistent basis for obtaining data, a set procedure had to be established. This assured obtaining continuous or "smooth" data. Time was not available to follow some of the elaborate techniques given in the literature (23,

29, 50, 51) to obtain exact current-voltage data.

The problem of developing a standard technique for data taking is very common with the oxygen electrode (9). Varying techniques were often used in the early studies of the oxygen electrode. Many times the exact technique was not described accurately. The consequence of this was irreproducibility of data. With this in mind, the data taking procedure of these experiments is exactly specified in the apparatus section. Moreover, it should be recognized that the exact current-voltage curves were not necessary for solution of the thesis problem, i.e. the nature of the type of oxygen overvoltage at the anode can be determined without exact data.

The difference in the upward and downward scans is actually due to a certain amount of "overshoot" from changing the potential and recording the current at a fixed time (30 seconds) after the change. The same argument applies to both the downward scan and the upward scan; however, in practice, the downward scan was much more stable. Stability, here, is defined as the rate at which the current responded to a voltage change. So, even though the current density values for the upward scan are higher, the results of the downward scan are more reliable. This is further supported as i_o for the downward scan is closer to the literature values than is the i_o for the upward scan. (The same behavior is present in experiments with the standard cell, i.e. in all cases, the upward scan produced higher currents. The same explanation for this phenomenon applies to the standard cell as to the "free electrolyte" cell.)

The exact comparison of Tafel slopes and i_o's with literature values is very difficult, as noted earlier. In particular, experimental

conditions as given in the literature are generally controlled much more rigorously than was feasible, or even desirable, for these experiments. An example of the extreme in control of experimental conditions is that of Kheifets and Rivlin (52). These authors used twice distilled water for preparation of the sulfuric acid solution. The sulfuric acid was chemically pure, distilled twice, and only the middle fraction of the final distillation was used. All apparatus was made of glass. The temperature was controlled to $\pm$ 0.1° C. Preanodization was carried out for 10-15 days to ensure a stable, constant oxygen layer on the anode. In contrast to these conditions, the experiments of this work were performed in a cell open to the air; preanodization was 25 minutes; singly distilled water was used with stockroom H_2SO_4 (98.5% by weight). Contamination of the solution and the electrode surface was inevitable. However, when one considers the ultimate use of the water electrolysis cell, the lack of purity of experimental conditions is easily justified. The actual cell in space cabin operation will be operating on air which contains water vapor exhaled by the cabin's occupants. This is certainly not a pure system. Therefore, experimental tests were performed without strict regard for system purity. The excellent agreement of experimental results with literature values shows that system purity was a minor experimental factor; this was most likely due to the large electrode area, 61.9 cm^2, which would "average out" any impurity effects.

Finally, with regard to the "free electrolyte" cell results, one notes that IR losses only become significant at a current density above 10^{-2} A/cm^2 or 700 mA. Minor errors in calculation result from the inaccuracy of the measurement of the distance between the anode and cathode. In general, a distance of 2.5 cm was used. The actual cell

in spaceship operation has a design anode-cathode separation of approximately 0.1 cm. This small separation gives a negligible IR loss, and only a very dry electrolyte could cause a measurable IR loss. However, as will be demonstrated later, a dry electrolyte has more serious consequences than an increased IR loss. Therefore, in the actual cell, IR losses do not constitute a significant portion of cell overvoltage.

2. Standard Cell Results.

The results of experiments performed on the standard cell apparatus are presented in Figures 20 to 22. There was no need to correct these curves for IR loss because the current was never high enough (approximately one amp) for IR loss to have a significant effect (greater than 10 mV).

Two features of these results are immediately evident:

1. A difference in the current-voltage curves of the upward and downward voltage scans.
2. A linear semi-log region and a non-linear, sharply increasing high-voltage region.

The difference between the upward and downward scan results is due to experimental technique as described in the discussion of the free electrolyte.

The second evident feature, namely the existence of two regions of the current-voltage curve, is unexpected. The initial linear semi-log region has the typical oxygen evolution parameters. Slopes range from 0.15 to 0.177; exchange current densities range from 8.5×10^{-9} to 9.2×10^{-10}. These are in good agreement with the literature values for anodic oxygen evolution.

There is no reason, a priori, to expect the non-linear semi-log

region of the current-voltage curves. This region begins at current densities between 10^{-3} and 10^{-4} A/cm^2. It is characterized by an increasingly steep rise in voltage with respect to current density.

There is one significant feature of the standard cell current-voltage curves which is not readily apparent. The magnitude of the current densities at higher potentials varied significantly among the standard cells. In other words, the characteristics of the non-linear semi-log region vary widely among the various standard cell assemblies. For example, at a potential of 2.61 V vs NHE the current density is 1.3×10^{-2} A/cm^2 in one case and 3.6×10^{-3} A/cm^2 in another. Similarly, the deviation from linear semi-log behavior begins at significantly different current densities.

The explanation of this non-linear section of the standard cell's Tafel plots is the heart of the discussion section of this work. Such an explanation if pursued below in the comparison of results of the "free electrolyte" cell and the standard cell.

3. Comparison of "Free Electrolyte" Results and Standard Cell Results.

Figure 24 is a comparison of the downward scan current-voltage curves of the "free electrolyte" cell and the standard cell The "free electrolyte" cell displays a linear Tafel plot which is explained above. The standard cell has a linear Tafel region and a non-linear region. The standard cell current-voltage curve is essentially the same as that of the "free electrolyte" cell at lower current densities (10^{-6} to 10^{-4} A/cm^2) but diverges at higher current densities. The standard cell shows lower current densities at the same voltage than that of the "free electrolyte". Moreover, the divergence increases with increasing current

densities (or increasing voltages). For example, at an anode potential of 2.13 volts vs NHE the free electrolyte current density is $1.30 \times 10^{-3} A/cm^2$ and that of the standard cell is $5.6 \times 10^{-4} A/cm^2$, while at an anode potential of 2.33 V vs NHE the free electrolyte current density is $1.85 \times 10^{-2} A/cm^2$ and that of the standard cell is $2.10 \times 10^{-3} A/cm^2$.

One notices that the current-voltage curves of both cells are not identical at lower current densities. The difference is very minor and is due to different anode pretreatment conditions. Although all cells were operated with 25 minutes of preanodization at approximately 0.8 amps, other preanodization conditions effected minor differences in the Tafel slopes and intercepts. For example, the standard cell apparatus was disassembled after a set of data had been obtained, which caused the anode to be removed from the sulfuric acid solution for a time. This had a minor effect on the nature of the platinum surface; consequently, a minor difference in the Tafel slope and intercept is observed.

At this point it is beneficial to briefly summarize the experimental results of this work, before interpreting them. These results can be listed as follows:

1. The "free electrolyte" exhibits Tafel behavior throughout the current density range investigated, when the results are corrected from IR losses.
2. The standard cell follows Tafel behavior below 10^{-3} to $10^{-4} A/cm^2$ and then deviates from the linearity of the semi-lot plot. This deviation is toward lower current densities than the "free electrolyte" cell exhibits at a given

potential.

3. The standard cells exhibit significantly different behavior in the non-linear portion of the semi-log current-voltage plots.

B. Physical and Electrochemical Implications of Experimental Results.

Why does the standard cell behave as described above? Apparently, the sole limiting step in the electrochemical process is not electron transfer at the anode surface, because the standard cell does not exhibit Tafel behavior at all potentials investigated. There are several possible reasons which might explain the aforementioned phenomena. The possibilities are:

1. Concentration polarization.
2. IR losses.
3. Adsorption.
4. Absorption of water.
5. Surface coverage by oxygen.

It is important to be certain that any explanation covers not only the experimental results of this work but also the findings of previous studies, especially those of Bloom (8). In particular, any explanation or "theory" must take into account the positive effects which resulted from cycling Bloom's standard cell.

Each of the above possibilities is discussed in detail below by 1) assuming the theory is correct, 2) presenting evidence to support the theory, 3) presenting evidence to negate the theory, and, 4) evaluating the theory by weighing the evidence.

1. Concentration Polarization.

The possibility and likelihood of concentration polarization at

the anode has been discussed above in "Literature Search" section. In particular, Bloom (8) gives an approximate mathematical approach to show that concentration polarization is negligible. This author has already pointed out in the "Literature Search" section that one of Bloom's assumptions is possibly incorrect, namely that the diffusivity of H^+ in a silica gel matrix could be considerably different from its diffusivity in sulfuric acid. Because of this possible error, Bloom's conclusion that negligible concentration polarization exists is suspect.

Clifford et.al. (13) claim that there is strong concentration polarization. They present data, which, when corrected for IR loss, strongly negate their claim. Clifford gives a Tafel plot with a slope and intercept which agree well with the literature values for the anodic evolution of oxygen; yet, he does not recognize this and still claims concentration polarization to be the major component of anode overvoltage. His data clearly support electron transfer control. One must conclude that he has misinterpreted his results. This has also been discussed in the "Literature Search" section.

Suppose that concentration polarization does indeed exist in the experiments presented in this work and in Bloom's work. Then concentration polarization must explain the following phenomena:

1. Current densities are lower than expected.
2. There is improvement of the electrochemical system after it has been turned off for five seconds.

As the anode potential increases from 1.7 V vs NHE toward higher potentials, electrochemical kinetics dictate that oxygen must be evolved faster and faster. The higher the voltage, the higher is the current and evolution of oxygen. This requires, also, that a given

water molecule must be able to diffuse to the anode as rapidly as it reacts at the surface. If the diffusion process is slow compared to the rate of reaction, the current will be limited by the rate of diffusion. This rate will necessarily be slower than the electrokinetic process, and hence a lower current is obtained. This agrees with the experimental results of this work.

Consider now the second point, that of improvement of cell conditions by turning the cell off. Suppose that Bloom's cell is operating and a concentration gradient of water exists near the surface of the electrode. What happens when the cell is turned off? The diffusion process continues, independent of whether or not the cell is connected or disconnected; the diffusion process occurs in a direction so as to relieve the concentration gradient. More water molecules become available at the surface. When the cell is reconnected the initial current is higher due to the presence of more water molecules at the anode surface. This agrees with Bloom's experimental results.

Conceivably, then, concentration can be seen to explain the observed phenomena. However, closer consideration of what should actually occur if concentration polarization were the controlling factor leads to some further hypotheses. First of all, if diffusion controls the rate of reaction (i.e. current), then the current must reach a constant or limiting value (see "Theory" section). As the water diffuses toward the surface, its rate depends only on the physical properties of the system, not the anode potential. As the potential is increased, the reaction rate can only be as great as the rate of diffusion of water molecules to the anode surface. This depends solely on the diffusion coefficient and mixing effects, which are not functions of the

potential. No limiting current was ever reached in these experiments; the potential was increased as high as 3 volts vs NHE. Although the standard cell current-voltage plots seem to approach a limiting current, one must realize that these are semi-log plots; on linear coordinates, no semblance of a limiting current is approached.

Secondly, consider the relieving of concentration "stresses" which would occur while the cell is disconnected. The diffusion of water molecules to the surface of the electrode must be rapid enough so that significant improvement of the power characteristics occurs in five seconds. Clearly, creation of a diffusion gradient in five minutes cannot be relieved by diffusion in five seconds.

In light of the above considerations, the existence of significant concentration polarization can safely be discounted.

2. IR losses.

Although IR losses are discussed above, not all aspects of this phenomenon have been investigated to this point. In particular, in the standard cell experiments of this work, a membrane is present in the cell which is not present in the "free electrolyte" cell. Secondly, in Bloom's experiments water is absorbed by the gel from the passing air stream and this decreases cell resistance. These two points are considered separately below.

Although there is an additional resistance due to the presence of the membrane, this was originally assumed to be negligible. The membrane was saturated with 8M H_2SO_4 for two weeks prior its use in experiments. Suppose, however, that the membrane does have a large resistance. This could account for a decrease in current (compared to the "free electrolyte"). This could not account, however, for any

improvement obtained by cycling. The membrane resistance is not a function of time; hence, no improvement in current would be expected from cyclic operation of the cell. In conclusion, large membrane resistance is not a real possibility in explaining improvement in cell performance due to cyclic operation.

Consider what happens to the gel electrolyte during the "off" cycle of Bloom's experiments. Water is absorbed from the passing humid air stream. This has the effect of lowering the resistance of the electrolyte, hence increasing the current through it once the cell is reconnected. However, a simple mass balance[1] shows that during the five seconds in which the cell is disconnected, the total amount of water in the cell increases by less than 0.005% of the original amount. This increase in water content is negligible and has no measurable effect on the electrolyte resistivity. Another negative consideration is the erratic current behavior at high currents, as observed in the experiments of this work. A simple IR loss is a smooth, continuous effect. Furthermore, one should consider the wide variance in cell behavior among standard cells. One could argue that the cells were prepared differently in terms of the amount of gel applied and that this could account for the IR loss being different among standard cells Bloom (8), however has shown that the amount of silica in the gel (10 weight per cent) has very little effect on the resistivity of the electrolyte. Therefore, the resistance due to the gel is essentially the same among standard cells. Likewise, the membrane resistance is idential from cell

[1]This mass balance was performed by using the rate of water absorption data of Connor (14). These data were checked (by Faraday's law) against Bloom's steady state current of 0.92 amps. Agreement was found to be within 3%, hence verifying both Connor's data and Bloom's current measurement technique. (See Appendix.)

to cell. Therefore, IR losses cannot explain the varying behavior of the standard cells.

With so much evidence against it, IR loss cannot be a real possibility in explaining the results of this work and of Bloom's (69) work.

3. Water Absorbtion and Overvoltage Decrease.

A net amount of water is absorbed by the electrolyte during the "off" cycle; this causes a decrease in the concentration of the sulfuric acid electrolyte. According to the findings of Kheifets and Rivlin (51) and Efimov and Izgaryshev (23), a shift toward a lower H_2SO_4 concentration causes an increase in current. The amount of this shift depends on the concentration and the potential. According to the data of Efimov and Izgaryshev, (see Figure 11) Bloom's experiments were performed in a very concentration-sensitive range. Hence, a small change in sulfuric acid concentration could produce a relatively large change in current (at a given potential). However, as pointed out in the argument against significant IR losses, the amount of water absorbed by the gel electrolyte in five seconds is very small compared to the total amount of water in the electrolyte. But, there is one further consideration here. The absorbed water can be considered to exist only at the protruding electrode surface In this case, the amount of water absorbed must be compared to the total amount of water which exists in the Nernst diffusion layer. If one takes a common value of 0.005 cm as the thickness of the diffusion layer and compares the amount of water absorbed to the volume of the diffusion layer, one finds that the change in concentration in the diffusion layer is only 0.13% (the calculations are presented in the Appendix). By examining Figure 11, one

can see that this composition change has a small effect on the current.

A further consideration is that water adsorption could not cause the non-linear section of the Tafel plots presented in this work. Since the experiments of this work were carried out in an essentially infinite supply of 8.0 M H_2SO_4, water adsorption could have had no effect on the experiments. The electrode surface "saw" only 8.0 M H_2SO_4 at all times. Hence, it can safely be concluded that water adsorption is not a viable explanation of experimental results.

4. Adsorption.

The standard cell data of this work bear a definite similarity to the data of Efimov and Izgaryshev (see Figure 11). On a current-voltage plot a Tafel region is followed by a region of steep slope. The data of Efimov and Izgaryshev exhibit another Tafel region after the region of steep slope; however, their anode potentials are considerably higher in the upper Tafel region than any of the potentials investigated in this work. Nevertheless, the question arises as to whether or not the presence of silica gel could act so as to enhance the adsorption process. As in previous cases, the discussion continues assuming that this is so, i.e. the standard cell results are due to adsorption phenomena.

The first point to be addressed is that of the "jumps" in current which are observed at higher current densities. One would not ordinarily expect this type of phenomenon in an adsorption process. Current-voltage behavior which accompanies ordinary adsorption processes is smooth. However, the anodic evolution of oxygen has been shown (23) to possess this erratic behavior. Efimov and Izgaryshev explained this in the following way: The species which are about to be adsorbed (e.g.

sulfate and persulfate ions) are violently disturbed by the oxygen bubbles evolved at the surface. Hence, the adsorption of these speciedis somewhat irregular. In support of this interpretation, Efimov and Izgrayshev cited the improvement due to stirring. They noted a 20-30 mV enhancement caused by more continuous adsorption of the sulfate and persulfate ions. Hence, the above explanation of Efimov and Izgaryshev could account for the unsteady current behavior noted in the experiments of this work.

The most important question to be asked is whether or not this proposed adsorption phenomenon can explain the increased current caused by Bloom's cycling (8). Consider one complete cycle:

a. The cell is in operation.

b. The cell is disconnected for approximately five seconds.

c. The cell is then reconnected.

Each of these steps in the cycle is discussed separately below:

a. The cell is in operation: At the anode surface there are two competing adsorption processes. The first is the adsorption of O_2 and formation of a monolayer of adsorbed oxygen. This process enhances the evolution of oxygen and causes an increase in current. The second (proposed) adsorption process is that of sulfate and persulfate ions. According to the data of Efimov and Izgaryshev (23), this decreases the current. The relative rates of adsorption of oxygen and sulfate and persulfate ions are unknown.

b. The cell is disconnected: Evolution of oxygen drops rapidly. The species which were adsorbed during cell operation are subsequently desorbed. The oxygen monolayer desorbs;

this is deterimental to the evolution of oxygen. The sulfate and persulfate ions desorb; this enchances the evolution of oxygen. The relative rates of desorption are unknown.

c. The cell is reconnected. Oxygen evolution begins immediately on the anode surface which is present at the end of the second process. The initial rate of oxygen evolution depends on the nature of the anode surface. If the surface of the anode is improved over what it was before the cell was disconnected, the initial current will be correspondingly higher. The converse is also true. Hence, it is possible to obtain an increase in initial current due to cycling. Obviously, this depends on the relative rates of adsorption and desorption of the various species.

The "nature" of the anode surface can be described by the coverage, θ, of each species. The greater the coverage by adsorbed O_2, the larger the current. The greater the coverage by sulfate and persulfate ions, the smaller the current. A bare Pt site is better for the evolution of O_2 than a site with adsorbed sulfate or persulfate ions. It is worse than a site with an adsorbed O_2 molecule.

Bloom further notes an optimum "off" cycle time. Can this be explained by the above adosorption and desorption processes? This question is equivalent to one which asks if the relative adsorption and desorption rates can be such that the surface reaches an optimum state. The answer is clearly yes. For example, suppose that when the cell is disconnected, sulfate and persulfate ions desorb rapidly and are essentially desorbed after five seconds. Any extension of this "off"

time beyond five seconds will be detrimental to the anode surface; O_2 will be desorbing and bare Pt sites will be formed. This is not a net benefit to the anode surface. Similarly if the "off" time is less than five seconds, all the sulfate and persulfate ions will not have desorbed. Consequently, current will not be as great as it could be, once the cell is reconnected. Therefore, an optimum "off" time of five seconds may exist.

One other point to be considered is the difference in cyclic behavior between electrode materials. If adsorption processes exist, one would expect the specific behavior to be dependent on the type of electrode material. Adsorption and desorption rates could exist which fit the experimental data of both electrode materials which Bloom studied.

It has now been established that adsorption processes, as described above, could account for the important results of this work and Bloom's work (8). It must furthermore be established that these adsorption processes are consistent with other less important observations.

The most obvious inconsistency lies in a comparison of the standard cell current-voltage curves of this work and those of Efimov and Izgaryshev. The steep slope of their work begins at current densities of 10^{-2} A/cm^2 whereas this occurs at 10^{-4} A/cm^2 in this work. Since there was no steep slope in the "free electrolyte" results of this work, one must conclude that the proposed adsorption is due to the presence of silica. However, silica was originally chosen for the water vapor electrolysis cell because it is extremely inert. In fact, commercial silica, such as that used in this work, is made by a process using a sulfuric acid bath. One would not expect the silica gel used in these experiments

to affect the platinum surface so as to make it sensitive to adsorption.

Strong evidence against the proposition of significant adsorption processes is the remarkable variation which was noticed in the current-voltage behavior of different standard cells (see Figure 23). The example given above is that at an anode potential of 2.61 V vs NHE, one standard cell had a current density of 1.3×10^{-2} A/cm^2 and another standard cell had a current density of 3.6 V 10^{-3} A/cm^2. This is a difference of three hundred percent! Even if adsorption processes are responsible for the standard cell behavior and silica enhances these adsorption processes, there should not be such a large difference in behavior from cell to cell. The silica gel used in all experiments was taken from the same batch. Since the silica gel itself did not differ from experiment to experiment, this cannot be responsible for the unusual differences noted above.

5. Oxygen Coverage.

Thus far, all of the conventional possibilities have been shown to be inconsistent with experimental results. Hence one must turn to an "unconventional" explanation of the experimental results. Yet, it is possible to learn much from the type of arguments presented in the discussion of the conventional possibilities. In particular, the arguments regarding electrode surface coverage are attractive.

A fundamental difference between the standard cell and the "free electrolye" cell is the presence of a thick, viscous electrolyte covering the anode. It is possible, therefore, that evolved oxygen will have difficulty in escaping from the electrolyte. In fact, it is possible that an evolved oxygen bubble could remain on the surface of the electrode until conditions are such that it will escape. If bubbles

do remain on the surface, then the area available for electrochemical reaction is decreased. Consequently, the cell current is less and current density based on the total cell area is also decreased. In other words, the explanation being proposed here is this: Because of the presence of a thick, viscous electrolyte on the surface of the electrode, evolved oxygen bubbles are trapped on the anode surface. This decreases the area available for electrolysis. Further implications of this "theory" are explored below.

Consider how the above argument applies to the results of this work. First of all, the difference between the "free electrolyte" behavior and standard cell behavior is most pronounced at higher currents. One might expect that, if oxygen is trapped on the surface, the amount of electrode surface covered by gaseous O_2 would increase with increasing oxygen evolution. This is precisely what is found, i.e. the higher the current the more pronounced is the surface coverage effect. Consequently, the current density characteristics of the standard cell deviate most from the "free electrolyte" behavior at higher currents.

The most natural question at this point is, "Why doesn't this deviating behavior show up at even lower current densities?" There are two possible answers: 1) The rate of oxygen evolution is so small at low current densities that essentially no measurable surface coverage is observed, and 2) the evolved bubbles might be so small that they easily find a path away from the electrode surface.

The proposition of bubble entrapment is attractive from the standpoint of explaining the high degree of current "jumps" or unsteadiness at high currents. One would expect that if a large bubble breaks loose from the surface, there would be a small but rapid rise in the

observed current.

Bloom's results can be treated by almost identical surface coverage arguments as given for the adsorption processes. The following situation can easily be hypothesized: The cell is in operation; oxygen bubbles cover part of the electrode surface. These bubbles have reached a steady state where they are removed into the passing air stream at the same rate they are formed on the surface. The cell is disconnected. No more bubbles are evolved; however some bubbles still escape from the electrode surface. After five seconds the cell is reconnected. Now, the surface has virtually no bubbles remaining on it. Therefore, there is an initial current surge utilizing the full electrode surface. Gradually, the surface reaches a steady state coverage again, and the cycle is repeated.

The most important assumption in this explanation is that the bubbles can escape from the surface in a matter of seconds when the cell is disconnected. It is important to keep in mind that the bubbles must not necessarily be completely removed from the gel into the passing air stream. <u>The bubbles need only be removed from the electrode surface</u>. This could be a very small distance indeed. All that is required for a current surge is that the anode surface be in contact with the sulfuric acid solution and that there be few or no "bare spots" on the electrode surface.

Although the nature of oxygen bubble removal is unclear, an analogy to Bloom's fuel cell effect appears attractive. Bloom noticed that when he turned his cell off it "acted as a fuel cell, consuming hydrogen and oxygen to make water". He noticed the bubble in his hydrogen collection bubble meter drop steadily, thereby signifying the

consumption of hydrogen. Had the hydrogen not been in a closed system (i.e. simply vented instead of trapped by a soap bubble in the bubble meter), Bloom would not have seen a prolonged fuel cell effect. The hydrogen would have escaped into the atmosphere instead of being "sucked in" by the cell. Nevertheless, this fuel cell effect raises the interesting possibility that any oxygen and hydrogen remaining on the surface of the electrode will be consumed by the fuel cell effect. In the case proposed here, oxygen and hydrogen are both trapped by the viscous gel. This would mean that the phenomenon of bubble entrapment by the gel on the electrode surface not only causes lower than expected currents but also causes their rapid removal when the cell is disconnected.

The oxygen bubble can now be seen as having two possible paths for removal from the electrode surface: 1) natural density differences, surface forces, and surface tensions, and 2) the fuel cell effect.

Bloom's investigation of cyclic behavior shows that different electrode materials exhibit different cyclic characteristics. Although these findings have already been shown to be suspect (see "Literature Search") they are discussed here. In particular, in the immediate region of zero "off" time, the specific power consumption of bright platinum increased with decreasing "off" time, the reverse of the platimum-tantulum cell case. At first glance, these results appear to contradict the oxygen entrapment explanation. Platinum-tantulum has a higher specific area than bright platinum. Consequently the current density should be higher at a given potential and oxygen entrapment should also be greater. One would therefore expect more of an entrapment effect on the platinum-tantulum screen than on the bright platinum screen.

Bloom offers an explanation for the phenomena discussed above.

This turns out to fit very well into the picture of oxygen entrapment and fuel cell removal of entrapped oxygen. Bloom noticed a difference in the degree to which the fuel cell reaction was maintained on the Pt-Ta electrode and on the bright platinum electrode. In particular he noted that the Pt-Ta electrode used up the hydrogen very quickly and exhibited a strong fuel cell reaction. The bright platinum electrode did not exhibit as strong a fuel cell reaction as the Pt-Ta electrode, and, in fact, was relatively weak. If this is true and the theory of oxygen entrapment is held, then one would expect that in the neighborhood of zero "off" time more oxygen would be removed from the surface of the Pt-Ta electrode and its specific power consumption correspondingly lower than that of the bright electrode. This is, in fact, what Bloom observed. It was only in this area, i.e. specific power consumption near zero "off" time, that Bloom noticed a difference between the two electrode types. Why this different susceptibility existed for the fuel cell reaction is still another question. Bloom offers a possible explanation of differences in the adsorbed conducting monolayer of oxygen on the two types, but concedes that,"No explanation is presently available for the effect."

The other path of oxygen removal, i.e. out through the gel, should also be considered here. In this case the situation is also complex.

If oxygen entrapment occurs, then it is important to consider what factors influence its enhancement and its abatement. Bubble size is certainly an important consideration, although it is not obvious if smaller or larger bubbles are more easily removed. Similarly, gel thickness and gel viscosity are very important. The anode surface and surface

forces also may play a major role in controlling oxygen entrapment. Moreover, one surface might give rise to small bubbles and another to large bubbles. The specific pretreatment of a given electrode material may also be a factor. In other words, different electrodes of the same basic material may exhibit different bubble forming and entrapping characteristics. All of these factors must be taken into account to be able to safely predict the behavior of a given cell. Obviously, little is known about any of these factors. Therefore, particular results such as Bloom's work on different electrodes, are extremely difficult to evaluate. For example, the bright platinum screen might evolve very small bubbles which are more easily removed from the electrode surface through the gel than the bubbles generated by the Pt-Ta electrode. At present, there is no way of determining exactly what occurs at a particular electrode.

Finally, there is the interesting result of this work that there can be significant differences in the current-voltage relationship from one standard cell to another. This can be explained by the fact that there is no rigorous, standard method to spread the gel onto the electrodes. If the gel thickness varies from standard cell to standard cell, then the degree of oxygen bubble entrapment will also vary. This is what most likely occurs. The gel is spread onto the anode with a stainless steel spatula. It is pressed through the screen to ensure total screen coverage. However, the gel thickness is not uniform over the screen. Nor is the gel thickness the same from cell to cell. There is no way of determining how much the thickness varies, but it is certain that there is no specific uniformity. Consequently, entrapment is likely to vary from cell to cell. This is, in fact, found to be the case, i.e. current varies significantly from cell to cell at higher voltages.

Of all the evidence presented above, very little, if any, can be considered to be positive evidence. All evidence has been used to determine why a particular theory can not prevail, and how one theory, oxygen entrapment, can be shown to account for the accompanying experimental results. However, no evidence has been presented which positively identifies entrapped oxygen as the "culprit". Instead, arguments have been presented to show that oxygen entrapment can explain all.

Three cases of positive evidence are presented below:

1. The "anode effect" of Efimov and Izgrayshev.
2. Literature mention of oxygen removal to prevent "mass transfer" effects.
3. Vibration of the standard cell.

The "anode effect" of Efimov and Izgaryshev (8) is not the same as the oxygen entrapment which is proposed in this work. It is, however, similar in nature. What Efimov and Izgaryshev found was that at very high voltages (>3.5 V) large oxygen bubbles became paralyzed on the anode surface. The presence of these bubbles caused a sharp decrease in cell current because available surface area was severely diminshed. This is similar to the proposal of this work, namely that entrapped surface oxygen has a detrimental effect on cell current. Although the cause of paralyzed oxygen on the surface is different in the two cases, the result is essentially the same.

Occasionally in the literature (e.g. 51) there is a reference to the experimental technique of passing nitrogen over the anode surface. Although the reasons given for use of this technique are often unclear, it is usually done to prevent "mass transfer" effects. In this case, what is probably meant is the removal of oxygen from the electrode surface

to ensure a continuously "clear" surface.

Finally, during the experimental work of this thesis, the possibility of oxygen entrapment was realized. Consequently, during operation at higher currents the cell was banged with the handle of a screwdriver. The result was a small jump in the current. This unscientific procedure was repeated periodically and it generally produced the same result. The cell unit was assembled very firmly, so that it was difficult to cause a significant disturbance within the cell itself. Moreover, the procedure of knocking the cell was limited because this caused splashing of the sulfuric acid solution in which the total cell was immersed. This was very hazardous to the operator. Although this minor experiment is inconclusive, it offers some positive evidence that oxygen is, in fact, trapped on the screen. Work is presently in progress at Battelle Institute, Ohio, in which the cell is being vibration-tested. These results could provide further evidence of oxygen entrapment.

VIII. CONCLUSIONS AND RECOMMENDATIONS

The experimental results of this work have shown that anode overvoltage of the electrolysis of water vapor in 8 M H_2SO_4 silica gel electrolyte at bright platinum electrodes is electron transfer controlled throughout the experimental range of anode potentials. The evidence for this is the agreement between the values of Tafel slopes and exchange current densities of this work and literature values. Activation control is also assumed to be the determining factor at high standard cell anode potentials, although the surface area available for reaction is decreased.

Furthermore, the results of this work have been shown to be compatible with a theory of "oxygen entrapment" at the standard cell anode. Other possible explanations are discounted for a variety of contradictions with experimental results. "Oxygen entrapment" as such, is the situation whereby oxygen evolved at the anode surface becomes trapped due to the presence of a thick, viscous gel electrolyte. Such entrapment causes a decrease in the available area for electrochemical reaction. Consequently, there is a decrease in the effective current density. The results of Bloom's (8) experiments on cyclic operation of the water vapor electrolysis cell have been shown to be compatible with "oxygen entrapment" and its removal from the electrode surface when the cell is disconnected.

The majority of evidence for the existence of oxygen entrapment is indirect. Although there is a significant accumulation of indirect evidence, it would be beneficial to have an equal arsenal of direct evidence. Unfortunately, little direct, or positive, evidence exists. Therefore, it is recommended here that methods be devised whereby direct evidence can be obtained. This is understandably difficult because visual

methods are necessarily excluded due to the nature of the cell. Vibration testing, under carefully controlled experimental conditions, could yield valuable data. Moreover, a fixed method of gel preparation and application to the anode screen is recommended. Finally, quantitative comparison of results using different gel matrix materials could yield valuable information. All of the experiments suggested above deal with a different aspect of the formation and removal of entrapped oxygen, a new area of experimental and analytical investigation which has been identified by this thesis.

IX. NOMENCLATURE

a = activity

a = constant in Tafel equation

A = constant in Tafel equation

A = surface area

b = exponent constant

C = concentration

C = capacitance

D = diffusion coefficient

e = electron

E = potential

$E_{1/2}$ = half-wave potential

F = activity coefficient

F = Faraday constant

G = Gibbs free energy

i = stoichiometric number

i = current density

I = electrochemical species

k = Randles - Sevcik constant

k = rate constant

m = number of hydrogen ions

M = molarity

n = number of electrons

n = number of equivalents

N = normality

N = flux

Q = charge

r = speed of rotation

R = gas law constant

t = time

t = transference number

T = absolute temperature

v = sweep rate

x = linear dimension

z = number of water molecules

Subscripts and Superscripts

a = anodic

Ad = adsorption

b = bulk phase

b = backward

c = cathodic

d = diffusion

dl = double layer

f = forward

h = heterogeneous

L = limiting

L-L = liquid-liquid

Ox = oxidized form

p = peak current

Red = reduced form

S = standard case

o = standard case

Greek Letters

α = transfer coefficient

δ = diffusion layer

ε = electrochemical potential

ε_0 = equilibrium potential

ζ = zeta potential

η = overvoltage

θ = C_{Ox}/C_{Red}

ν = stoichiometric coefficient

ρ = resistivity

ψ = $(D_{Ox}/D_{Red})^{1/2}$

X. BIBLIOGRAPHY

1. Adams, R. N. Electrochemistry at Solid Electrodes, Marcel Dekker, Inc., New York, 1969.

2. Adams, R. N. Electrochemistry at Solid Electrodes, p. 43 Marcel Dekker, Inc., New York, 1969.

3. Appleby, A. J., J. Electroanal. Chem., 35, 193 (1972).

4. Bain, H. G., Trans. Am. Electrochem. Soc., 78, 173 (1940).

5. Beck, T. R. and R. M. Moulton, J. Electrochem. Soc., 103, 247 (1956).

6. Biegler, T., and R. Woods, J. Electroanal. Chem., 20, 73 (1969).

7. Bircumshaw, L. L. and A. C. Riddiford, Quart. Revs. (London) 6, 157 (1952).

8. Bloom, A. M., Center for Air Environment Studies, Pennsylvania State University, CAES 200-71, NASA Grant NGR-39-009-123, 1971.

9. Bockris, J. O'M., and A. K. M. S. Huq, Proc. Roy. Soc. (London) A 237, 277 (1956).

10. Bold, W. and M. W. Breiter, Electrochim. Acta., 5, 145 (1961).

11. Bowden, F. P.,Proc. Roy. Soc. (London), A 125, 446 (1929).

12. Briner, E. H. Haefeli, and H. Pillard, Helv. Chim. Acta., 20, 1510 (1937).

13. Clifford, J. E., J. A. Gurklis, J. G. Beach, E. S. Kolic, E. W. Winter, A. C. Secrest, J. T. Gates and C. L. Faust, Batelle Memorial Institute, NASA CR-771, 1967.

14. Connor, W. J., B. M. Greenough, G. M. Cook, Lockhead Missiles and Space Co., NASA Contract NAS-2-2630, Final Report, 1966.

15. Conway, B. E. and E. Gileadi, Trans. Faraday Soc., 58, 2493 (1962).

16. Conway, B. E., J. Electroanal. Chem., 8, 486 (1965).

17. Damjanovic, A., M. A. Genshua, and J. O'M. Bockris, J. Phys. Chem., 70, 3761 (1966).

18. deBethune, J. J. and N. A. S. Loud, Standard Aquaeous Electrode Potentials and Temperature Coefficients, Clifford A. Hempel, Skokie, Ill., 1964.

19. Delahay, Paul, New Instrumental Methods in Electrochemistry, pp. 48-57, Interscience, New York, 1954.

20. Delahay, Paul, New Instrumental Methods in Electrochemistry, pp.17-18, Interscience, New York, 1954.

21. Delahay, Paul, New Instrumental Methods in Electrochemistry, p. 69, Interscience, New York, 1954.

22. Delahay, Paul, New Instrumental Methods in Electrochemistry, pp. 133-134, Interscience, New York, 1954.

23. Efimov, E. A. and N. A. Izgrayshev, Zh. Fiz. Khim., 31, 1141 (1957).

24. Engel, A. J., ASEE - NASA Summer Institute, Final Report, 1967.

25. Feldberg, S. W., C. G. Enke, and C. E. Bricker, J. Electrochem., 110, 826 (1963).

26. Foerster, F. A., Z. Physick. Chem., 51, 356 (1906).

27. Frumkin, A. N., Electrochim. Acta., 5, 265 (1961).

28. Frumkin, A. N., Proc. CITCE, 9, 396 (1959).

29. Gerovich, M. A., R. I. Kaganovich, V. A. Vergelesov, and L. N. Gorokhov, Dokl. Akad. Nauk SSSR, 114, 1049 (1957).

30. Gerisher, H., Z. Physik. Chem. N. F., 26, 223 (1960).

31. Giver, J., Z. Electrochem., 63, 386 (1959).

32. Glasstone, S., K. J. Laidler, and H. Eyring, The Theory of Rate Processes, McGraw - Hill, New York, 1941.

33. Grube, G , Z. Electrochem., 16, 621 (1910).

34. Haber, F., Z. Anorg. Allgem. Chem., 51, 356 (1906).

35. Hickling, A. and W. H. Wilson, Nature, 164, 673 (1949).

36. Hoar, T. P., Proc. Roy Soc. (London) A 142, 628 (1933).

37. Hoare, James, P., Electrochemistry of Oxygen, Wiley, New York, 1968.

38. Hoare, James, P., Electrochemistry of Oxygen, p. 28, Wiley, New York, 1968.

39. Hoare, James, P., Electrochemistry of Oxygen, p. 34, Wiley, New York, 1968.

40. Hoare, James, P., Electrochemistry of Oxygen, pp. 32-38, Wiley, New York, 1968.

41. Hoare, James, P., Electrochemistry of Oxygen, p. 84, Wiley, New York, 1968.

42. Hoare, James, P., Electrochemistry of Oxygen, pp. 84-85, Wiley, New York, 1968.

43. Hoare, James, P., Electrochemistry of Oxygen, p. 88, Wiley, New York, 1968.

44. Hoare, James, P., Electrochemistry of Oxygen, p. 125, Wiley, New York, 1968.

45. Hoare, J. P., J. Electrochem. Soc., 109, 858 (1962).

46. Hoare, J. P., J. Electrochem. Soc., 112, 602 (1965).

47. Hoare, J. P., J. Electrochem. Soc., 112, 849 (1965).

48. Izgaryshev, N. A. and E. A. Efimov, Zh. Fiz. Khim., 31, 1141 (1957).

49. Julian, D. B. and W. R. Ruby, J. Am. Chem. Soc., 72, 4719 (1950).

50. Kaganovich, R. I., M. A. Gerovich, and E. Kh. Enikeev, Dokl. Akad. Nauk. SSSR, 108, 107 (1956).

51. Kheifets, V. L. and I. Ya. Rivlin, Zh. Prikl., 28, 1291 (1955).

52. Koltoff, I. M. and J. J. Lingane, Polarography, 2nd ed., Interscience, New York - London, 1952.

53. Krushcheva, E. I. N. A. Shumilova, and M. R. Tarasevich, Elektrokhimiya, 1, 730 (1965).

54. Laitenen, H. A. and C. G. Enke, J. Electrochem. Soc., 107, 773 (1960).

55. Latimer, W. M., Oxidation Potentials, 2nd ed., Prentice - Hall, Englewood Cliffs, New Jersey, 1952.

56. Latimer, W. M., Oxidation Potentials, 2nd ed., p. 39, Prentice - Hall, Englewood Cliffs, New Jersey, 1952.

57. Lederer, E. L., Kolloid - Z. 44, 108 (1928).

58. Lee, T. J., J. Am. Chem. Soc., 74, 5001 (1952).

59. Levich, B., Acta. Physiochem., U.R.S.S., 17, 257 (1942).

60. Levich, B., Acta. Physiochem., U.R.S.S., 17, 259 (1942).

61. Levich, B., J. Phys. Chem. (U.S.S.R.), 21, 689 (1947); 22, 575, 711, 721 (1948).

62. Lewartowicz, E., J. Electroanal. Chem., 6, 11 (1963).

63 Lorenz, R., Z. Elecktrochem., 14, 781 (1908).

64. Lorenz, R., and H. Hauser, Z. Anorg. Allgem. Chem., 51, 81 (1906).

65. Lorenz, R. and P. E. Speilman, Z. Elektrochem , 15, 293 (1909).

66. Lorenz, R. and P. E. Speilman, Z. Elektrochem., 15, 349 (1909).

67. Nagel, K. and H. Dietz, Electrochim. Acta., 4, 141 (1961).

68. Nicholson, M. M., J. Am. Chem. Soc., 76, 2539 (1954).

69. Ord, J. L. and F. C. Ho, J. Electrochem. Soc., 118, 46 (1971).

70. Parsons, R. and W. H. M. Visscher, J. Electroanal. Chem., 36, 329 (1972).

71. Reddy, A. K. N., M. Genshaw, and J. O'M. Bockris, J. Electroanal. Chem., 8, 406 (1964).

72. Roughton, J. E., J. Appl. Chem., 1 (S2), S143 (1951).

73. Schuldiner, S., and R. M. Roe, J. Electrochem. Soc., 110, 332 (1963).

74. Schuldiner, S., and T. B. Warner, J. Electrochem. Soc., 112, 212 (1965).

75. Speilman, P. E., Trans. Faraday Soc., 5, 88 (1909).

76. Thacker, R. and J. P. Hoare, J. Electroanal. Chem., 30, 1 (1971).

77. Trachtenberg, Isaac, J. Electrochem. Soc., 3, 376 (1964).

78. Tsukamoto, T., T. Kambara, and I. Tachi, Sbornik Mezinarod. Polarog. Sjezdu Praze, 1st cong., Pt. I, Proc., pp. 525-541 (1951).

79. Vetter, K. J., Electrochemical Kinetics, Academic Press, New York, 1967.

80. Vetter, K. J., Electrochemical Kinetics, p. 232, Academic Press, New York, 1967.

81. Vetter, K. J., Electrochemical Kinetics, pp. 283-334, Academic Press, New York, 1967.

82. Vetter, K. J., Electrochemical Kinetics, p. 75, Academic Press, New York, 1967.

83. Vetter, K. J., Electrochemical Kinetics, pp. 47-52, Academic Press, New York, 1967.

84. Vetter, K. J., Electrochemical Kinetics, p. 644, Academic Press, New York, 1967.

85. Vetter, K. J., Electrochemical Kinetics, pp. 22-35, 53-73, Academic Press, New York, 1967.

86. Watanabe, N., and M.A.V. Devanatan, J. Electrochem. Soc., 111, 615 (1964).

APPENDICES

A. Appendix A - Experimental Data.

The experimental data are presented from which Figures 18-24 were constructed. The data are presented in tables of anode potential versus reference electrode potential, cell current, and cell current density. Of course, current density was not a datum which was recorded during the experiments. However, Figures 18-24 are plots of potential versus current density, and therefore, current density is also tabulated to facilitate any checking with the plotted results. All current densities were obtained by dividing the current by the electrode surface area, 61.9 cm^2. Experimental notes and conditions are presented as they appeared on the original data sheets. The reference electrode was a mercury-mercurous sulfate sleeve junction electrode with a potential of +0.61 V versus the normal hydrogen electrode, +0.0 V.

Table 6

FREE ELECTROLYTE - DOWNWARD SCAN

FIGURE 18, #1

Preanodization = 25 minutes at 1000 mA
Interelectrode distance = 2.5 cm

E vs Ref (Volts)	I (mA)	i (A/cm^2)
2.00	3200	5.18×10^{-2}
1.98	-	-
1.96	2700	4.38×10^{-2}
1.94	-	-
1.92	2300	3.72×10^{-2}
1.88	2000	3.24×10^{-2}
1.86	1800	2.92×10^{-2}
1.84	1600	2.59×10^{-2}
1.82	1500	2.43×10^{-2}
1.80	1350	2.19×10^{-2}
1.78	1150	1.86×10^{-2}
1.76*	1050*	1.70×10^{-2}
1.74	940	1.52×10^{-2}
1.72	760	1.23×10^{-2}
1.70	620	1.00×10^{-2}
1.68	495	8.00×10^{-3}
1.66	405	6.56×10^{-3}
1.64	330	5.35×10^{-3}
1.62	275	4.45×10^{-3}
1.60	200	3.24×10^{-3}
1.58	165	2.67×10^{-3}
1.56	135	2.19×10^{-3}

Table 6 (Concluded)

E vs Ref (Volts)	I (mA)	I (A/cm^2)
1.54*	105*	1.70×10^{-3}
1.52	81	1.31×10^{-3}
1.50	56.5	9.15×10^{-4}
1.48	40.0	6.47×10^{-4}
1.46	31.0	5.02×10^{-4}
1.44	23.5	3.80×10^{-4}
1.42	19.5	3.15×10^{-4}
1.40	14.0	2.27×10^{-4}
1.38	12.0	1.94×10^{-4}
1.36	8.40	1.36×10^{-4}
1.34*	6.30*	1.02×10^{-4}
1.32	4.20	6.80×10^{-5}
1.30	2.90	4.70×10^{-5}
1.28	2.30	3.72×10^{-5}
1.26	1.65	2.67×10^{-5}
1.24	1.30	2.11×10^{-5}
1.22	1.10	1.78×10^{-5}
1.20	0.81	1.31×10^{-5}
1.18	0.54	8.25×10^{-6}
1.16	0.37	6.0×10^{-6}
1.14	0.285	4.61×10^{-6}
1.12	0.19	3.08×10^{-6}

*Current jump noted.
Temp. = 80°F.
Air Flow Rate = 24 cm^3/sec.
Rel. Hum. = 51%.
8.1 M H_2SO_4 solution.

Table 7

FREE ELECTROLYTE - UPWARD SCAN

FIGURE 19, #2

Preanodization = 25 minutes at 820 mA
Interelectroce distance = 2.5 cm

E vs Ref (Volts)	I (mA)	i (A/cm^2)
1.12	1.10	1.78×10^{-5}
1.14	1.25	2.02×10^{-5}
1.16	1.45	2.35×10^{-5}
1.18	-	-
1.20	2.60	4.21×10^{-5}
1.22	-	-
1.24	4.80	7.77×10^{-5}
1.26	-	-
1.28	9.0	1.45×10^{-4}
1.30	-	-
1.32	15.0	2.43×10^{-4}
1.34	-	-
1.36	30.0	4.86×10^{-4}
1.38	-	-
1.40	45.0	7.29×10^{-4}
1.42	58.0	9.40×10^{-4}
1.44	69.0	1.11×10^{-3}
1.46	91.5	1.47×10^{-3}
1.48	130	2.11×10^{-3}
1.50	155	2.55×10^{-3}
1.52	-	-
1.54	250	4.04×10^{-3}

Table 7 (Concluded)

E vs Ref (Volts)	I (mA)	i (A/cm^2)
1.56	-	-
1.58	330	5.34×10^{-3}
1.60	-	-
1.62	400	6.48×10^{-3}
1.64	480	7.77×10^{-3}
1.66	530	8.57×10^{-3}
1.68	585	9.46×10^{-3}
1.70	-	-
1.72	690	1.11×10^{-2}
1.74	-	-
1.76	770	1.25×10^{-2}
1.78	-	-
1.80	890	1.44×10^{-2}
1.82	-	-
1.84	1150	1.86×10^{-2}
1.86	1400	2.27×10^{-2}
1.88	-	-
1.90	-	-
1.92	1500	2.43×10^{-2}
1.94	-	-
1.96	1700	2.75×10^{-2}
1.98	-	-
2.00	1850	2.99×10^{-2}

Experimental note: At low currents (1-10 mA) the current decreased after a step change in potential.

Table 8

DOWNWARD SCAN

FIGURE 19, #3

E vs Ref (Volts)	I (mA)	i (A/cm^2)
2.00	1900	3.07×10^{-2}
1.98	1700	2.75×10^{-2}
1.96	-	-
1.94	1450	2.34×10^{-2}
1.92	-	-
1.90	1250	2.02×10^{-2}
1.88	-	-
1.86	990	1.60×10^{-2}
1.84	865	1.40×10^{-2}
1.82	780	1.26×10^{-2}
1.80	695	1.12×10^{-2}
1.78	615	9.95×10^{-3}
1.76	540	8.75×10^{-3}
1.74	460	7.45×10^{-3}
1.72	415	6.72×10^{-3}
1.70	-	-
1.68	310	5.02×10^{-3}
1.66	-	-
1.64	225	3.64×10^{-3}
1.62	-	-
1.60	160	$2\ 59 \times 10^{-3}$
1.58	130	2.11×10^{-3}
1.56	-	-

Table 8 (Concluded)

E vs Ref (Volts)	I (mA)	I (A/cm^2)
1.54	84.0	1.36×10^{-3}
1.52	66.5	1.08×10^{-3}
1.50	52.5	8.50×10^{-4}
1.48	37.5	6.06×10^{-4}
1.46	-	-
1.44	26.0	4.21×10^{-4}
1.42	-	-
1.40	20.5	3.32×10^{-4}
1.38	12.5	2.02×10^{-4}
1.36	9.70	1.57×10^{-4}
1.34	7.15	1.16×10^{-4}
1.32	5.40	8.75×10^{-5}
1.30	4.10	6.65×10^{-5}
1.28	2.90	4.70×10^{-5}
1.26	-	-
1.24	2.00	3.22×10^{-5}
1.22	1.40	2.27×10^{-5}
1.20	1.15	1.86×10^{-5}
1.18	.77	1.25×10^{-5}
1.16	.60	9.70×10^{-6}
1.14	.45	7.30×10^{-6}
1.12	.35	5.67×10^{-6}

Temp. = 80°F.
Air Flow Rate = 24 cm^3/Sec.
Rel. Hum. = 50%.
8.1 M H_2SO_4 solution.

Table 9

STANDARD CELL - UPWARD SCAN

FIGURE 20, #1

Preanodization = 15 minutes at 800 mA
Interelectrode distance = 2.5 cm

E vs Ref (Volts)	I (mA)	i (A/cm^2)
1.12	0.330	5.35×10^{-6}
1.14	0.490	7.95×10^{-6}
1.16	0.660	1.08×10^{-5}
1.18	0.990	1.61×10^{-5}
1.20	1.45	2.35×10^{-5}
1.22	2.10	3.40×10^{-5}
1.24	2.65	4.29×10^{-5}
1.26	3.80	6.15×10^{-5}
1.28	4.90	7.95×10^{-5}
1.30	6.50	1.05×10^{-4}
1.32	8.90	1.44×10^{-4}
1.34	12.0	1.94×10^{-4}
1.36	15.0	2.42×10^{-4}
1.38	21.5	3.45×10^{-4}
1.40	28.5	4.62×10^{-4}
1.42	-	-
1.44	47.0	7.60×10^{-4}
1.46	-	-
1.48	77.5	1.25×10^{-3}
1.50	93.0	1.51×10^{-3}
1.52	120	1.94×10^{-3}
1.54	-	-

Table 9 (Concluded)

E vs Ref (Volts)	I (mA)	i (A/cm^2)
1.56	160	2.59×10^{-3}
1.58	-	-
1.60	210	3.40×10^{-3}
1.62	-	-
1.64	265	4.28×10^{-3}
1.66	-	-
1.68	330	5.34×10^{-3}
1.70	-	-
1.72	390	6.30×10^{-3}
1.74	-	-
1.76	450	7.28×10^{-3}
1.78	-	-
1.80	510	8.25×10^{-3}
1.82	-	-
1.84	575	9.30×10^{-3}
1.86	-	-
1.88	655	1.06×10^{-2}
1.90	-	-
1.92	690	1.12×10^{-2}
1.94	735	1.19×10^{-2}
1.96	775	1.25×10^{-2}
1.98	800	1.29×10^{-2}
2.00	830	1.34×10^{-2}

Air flow Rate = 24 cm^3/Sec.
Temp. = 81°F.
Rel. Hum. = 50%.
Experimental Note: Instability of current recorder above 600 mA; "jumpiness".

Table 10

DOWNWARD SCAN

FIGURE 20, #2

E vs Ref (Volts)	I (mA)	i (A/cm^2)
2.00	810	1.31×10^{-2}
1.98	-	-
1.96	725	1.17×10^{-2}
1.94	-	-
1.92	640	1.03×10^{-2}
1.90	-	-
1.88	560	9.06×10^{-3}
1.86	-	-
1.84	505	8.18×10^{-3}
1.82	-	-
1.80	430	6.96×10^{-3}
1.78	-	-
1.76	360	5.82×10^{-3}
1.74	-	-
1.72	300	4.86×10^{-3}
1.70	-	-
1.68	245	3.96×10^{-3}
1.66	-	-
1.64	190	3.08×10^{-3}
1.62	-	-
1.60	155	2.51×10^{-3}
1.58	-	-
1.56	115	$1,86 \times 10^{-3}$

Table 10 (Concluded)

E vs Ref (Volts)	I (mA)	i (A/cm^2)
1.54	-	-
1.52	74	1.20×10^{-3}
1.50	-	-
1.48	46	7.45×10^{-4}
1.46	-	-
1.44	27.5	4.45×10^{-4}
1.42	-	-
1.40	17.5	2.84×10^{-4}
1.38	-	-
1.36	11.5	1.86×10^{-4}
1.34	-	-
1.32	6.30	1.02×10^{-4}
1.30	4.65	7.50×10^{-5}
1.28	3.40	5.49×10^{-5}
1.26	2.50	4.03×10^{-5}
1.24	1.80	2.91×10^{-5}
1.22	-	-
1.20	1.25	2.02×10^{-5}
1.18	0.775	1.25×10^{-5}
1.16	0.60	9.70×10^{-6}
1.14	0.42	6.80×10^{-6}
1.12	0.33	5.34×10^{-6}

Table 11

STANDARD CELL - DOWNWARD SCAN

FIGURE 21, #3

Preanodization = 20 minutes at 700 mA
Interelectrode distance = 2.5 cm

E vs Ref (Volts)	I (mA)	i (A/cm^2)
2.00	670	1.08×10^{-2}
1.98	615	9.95×10^{-3}
1.96	595	9.60×10^{-3}
1.94	560	9.05×10^{-3}
1.92	530	8.57×10^{-3}
1.90	500	8.09×10^{-3}
1.88	455	7.35×10^{-3}
1.86	430	6.95×10^{-3}
1.84	400	6.47×10^{-3}
1.82	370	5.98×10^{-3}
1.80	-	-
1.78	310	5.01×10^{-3}
1.76	-	-
1.74	260	4.21×10^{-3}
1.72	-	-
1.70	210	3.40×10^{-3}
1.68	-	-
1.66	170	2.75×10^{-3}
1.64	-	-
1.62	130	2.10×10^{-3}
1.60	-	-
1.58	100	1.62×10^{-3}

Table 11 (Concluded)

E vs Ref (Volts)	I (mA)	i (A/cm^2)
1.56	69	1.12×10^{-3}
1.54	56	9.05×10^{-4}
1.52	46.5	7.51×10^{-4}
1.50	38.5	6.21×10^{-4}
1.48	27.5	4.45×10^{-4}
1.46	22.5	3.64×10^{-4}
1.44	18.0	2.91×10^{-4}
1.42	-	-
1.40	12.0	1.94×10^{-4}
1.38	9.20	1.49×10^{-4}
1.36	7.00	1.13×10^{-4}
1.34	5.00	8.08×10^{-5}
1.32	4.20	6.78×10^{-5}
1.30	3.15	5.09×10^{-5}
1.28	2.35	3.80×10^{-5}
1.26	1.90	3.07×10^{-5}
1.24	1.45	2.34×10^{-5}
1.22	1.20	1.94×10^{-5}
1.20	0.86	1.39×10^{-5}
1.18	0.595	9.61×10^{-6}
1.16	0.410	6.62×10^{-6}
1.14	0.330	5.33×10^{-6}
1.12	0.265	4.28×10^{-6}

Air Flow Rate = 24 cm^3/Sec.
Temp. = 76°F.
Rel. Hum. = 50%

Table 12

STANDARD CELL - UPWARD SCAN

FIGURE 21, #4

E vs Ref (Volts)	I (mA)	i (A/cm^2)
1.12	0.250	4.03×10^{-6}
1.14	0.355	5.74×10^{-6}
1.16	0.460	7.44×10^{-6}
1.18	0.720	1.16×10^{-5}
1.20	1.20	1.94×10^{-5}
1.22	1.60	2.59×10^{-5}
1.24	2.25	3.64×10^{-5}
1.26	2.90	4.69×10^{-5}
1.28	3.95	6.39×10^{-5}
1.30	5.65	9.12×10^{-5}
1.32	7.40	1.20×10^{-4}
1.34	9.65	1.53×10^{-4}
1.36	11.0	1.78×10^{-4}
1.38	14.0	2.26×10^{-4}
1.40	19.0	3.07×10^{-4}
1.42	26 5	4.12×10^{-4}
1.44	33.0	5.33×10^{-4}
1.46	*	*
1.48	51.0	8.25×10^{-4}
1.50	58.0	9.38×10^{-4}
1.52	68.0	1.10×10^{-3}
1.54	81.0	1.31×10^{-3}
1.56	120	1.94×10^{-3}

Table 12 (Continued)

E vs Ref (Volts)	I (mA)	i (A/cm^2)
1.58	-	-
1.60	170	2.75×10^{-3}
1.62	-	-
1.64	230	3.72×10^{-3}
1.66	-	-
1.68	290	4.69×10^{-3}
1.70	-	-
1.72	350	5.66×10^{-3}
1.74	-	-
1.76	415	6.70×10^{-3}
1.78	-	-
1.80	490	7.92×10^{-3}
1.82	-	-
1.84	555	8.96×10^{-3}
1.86	-	-
1.88	620	1.00×10^{-2}
1.90	-	-
1.92	700	1.13×10^{-2}
1.94	735	1.19×10^{-2}
1.96	-	-
1.98	770	1.25×10^{-2}
2.00	815	1.32×10^{-2}

*Gradually decreasing current after step change in potential.

Experimental note: No limiting current reached even up to 3 amps.

Table 13

STANDARD CELL - UPWARD SCAN

FIGURE 22, #5

Preanodization = 20 minutes at 850 mA
Interelectrode distance = 2.5 cm

E vs Ref (Volts)	I (mA)	i (A/cm^2)
1.14	0.21	3.45×10^{-6}
1.16	0.30	4.92×10^{-6}
1.18	0.41	6.72×10^{-6}
1.20	0.56	9.20×10^{-6}
1.22	0.90	1.48×10^{-5}
1.24	1.30	2.13×10^{-5}
1.26	1.70	2.79×10^{-5}
1.28	2.20	3.61×10^{-5}
1.30	3.30	5.41×10^{-5}
1.32	3.90	6.40×10^{-5}
1.34	5.30	8.70×10^{-5}
1.36	6.70	1.10×10^{-4}
1.38	8.60	1.41×10^{-4}
1.40	12	1.97×10^{-4}
1.42	13	2.13×10^{-4}
1.44	16	2.62×10^{-4}
1.46	21	3.44×10^{-4}
1.48	25.5	4.18×10^{-4}
1.50	30.5	5.00×10^{-4}
1.52	34.5	5.65×10^{-4}
1.54	40	6.56×10^{-4}
1.56	46	7.55×10^{-4}

Table 13 (Concluded)

E vs Ref (Volts)	I (mA)	i (A/cm^2)
1.58	53.5	8.77×10^{-4}
1.60	62.5	9.90×10^{-4}
1.62	67	1.08×10^{-3}
1.64	77	1.24×10^{-3}
1.66	87	1.42×10^{-3}
1.68	96	1.55×10^{-3}
1.70	125	2.02×10^{-3}
1.72	130	2.11×10^{-3}
1.74	140	2.27×10^{-3}
1.76	150	2.43×10^{-3}
1.78	160	2.59×10^{-3}
1.80	175	2.83×10^{-3}
1.82	190	3.07×10^{-3}
1.84	200	3.23×10^{-3}
1.86	210	3.40×10^{-3}
1.88	230	3.72×10^{-3}
1.90	235	3.80×10^{-3}
1.92	240	3.88×10^{-3}
1.94	250	4.04×10^{-3}
1.96	265	4.29×10^{-3}
1.98	275	4.45×10^{-3}
2.00	285	4.61×10^{-3}

Table 14

STANDARD CELL - DOWNWARD SCAN

FIGURE 22, #6

E vs Ref (Volts)	I (mA)	i (A/cm^2)
2.00	230 ±5	3.72×10^{-3}
1.98	215	3.48×10^{-3}
1.96	205	3.32×10^{-3}
1.94	190	3.07×10^{-3}
1.92	185	2.99×10^{-3}
1.90	175	2.83×10^{-3}
1.88	165	2.67×10^{-3}
1.86	155	2.51×10^{-3}
1.84	145	2.35×10^{-3}
1.82	135	2.19×10^{-3}
1.80	130	2.11×10^{-3}
1.78	120	1.94×10^{-3}
1.76	110	1.78×10^{-3}
1.74	100	1.62×10^{-3}
1.72	79	1.28×10^{-3}
1.70	70	1.13×10^{-3}
1.68	63	1.02×10^{-3}
1.66	56	9.06×10^{-4}
1.64	51	8.25×10^{-4}
1.62	45	7.28×10^{-4}
1.60	40	6.47×10^{-4}
1.58	35	5.66×10^{-4}
1.56	31	5.01×10^{-4}

Table 14 (Concluded)

E vs Ref (Volts)	I (mA)	i (A/cm^2)
1.54	26	4.21×10^{-4}
1.52	23	3.72×10^{-4}
1.50	19	3.07×10^{-4}
1.48	17	2.75×10^{-4}
1.46	14	2.26×10^{-4}
1.44	12	1.94×10^{-4}
1.42	8.5	1.38×10^{-4}
1.40	7.15	1.06×10^{-5}
1.38	5.6	9.06×10^{-5}
1.36	4.25	6.87×10^{-5}
1.34	3.30	5.34×10^{-5}
1.32	2.50	4.04×10^{-5}
1.30	2.10	3.40×10^{-5}
1.28	1.60	2.59×10^{-5}
1.26	1.25	2.15×10^{-5}
1.24	0.895	1.45×10^{-5}
1.22	0.610	9.90×10^{-6}
1.20	0.460	7.45×10^{-6}
1.18	0.355	5.75×10^{-6}
1.16	0.250	4.04×10^{-6}
1.14	0.200	3.23×10^{-6}
1.12	0.140	2.26×10^{-6}

Temp. = 76°F.
Air Flow Rate = 24 cm^3/sec.
Rel. Hum. = 50%.

B. Appendix B - Sample Calculations.

1. IR Loss.

$$IR = il\rho$$

$$i = \frac{I}{A} = \frac{3.2\ A}{6.19\ cm^2} = 5.18 \times 10^{-2}\ a/cm^2$$

$$\rho = 1.91 \text{ ohm cm (ref. 72)}$$

$$l = 2.5 \text{ cm}$$

$$IR = (5.18 \times 10^{-2}\ A/cm^2)\ (1.91 \text{ ohm cm})\ (2.5 \text{ cm})$$

$$IR = 0.25 \text{ volt}$$

The IR corrected anode potential is, therefore,

$$2.00\ V - 0.25V = 1.75V \text{ vs Ref.}$$

2. Water adsorption - mass balance; verification of steady state current.

$$H_2O \text{ absorption rate} = \frac{0.33\ gm^{1}}{hr} \times \frac{hr}{3600\ sec} \times \frac{1\ mole}{18\ gm}$$

$$= 5.1 \times 10^{-6} \text{ moles O/sec.}$$

$$= 2.55 \times 10^{-6} \text{ moles } O_2/\text{sec.}$$

now,

$$0.92\ A = \text{how many moles } O_2/\text{sec?}$$

$$1\ A = \frac{1\ coul}{sec} \times \frac{1}{97000} \frac{mole\ e^-}{coul} \times \frac{mole\ O_2}{4\ moles\ e^-}$$

$$0.92\ A = 0.92 \frac{coul}{sec} \times \frac{1}{97000} \frac{mole\ e^-}{coul} \times \frac{moles\ O_2}{4\ moles\ e^-}$$

$$= 2.38 \times 10^{-6} \text{ moles } O_2/\text{sec.}$$

$$100\% \times \frac{2.38 \times 10^{-6} \text{ moles } O_2/\text{sec.}}{2.55 \times 10^{-6} \text{ moles } O_2/\text{sec.}} = 94\%$$

[1]See Figure 25.

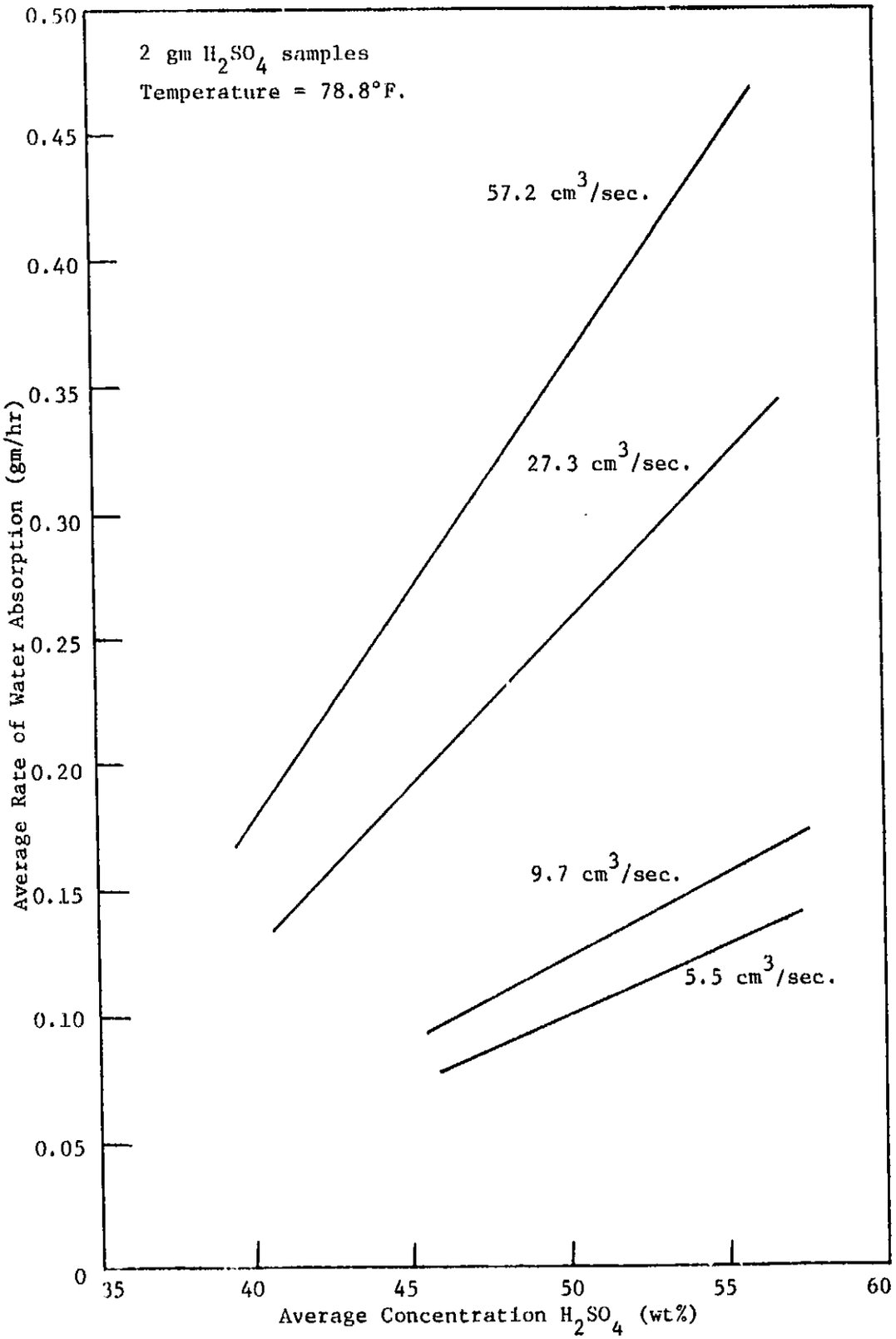

Figure. 25 WATER ABSORPTION RATE ON H_2SO_4 AT DIFFERENT GAS FLOW RATES.

Hence, steady state current has been checked by water absorption data to within 6%.

3. Volume of water absorbed in 5 seconds.

$$V_{5sec} = \frac{.33 \text{ gm}}{\text{hr}} \times \frac{\text{hr}}{3600 \text{ sec}} \times \frac{\text{cm}^3}{\text{g}} \times 5 \text{ sec.}$$

$$= 4.1 \times 10^{-4} \text{ cm}^3$$

Volume in cell

$$V_{cell} = 0.1 \text{ cm deep} \times 4 \text{ in}^2 \times (2.54 \text{ cm/in}^2)$$

$$= 2.58 \text{ cm}^3$$

Relative Volumes

$$100\% \times \frac{V_{5 \text{ sec}}}{V_{cell}} = \frac{4.1 \times 10^{-4}}{2.58 \text{ cm}} = 0.00036\%$$

Volume in diffusion layer

$$V_{d.l.} = 0.005 \text{ cm} \times 6.19 \text{ cm}^2 = .31 \text{ cm}^3$$

Relative Volumes

$$100\% \times \frac{V_{5 \text{ sec}}}{V_{d.l.}} = \frac{4.1 \times 10^{-4} \text{ cm}^3}{0.31 \text{ cm}^3} = 0.13\%$$